University of Technology, Sydney

Master Thesis

Performance analysis of a new single effect hot water absorption chiller system

Author:
Saket Sinha

Supervisor:
Associate Professor Quang Ha

A thesis submitted in partial fulfillment of the requirements for the degree of Master of Engineering Research

in the

Faculty of Engineering and Information Technology
School of Electrical, Mechanical and Mechatronics Systems

October 2015

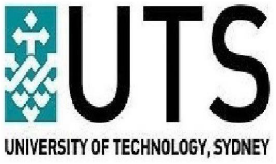

Certificate of Authorship

I certify that the work in this thesis has not previously been submitted for a degree nor has it been submitted as part of requirements for a degree except as fully acknowledged within the text.

I also certify that the thesis has been written by me. Any help that I have received in my research work and the preparation of the thesis itself has been acknowledged.In addition, I certify that all information sources and literature used are indicated in the thesis.

Signed: _____

Date: _____

"Well the basic thesis is that there's a god in heaven who is all powerful who wants to help people. And that - he will answer prayer, and does miraculous things in people's lives. And so I've documented some of these wonderful things."

Saket Sinha

Performance analysis of a new single effect hot water absorption chiller system

Saket Sinha

Abstract

Conventional air conditioning significantly contributes to primary electricity consumption. The rise in living standards and working conditions combined with the increasing usage of renewable energy has led to a great expansion of modern air conditioning systems. Among existing chiller systems, absorption machines are promising as they use less electrical power and electric utilities. Another advantage of absorption units is that the working fluids are not harmful to the environment. Thus, there is a high demand for small capacity absorption machines for residential and small office applications. However, high investment cost, additional equipment requirement and few manufacturers are the main reasons for these machines not being economically competitive with conventional compression machines. There is a lack of best practice guides, test procedures and adequate standards for their evaluation. Therefore, it is important to conduct research, starting from design and validation work, into modelling and energy optimisation in energy-efficient air conditioning systems.

This thesis aims to develop simple and accurate steady-state models of small capacity absorption machines based on experimental data obtained from a solar, single-effect, hot-water absorption machine, installed at UTS. These models are further used in a simulation tool for energy optimisation of this absorption machine. The thesis encompasses components of testing, modelling and energy optimisation of small capacity absorption machines. The first task is obtaining highly reliable data from our installation. This part involves several steps: test planning, data modelling, uncertainty estimation and analysis of results.

The second research task focuses on the development of small capacity absorption chiller models from the obtained dataset. The study involves two different modelling methods, namely adapted characteristic equation and multivariable polynomial regression. It is possible to use external water circuits as input parameters to develop highly accurate empirical models. The study describes statistical tests that assist in selecting the most appropriate models.

The last research task focuses on energy optimisation of the chiller plant. Here, water-cooled chilled water plants are considered. The chiller plant optimisation problem is formulated by developing multi-variable regression models using equipment performance data. The water-cooled chiller plant optimisation involves the optimal combination of equipment and operating levels for minimum electrical power consumption.

Acknowledgements

I am heartly thankful to my supervisor, Associate Professor Quang Ha, whose encouragement, guidance and support from the initial to the final level enabled me to develop my thesis. I thank him for guiding my thesis in a routine manner. I also thank my friends and parents for encouraging and motivating me on writing the thesis. I also thank university support in providing me appropriate resources for the project like the library. Thanks to the Research and Development staff who gave me help during my studies at the department. I also give my thanks to the Library for allowing me to borrow books related to my topic.

Lastly, I offer my regards and blessings to all those who supported me in any respect during completion of the project.

Contents

List of Figures

List of Tables

Dedicated to my Parents

Chapter 1

Introduction

1.1 Energy Context

Nature and human activities produce global warming that has severe consequences for the atmosphere. Volcanic eruptions, natural fluctuations in the climate system and fractional changes in solar radiation are natural causes of global warming. However, Nature produces only part of this world warming. The primary cause of global warming is human activities such as burning of fossil fuels producing heat-trapping greenhouse gas emissions. In recent years, the typical surface air temperature has increased by $0.74°C$. The Intergovernmental Panel on Climate Change (IPCC) ventures that by 2100, the worldwide average temperature will increase by a further $1.8°C$ to $4°C$. Worldwide average temperature will increase further unless the world makes a move to limit greenhouse gas emissions. Burning of fossil fuels influences our regular lives and has extreme results on Earth's environment and are the main cause of global warming. Melting polar ice caps, higher seismic movement, hurricanes, retreating glaciers and climbing ocean level are the major consequences of global warming. Higher concentration of ozone in the lower atmosphere, warmer climate and the environment in danger are major consequences of

global warming. Oil prices increased in the year 2008, and the level of the petroleum crisis increased in the seventies. Cost of energy will increase further by lack of fossil fuel sources supported by economic crisis and climate-related incidents. World primary consumption decreased by 1.1% in the year 2009 and this was the first decline since the year 1982. Figure 1.1 illustrates that oil is the world's leading fuel while coal remains the fastest growing fuel.

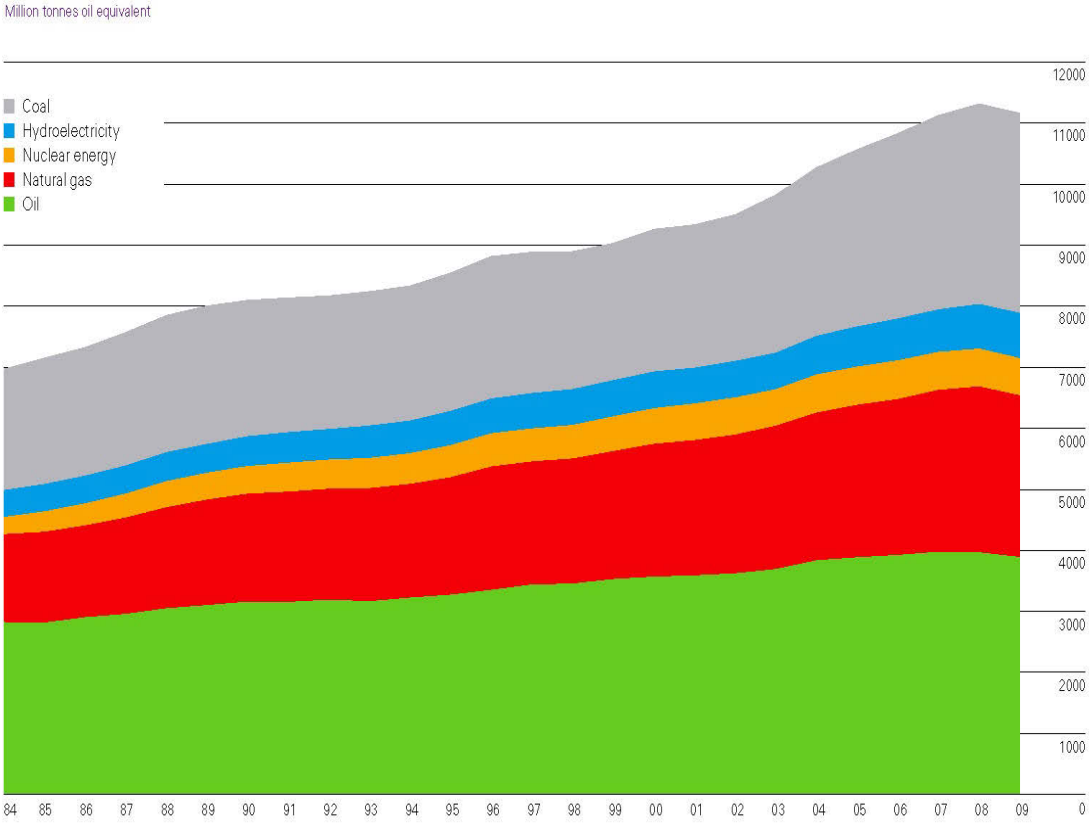

FIGURE 1.1: World primary energy consumption [1]

The Kyoto protocol adopted by world governments gathered in the Japanese city Kyoto identifies regulatory measurements to tackle climate change. The Kyoto protocol sets legally binding limits for greenhouse gas emissions for industrialised countries of the world. Rising carbon dioxide emission and prediction (Figure 1.2) have forced countries in the world to make significant efforts in the battle against emission reductions. The EU developed a climate and energy package in 2009 which proposed greenhouse gas cuts, increased use of renewables and

improved energy efficiency. Low carbon emissions, international funding and international carbon market are areas to invest money by 2015 and help countries adapt to climate change. The present environmental and economic crisis depends on current energy systems based on fossil fuels. Electrical air-conditioning units are significant contributors to primary energy consumption of both developed and developing countries. The reduced prices of air - conditioning units and lower electricity prices caused a great expansion of these systems. Worldwide sales of room air conditioners produce an adverse impact on electricity demand and the environment. Cooling and heating energy requirements projections (Figure 1.3) show the rising trend in the next decade. According to the International Energy Agency, the direct emissions from buildings along with indirect emissions from electricity use produce 30% of global CO_2 emissions.

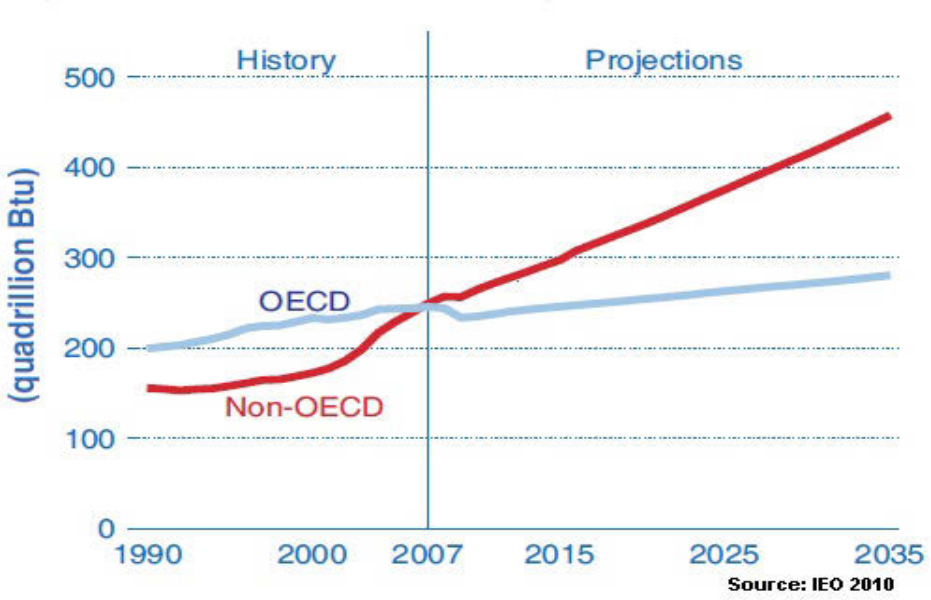

FIGURE 1.2: World energy - related carbon dioxide emissions by fuel type [30]

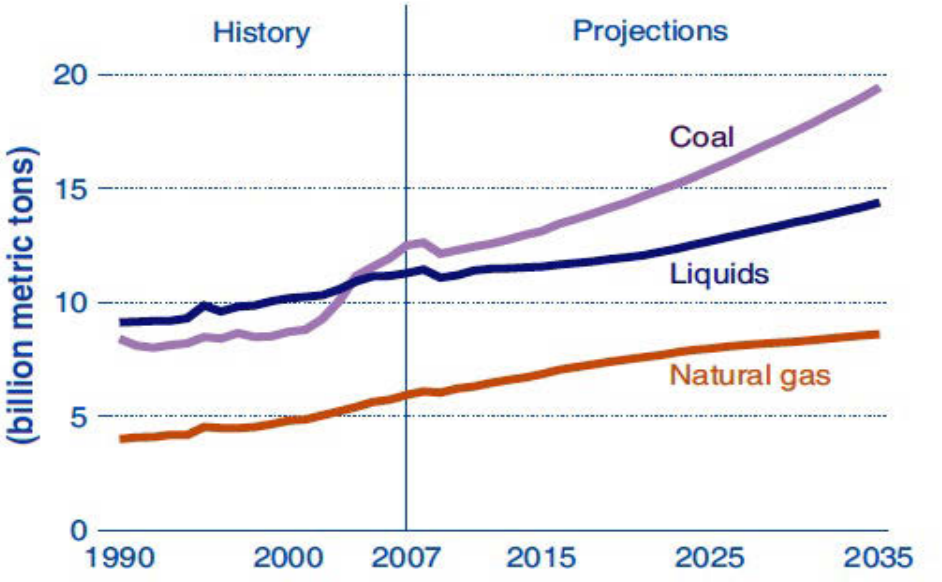

FIGURE 1.3: World energy consumption in developed and developing countries [30]

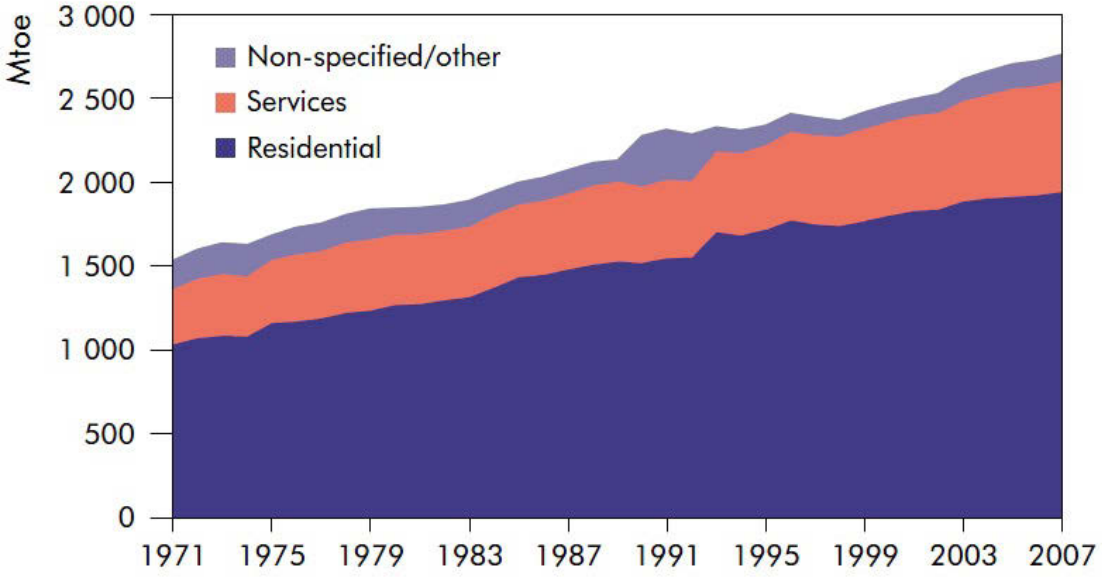

FIGURE 1.4: Global Energy consumption of buildings by sector [29]

Buildings consume 40% of world's total final energy consumption. Energy consumption of the building sector grew by 1.6% a year (Figure 1.4) between 1971 and 2007. Electricity used for space and water heating and air-conditioning is a major part of that energy. Space and water heating and air-conditioning make up one-third of total electricity consumed in buildings. Between 1995 to 2007, the United States had an annual growth of 3.1% in the building sector. The electricity consumption as a proportion of total energy consumption increased from 41% to 49% between 1990 to 2007. The residential and commercial sector consumed 72% according to DOE report while 27% use space and water heating and air-conditioning. However, total final energy consumption in China doubled from 2000 to 2007. The energy consumption for buildings increased by three times over the same period. The electricity used in buildings multiplied by 3 in a period between 1990 and 2007 for India. Brazil, Russia, India, China and the Middle East are fastest world construction markets and have further growth in demand for comfortable indoor conditions. World energy needs and rising climate changes are solved in part by renewable energy technologies.

Renewable energy sources useful for generating energy are solar energy, wind, falling water and various plants i.e. biomass. There is significant progress in the collection and improving of the conversion efficiency of these renewable energies. There has been progress in lowering maintenance costs and increasing applications of renewable energy systems. The advantages of cooling by solar energy are the relation between solar power and solar demand. Another choice is waste heat from combined heat and power plants for cooling. The high availability of solar radiation and waste heat during summer peak loads can use energy with heat driven cooling machines. Absorption systems are the most dominating technology among many technologies used for solar cooling and combined heat and power plants (CHP).

1.2 Background and motivation

Absorption machines use heat to produce cooling or heating because conventional compression devices use electricity and hence produce energy savings. They work on the absorption process where solid or liquid sorbent absorbs refrigerant molecules inside and changes their physical or chemical form. Absorption machines transform thermal energy into cooling power. Another advantage of absorption machines is that they use environmentally friendly working fluid pairs without depleting the ozone layer of the atmosphere. The absorption chillers range in capacity from medium (50-300 kW) to high (300 kW and up). However, small capacity absorption machines (less than 50 kW, less than 20 kW) have increased cooling demand in residential and small office applications. The market potential of small-scale cooling systems with absorption chillers is significant. Solar cooling and combined heat and power plant (CHP) systems have much lower operating costs and reduced CO_2 emissions, but there are many issues to solve before they become more competitive in the market than conventional compression systems. The results from monitoring of 150 small-scale solar cooling systems produced hints for improvements. Installations under real operating conditions provided field data showing shortcomings in the system's hydraulic design and control. Design of these systems requires computer simulations of different system configurations to find the best energy-cost performance. Electrical consumption of auxiliary equipment is under particular attention. Control of these absorption machines is sophisticated to increase overall performance. Therefore, economic feasibility is achieved by improving the performance of these thermal driven machines. Small-scale absorption machines are new, and have a lack of adequate standards, best practice guidelines and test procedures for their evaluation compared to conventional compression machines. The best method for performance analysis of absorption

machines uses real operating data from experimental work in equipped and monitored test facilities. Manufacturer catalogues of absorption machine provide poor information on their performance. System efficiency varies by actual conditions of applications. As a result, the research method involves experimental data analysis for getting correct and reliable mathematical models for further development. The modelling allows engineers to assess most economic operating conditions and optimal ways of control in air-conditioning systems. Authors have reported work on absorption chiller modelling, but no study compares different modelling approaches. A comprehensive study should consider both physical and empirical modelling approach and examines the differences providing guidelines for use of models.

This thesis contributes to performance analysis and modelling of small capacity commercial absorption machines taking into account external measurements. It is important to integrate this device into systems reducing energy consumption and providing environmental benefits for residential and light commercial buildings. This thesis will help software developers find methods to simulate these interactions using different modelling approaches.

1.3 Aims and Objectives

This thesis aims to produce comprehensive methodology for testing, modelling, performance analysis and optimisation for small capacity absorption chillers. The data for chilled water, cooling water and hot water develops different mathematical models for small capacity absorption machine.These models can further use testing and optimising operation of absorption machine in air-conditioning systems. The methods used in this thesis are derived from

experimental work and building energy system design. In order to achieve this aim, the following were defined:

- Comprehensive literature review is performed on absorption technology and standards including small capacity absorption machines and their integration into solar-assisted air-conditioning systems.
- Developing strategies for design and selection of proper air-conditioning in buildings capable of providing safe, healthier, productive and comfortable working environment to occupants. This is achieved by calculating cooling load of lift motor room by cooling load temperature difference method and radiant time series method.
- Develop various steady-state models based on experimental results using both physical and empirical approaches by thermodynamic modelling for the system.
- Establish simple analytical procedure to assess performance of absorption machines based on collected data by using previous research work and experience in this field.
- Total Power consumption of chiller plant is minimised to get the maximum available solar energy with an aim to keep the cost minimum for energy conservation of the system.

1.4 Research Approach

The thesis focuses on data analysis, model development and performance analysis of absorption chillers based on the Characteristic Equation model and multivariable polynomial regression model. Experimental data and computation methods are two essential components of this work. This research acts as a guideline to other researchers as a step by step procedure from test

planning to experimental work. It involves data analysis of models and optimisation useful for simulation software developers. The following research methodology is used to achieve the aims and objectives of the thesis:

1. A Comprehensive literature review is performed on available solar energy and the system capable of converting the solar energy into suitable form like heat and/or electricity.

2. Calculating cooling load of the lift motor room and comparing cooling load by cooling load temperature difference and radiant time series method for providing estimate of cooling required by absorption chiller system for lift motor room for 24 hours a day.

3. Experimental investigation involving measuring inlet and outlet cooling water, chilled water and hot water for the absorption chiller.

4. Thermodynamic modelling of absorption chiller, evacuated solar collectors, cooling tower and fan coil system.

5. The chilled, cooling and hot water measurements for absorption chiller is used for data modelling from first law of thermodynamics providing experimental heat absorbed by generator, absorber and heat rejected by condenser.

6. Performance analysis of solar hot water absorption chiller using multivariable polynomial regression model and characteristic equation model and comparison with experimental data for absorption chiller.

7. Total power consumption of chiller plant is minimised for energy conservation of solar hot water absorption chiller system.

1.5 Structure of the thesis

The thesis is divided into seven chapters and one Appendix where each Chapter focuses on interests of future researchers. The first Chapter of the thesis discusses the main factors affecting excessive primary energy consumption. The Chapter discusses the main causes affecting adverse impacts on the environment. Research in small capacity absorption machine reflects on possible solutions for conventional compression systems. Research objectives are selected and justified and a research approach is used to achieve these goals.

Chapter 2 provides a comprehensive literature review into R& D works by using PV technology for improving the energy efficiency of buildings for heating, ventilation and air- conditioning. The different solar air-conditioning systems describe the improving energy efficiency of buildings. Current status, research focus and existing difficulties/ barriers are researched for solar cooling of buildings. Different design of solar cooling systems have been designed for improving the energy efficiency of buildings. Various mathematical models and control design for different air-conditioning systems are investigated. Based on the literature Review possibilities of future research for different solar air-conditioning systems are suggested.

Chapter 3 provides the radiant time series method for performing design cooling load calculations, derived from the heat balance method. Radiant time series replaces cooling load temperature difference/ solar cooling load / cooling load factor (CLTD/SCL/CLF). Radiant time series calculates conductive heat gain on 24-term response part series and instantaneous radiant heat gains on 24-term ”radiant time series” for calculating cooling loads. This Chapter describes radiant time series method and generation of response factors and radiant time series coefficients and gives a brief comparison with the CLTD method.

The fourth Chapter provides testing procedures for commercial small capacity absorption machines. It attempts to create a standard procedure on earlier achievements and experience to create a performance map of an absorption machine by external measurements and generate the database for absorption machine modelling. The Chapter provides thermodynamic modelling of the absorption chiller, evacuated tube collectors, cooling tower and fan coil for absorption chiller system. It reflects on performance analysis of the absorption chiller.

Chapter 5 provides performance analysis of the absorption chiller based on experiments. Two different modelling methods are developed using both physical and empirical methods. Statistical limits are used to discuss and test the data.

Chapter 6 identifies absorption chiller limits and plans the chiller plant. It involves optimisation using the hybrid optimisation technique. The optimisation model formulation finds operating limits in the chiller plant for least electrical Power consumption. This Chapter takes into account performance of chillers, cooling towers and pumps and optimises Energy consumed based on required loads and ambient atmospheric conditions.

Chapter 7 summarises the results and works done in this thesis and thesis contributions providing a perspective for future research.

Chapter 2

Literature Review of solar air conditioning systems

2.1 Introduction

The energy production from coal and oil is likely to reduce significantly for the Organisation of Economic Corporation and Development. Thus, these nations have shown interests towards using renewable sources of energy and other non-fossil fuels based energy sources for balancing and satisfying their energy production and demand. Therefore, it appears that renewable sources of energy such as the generation of electricity by using photovoltaic cell may reduce the danger of an energy crisis in the future. Air conditioning of buildings is an important application of solar energy due to the location coincidence of building cooling loads with available solar power. On the other hand, solar technology for air conditioning of buildings has high installation costs and is not competitive with electricity driven or gas-fired air conditioning

systems in the business. However, solar air conditioning systems can become competitive in the market by lowering the cost of components and improving the performance of the system. The cost of solar air conditioning systems can be reduced by enhancing the performance of the system and reducing the area of solar collectors. Some of the proposed and under development solar driven refrigeration systems are sorption systems including liquid/vapour, solid/vapour absorption, adsorption, vapour compression and photovoltaic –vapour compression systems. Solar thermal technology and cold production technology are two main categories of solar cooling systems. The relevant solar technologies applications require the following components:

- Evacuated tube Collectors
- Flat-plate Collectors
- Photovoltaic cells
- Thermoelectric system
- Stationary non-imaging concentrating collectors
- Dish type concentrating collectors
- Linear focussing collectors
- Solar pond

The cooling technologies relevant are:

- Continuous adsorption
- Intermittent absorption

- Solid/gas absorption
- Diffusion
- Adsorption and
- Desiccant systems

2.2 Cooling Technologies

2.2.1 Single effect absorption air conditioning system

Figure 2.1 shows a schematic diagram of the single-effect solar absorption system. In this system, solar energy is gained through the collector and accumulates in the hot water tank. Then hot water from the water storage tank passes by generator and boils water vapour from a solution of lithium bromide and water. The water vapour cools down in the condenser and passes to the evaporator. In the evaporator, it again evaporates at low pressure providing cooling to the required space. During this time, a strong solution leaving the generator to the absorber passes through the heat exchanger and preheats the weak solution entering the generator. The strong solution absorbs water vapour leaving the evaporator in the absorber. The cooling water removes the heat by mixing and condensation.The heat rejection (cooling water) fluid flows through the absorber first and then to the condenser as the efficiency of the system has a greater influence of the absorber temperature than the condensing temperature. The ratio of heat transfer rate into the evaporator to the heat transfer rate into the generator is the performance coefficient of absorption air conditioning. The coefficient of performance (COP) of absorption systems with different working fluids are compared by Wilbur and Mitchell[69].

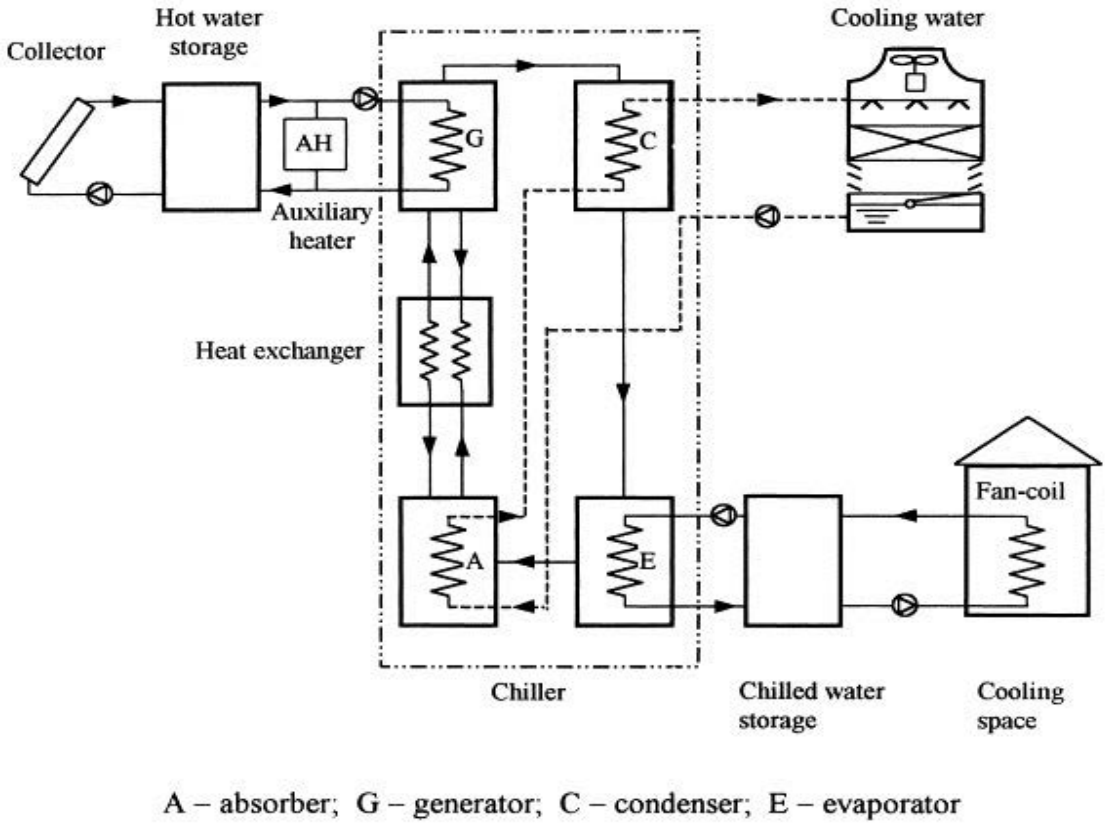

FIGURE 2.1: Schematic diagram of solar powered single-effect air-conditioning system [44]

Depending on the working fluid, absorption systems are divided into two categories. These are $LiBr - H_2O$ and $NH_3 - H_2O$ absorption refrigeration system. In $LiBr - H_2O$ system water is the refrigerant and LiBr is the absorbent whereas in $NH_3 - H_2O$ system water is the refrigerant, and NH_3 is used as the absorbent. The ammonia-water system has some disadvantages over the Lithium Bromide system.

- The coefficient of performance of $H_2O - NH_3$ is lower than $LiBr - H_2O$. The operating range for $H_2O - NH_3$ system is 10-15% lower solar fraction than $LiBr - H_2O$.

- $NH_3 - H_2O$ requires a higher inlet temperature than $LiBr - H_2O$. LiBr- H_2O requires generator inlet temperatures of $70 - 88°C$, while $H_2O - NH_3$ requires temperatures of

90-180°C. Therefore $H_2O - NH_3$ cooling system achieves lower COP using flat plate collectors.

- It requires higher pumping pressure and hence higher pumping power.

It is essential to have hot water storage in a solar absorption air conditioning system. Lof and Tybot[45] have reported that the optimal storage volume is about $50kg/m^2$ of collector area. It suggests that nominal storage amount for cooling purposes range from $80kg/m^2$ of collector area to $200kg/m^2$. A critical problem with a hot water storage tank is heat loss to surrounding.

Wilbur and Mancini[68] have reported that a dry cooling tower can replace the wet cooling tower. The wet cooling tower needs maintenance from average homeowners and uses solar powered absorption coolers for heat rejection. It is a lower performance air heated exchanger and will replace the dry cooling tower. The use of a dry cooling tower in place of the wet cooling tower can reduce the solar fraction by $10 - 20\%$. Therefore a dry cooling tower is recommended over the wet cooling tower as it requires lower maintenance and thus is more acceptable. Pressurised storage can be removed by incorporating a dry cooling tower to remove hot water storage.

Charter and Chen[10] have studied and compared air-cooled and water cooled systems. According to ASHRAE[3] the accepted standard is 35°C dry-bulb used in air-cooled unit and 25°C wet bulb used in water cooled system. The cooling temperature needed is higher in an air-cooled system than a water cooled system. Therefore, pressure is greater in an air-cooled system and that decreases the system COP. The temperature of heat rejection from water cooled system with the cooling tower is related to wet bulb temperature. However, in an air cooled unit the heat rejections from condenser and absorber are related to dry bulb temperature. For water cooled system, evaporator temperature is 5°C and generator inlet temperature is 78°C whereas

for air cooled system the generator temperature rises to $100°C$ for matching conditions. In addition Charters and Chen[10] have conducted experiments with high concentration LiBr, close to crystallization limit of the solution. A sudden temperature drop in the generator could cause crystal formation resulting in the "shutdown" of the system. The air-cooled system is improved by adding some salt such as LiSCN into $LiBr - H_2O$. The Addition of LiSCN can reduce vapour pressure and, therefore, prevent crystallization of the solution at the temperature corresponding to an air-cooled system. The new working fluid uses an air-cooled absorption refrigeration system with the generator temperature still above $100°C$.

Butz et al.[9] presented thermal and economic analysis of solar heated air conditioning systems. Hottel and Whillier[27], Bliss and Klien et al.[8,39] modelled the solar collector and neglected the thermal capacitance of the collector. It showed the output dependence on collector area. For example, annual system efficiency decreases as collector area increases.

Hu[28] modified the above analysis. He simulated the system performance by unsteady heating in the collector including the thermal capacitance of collector components for obtaining useful energy.

Blinn et al.[7] have applied a simulation of the transient model of $LiBr - H_2O$ air conditioner to the residential solar air-conditioning system used in southern United States. System performance degrades on use with on-off thermostat for chiller transient. Increasing the dead band of the thermostat can improve the system performance, frequency of cycling and decrease auxiliary consumption. The solar fraction is highest at lowest source temperature for flat plate collectors. Parallel heat auxiliary led to a larger fraction by solar than series heat auxiliary. Vapour compression yields higher solar fraction than either auxiliary modes and requires less auxiliary power. Chiller capacity and COP are a function of entering hot water and cooling

water temperature and is formulated with performance curves provided by the manufacturer or by experiments.

Munner and Uppal[51] developed a numerical simulation model for a commercially available solar absorption chiller. The model consists of performance data of a Yakazi-manufactured water-cooled system. It consists of a summer season's meteorological data for an arid location, the Sahara desert. Different collector type/areas and storage volumes are used to compute system performance. Their model shows a suitable ratio of collector area and storage volume. It also shows that the cooling water temperature is a function of inlet water temperature to the tower and ambient wet bulb temperature. In the dry conditions of the Sahara very low cooling water temperature are available which shows design load conditions of generator temperature as low as $80°C$.

TRNSYS[64] provides digital simulation of solar cooling systems and models for each part by a subroutine so that each input reference links to each output and each output to the corresponding input of another part.The University College Dublin, of the Commission of the European Community, provides a simulation of solar thermal systems.

Mansoori and Patel[46] have derived upper and lower limits of the coefficient of performance(COP) for absorption cooling cycles through the application of the first and second law of thermodynamics. The limits depend on the environmental temperature of the components of the cycle. They are also dependent on thermodynamic properties of refrigerants, absorbents and their mixtures. The authors perform a quantitative comparative study of different refrigerant-absorbent combinations as $H_2O - NH_3$, $NH_3 + NaSCN$ and $LiBr - H_2O$ with the use of upper and lower limits of COP used in solar absorption cooling cycles.

2.2.2 Adsorption air conditioning system

Figure 2.2 represents the schematics of an air conditioning unit. The system consists of three primary components: a water-cooled unit (the chiller), a tank of cold water, and an air-water heat exchanger(the fan coil). The adsorption chiller consists of two (water adsorber) heat exchangers and a tank of hot water (replenished by solar energy and gas combustion). It also consists of two air condensers, one evaporator and accessories such as valves and circulation pumps. The adsorbers are multi-tubular and have the same configuration as that for the tubes of a shell-and-tube heat exchanger. The adsorbers(I and II) are combined with the storage tanks together with the solar and gas heater to form central cooling systems or the adsorption chiller. The adsorbers(I and II) are responsible for cooling the water in the thermal storage tank. The heat exchange between stored cold water and air entering through the fan coil is used to supply conditioned air. Adsorber I receives methanol vapour from the evaporator at the bottom of the storage tank. Then Adsorber II goes into regeneration mode that characterises the desorption process followed by condensation of methanol in an air condenser. The regeneration of Adsorber II is produced by water heated by highly efficient solar collectors and a gas heater. The release of the heat of adsorption(from adsorber I) is through a secondary water circuit including a sky radiator and storage tank. A hydraulic network feeds the circuit. During the night time, water is cooled by irradiative exchanges with the sky and circulates through the tubes to improve the adsorption process. The electro valves and microcontrollers control the flow of water in the adsorbers. The entering air/cold water exchanger (the fan coil) is the secondary cooling system and is responsible for moving the necessary amount of cooled air to provide thermal comfort conditions inside the room.

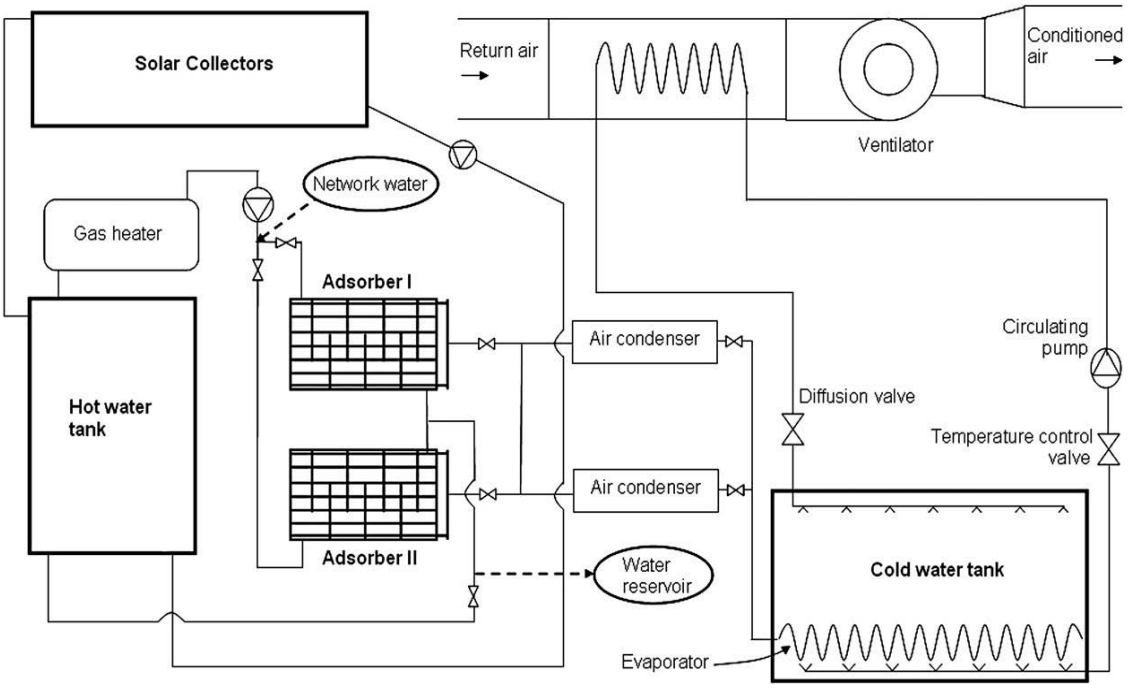

FIGURE 2.2: Schematic Layout of Central Air Conditioning Unit [42]

The adsorbent used for cooling purposes should have high adsorptive capacity at low pressures and ambient temperature and maintain the small capacity of adsorption at high temperatures and pressures. The adsorptive capacity of an adsorbent allows the adsorbent to retain vapours from a fluid at a lower temperature. The required temperature at the evaporator depends on adsorptive capacity under small pressures. On the other hand, the higher adsorptive capacity means higher level temperature for regenerating the adsorbent. The adsorbate is the working or refrigerant fluid that depends on the evaporator temperature. For an easy adsorption, it must possess high latent heat of vaporisation and small molecular dimensions. Since the chiller operates below $0°C$, methanol seems to be a good adsorbate because:

- Its molecules are small ($4 \times 10^{-4}\mu$) and are easily absorbed in micropores, with diameter smaller than $2 \times 10^{-3}\mu m$.

- It can evaporate at temperature mostly below $0°C$ (its melting point is $-94°C$).

- Its enthalpy of vaporisation is high ($1200kJ/kg$, at $-5°C$).
- Its average boiling point ($65°C$) is much higher than room temperature.
- Its working temperature is lower than the atmospheric one, which means a safety factor in the case of leakage.

The adsorbent material is activated carbon because of its close relationship with methanol; the thermophysical properties are those of the AC-35 produced by CECA(France). The activated carbon AC-35 is obtained from pinewood by heating to $95°C$ in the presence of water vapour. It has excellent micropores volume, the space corresponding to 78% of the total volume. The adsorbent bed consists of cylindrical grains of 2 mm diameter and 3 mm long on average. The maximum adsorption capacity of activated carbon methanol pair is about $0.3kg$ of adsorbate/kg of adsorbent. According to experimental studies, the regeneration temperature of the activated carbon AC-35 at this temperature ranges from $65°C$ to $100°C$.

Wang et al.[67] developed an adsorption air conditioning system powered by heat sources with temperatures close to $100°C$. Evacuated tube collectors are used for supplying hot water at this temperature. It has two adsorbers with 26 kg carbon inside each and methanol as the refrigerant. The cycle time of the system significantly influences the COP and SCP of the system. The cycle time of 30 min produced COP of 0.15 and a cooling power of 3.84 kW and a cycle time of 60 min produced a COP of 0.21 and cooling power of 3.03 kW. In both situations, evaporation temperature was close to $6°C$. The authors did several modifications to improve the performance of the system. They changed the adsorbers to a tube and plate heat exchanger keeping the same charge of carbon. In the adsorber carbon is placed outside the tubes, between the plates. The experimental conditions for this case were: a heat source temperature of $100°C$, and evaporation

temperature of $10°C$. It has a condensing temperature of $24°C$ and cycle time of 50 min. This new design has COP of 0.4 and cooling power of 3.80 kW.

Li et al.[43] established a novel model of the combined cycle of solar-powered adsorption-ejection refrigeration system to overcome the intermittent character of a single bed solar adsorption cycle. It has the following operating conditions: condensing temperature $40°C$, evaporating temperature of $10°C$, regenerating temperature $120°C$, and desorbing temperature $200°C$, using zeolite 13x - water as the working pair. The COP of the system is 0.4 under the above conditions.

In-SJTU experiments and performance testing on silica-gel water, 10 kW adsorption chiller has been done. System test is under the following conditions: $85°C$ hot water, chilled water outlet temperature of $10°C$ and cooling water temperature of $30°C$. Under these conditions, system COP reaches 0.4 and confirms that the adsorption chiller is efficient for refrigeration. Also, it is efficiently driven by a low-grade heat source. This silica-gel-water adsorption chiller has been commercialised and used in a green building project in Shanghai, solar cooling for green storage and also micro-CCHP systems.

Nunez et al.[52] developed and tested a silica-gel-water adsorption chiller with the nominal cooling power of 3.5 kW. It had two adsorbers, each one filled with 35 kg of adsorbent. The chiller operated at generation temperatures between 75 and $95°C$, heat sink temperatures between 25 and $35°C$ and evaporation temperature ranging between 10 to $20°C$. The COP varied between 0.4 and 0.6 according to experimental conditions. The author also compared the performance of the chiller to the performance of the Nishiyodo NAK 20/70 adsorption chiller and to Yasaky WFS SC-10 adsorption chiller. The figures of merit compared COP and cooling power density at different reduced temperatures.

Restuccia et al.[56] developed an adsorption chiller that employed silica gel impregnated with $CaCl_2$ as sorption material. The high sorption ability of up to 0.7 kg of water per kg of dry sorbent is the adsorbent and most of the water content desorbs at generation temperature between 90 and 100°C. The COP of the chiller is close to 0.6 when the condenser temperature is 35°C and generation temperature ranges from 85 to 95°C. It varied between 0.3 and 0.4 for condensation temperature of 40°C. The evaporation temperature during these experiments was 10°C. The SCP was 20 W/kg at generation temperature of 95°C and condensing temperature of 40°C.

2.2.3 Desiccant air conditioning system

The desiccant air conditioning system consists of the liquid desiccant cooling system and vapour compression heat pump as shown in figure 2.3. Absorber, regenerator, solution heat exchanger, compressor, and expansion valve are some of the components of the desiccant air conditioning systems. The absorber (or regenerator) integrates with the evaporator (or condenser) of the compression system. The evaporator of the system corresponds to a fin tube type heat exchanger. The refrigerant flows through tubes and solution supplied from spray tubes falls along the fin surface. The air flows up through between the fins in the opposite direction of solution flow. In the absorber, both solution and process air are cooled by evaporation of the refrigerant and air is dehumidified by direct contact with falling solution film. The regeneration air and solution heats by condensation of refrigerant and solution regenerate by direct accumulator contact with air. The heat exchange between hot regeneration side solution and cool process side solution occurs in the heat exchanger. The refrigerant vapour which flows out of the evaporator is compressed in the compressor and goes to the condenser. From the condenser, the refrigerant flows through the expansion valve and then into the evaporator. The

refrigerant from the evaporator returns to the system. The refrigerant vapour flows out of the compressor through the accumulator.

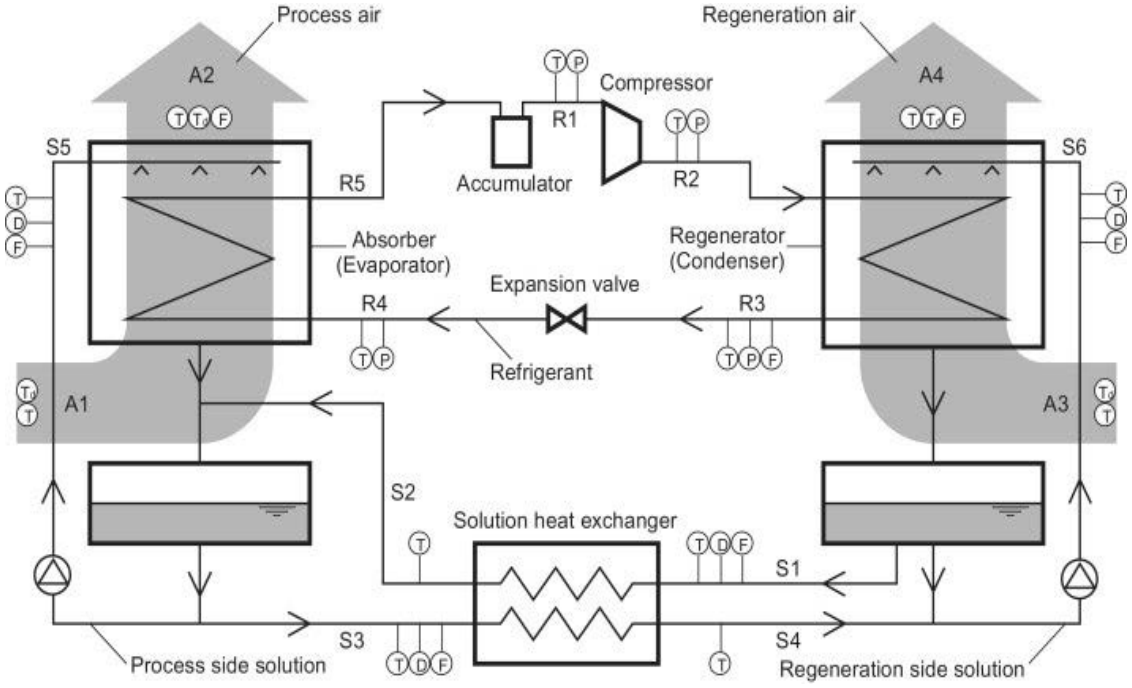

FIGURE 2.3: Schematic Diagram of hybrid liquid desiccant air-conditioning system [70]

The desiccant is a natural or synthetic substance capable of absorbing or adsorbing water vapour due to the difference of water vapour pressure between surrounding air and desiccant surface. They are in both liquid and solid states and both systems have their advantages and disadvantages. Liquid desiccants have the benefits of having lower regeneration temperature, flexibility in the utilisation and lower pressure drop on the airside. Solid desiccants are less subject to corrosion. Some examples of desiccant materials are lithium chloride, triethyl glycol and silica gels.

Another desiccant process uses a slowly rotating wheel coated with desiccant with part intercepting the incoming air stream and the rest being regenerated. Another arrangement uses packaging of solid desiccants to form adsorbent beds exposed to the incoming air stream thus taking up its moisture. These beds are moved periodically in the regeneration air stream

direction and returned to the process air stream. Liquid desiccants are sprayed into air streams or wetted into contact surfaces to absorb water vapour from incoming air. Liquid desiccants regenerate in a regenerator in a similar way to solid desiccants. Heating evaporates the water vapour that is absorbed previously out from the liquid desiccants.

Jain et al.[31] investigated four cycles (ventilation cycle, the recirculation cycle, the Dunkle Cycle and wet surface heat exchanger cycle) for various outdoor conditions as dry-bulb temperature and wet-bulb temperature of many cities in India. He evaluated the effect of heat exchangers and evaporative coolers on the cooling coefficient of performance (COP) and air volume circulation rate in different climatic conditions. However the cycle using the wet surface featured the best performance with respect to the other three cycles.

Two feasibility studies of solar desiccant cooling in different climatic zones of European Cities were conducted by Mavroudaki et al.[48] and Halliday et al.[21]. The regeneration of desiccant in high humidity climates is possible in high temperature and produces less energy savings.

Alizadeh et al.[2] designed, optimised and constructed a prototype of a forced-flow solar collector/ regenerator. They used an aqueous solution of calcium chloride as desiccant and studied the effect of parameters such as air and desiccant solution flow rate as well as climatic conditions on the regenerator's performance. The rate at which it removed water vapour from the weak desiccant solution measured the performance of regenerator. Therefore, it concludes that the performance of the regenerator increased as the air flow rate increased. The solar collector efficiency increased with the increase of air mass flow-rate. The maximum efficiency can be predicted by the value of the air flow rate.

Dai et al.[11] conducted a comparative study of a standalone vapour compression system, a

desiccant-associated vapour compression system and a desiccant and evaporative cooling associated vapour compression system. The authors found an increase of cold production by $38.8 - 76\%$ and of COP by $20 - 30\%$.

Mazzei et al.[49] used a computer simulation tool for comparing operating costs of desiccant and traditional systems. He predicted operating cost savings of 35% and thermal power reduction of up to 52%. He predicted operating cost savings to reach 87% where the desiccant regenerates by waste heat. The cost savings and cooling power reductions increase when using indirect evaporative cooling with desiccant dehumidification. The savings on operating costs depend on local electricity costs and varies from one country to another, even within the same country.

Henning et al.[26] conducted the parametric study of combined desiccant/chiller solar assisted cooling systems and showed not only feasibility but also primary energy savings of 50% with low increased overall costs.

Shen et al.[59] studied desiccant cooling systems and used molecular sieve 13xdesiccant wheel as an adsorbent. He also simulated water vapour and carbon dioxide removal from process air. The author conducted an optimisation study involving coefficient of performance, the temperature of desorption, the overall number of transfer units and the adsorption time.

Techajunta et al.[63] simulated solar energy in which incandescent electric bulbs were used to simulate solar energy. He used silica gel as adsorbent and also studied its regeneration with simulated solar energy. The regeneration rate from silica gel adsorbent depends on solar radiation intensity while its dependence on air flow rate was found to be weak.

Sanjev et al.[32] studied a liquid desiccant cooling system made of falling film tubular absorber and falling film regenerator and did the theoretical and experimental investigation of the cooling

system. The authors defined the wetness part to distinguish the uniformity of wetting of the surface of the dehumidifier and regenerator by the desiccant solution. He used it for performance evaluation of the desiccant cooling system. The study of the wetness factor helps designing viewpoint and contributes the calculation of the size of the contractors.

Kadoma et al.[17] investigated the impact of desiccant wheel speed, air velocity and regeneration temperature on the COP. The author showed that an optimal speed exists and found that COP decreased as air flow rate increased and, on the other hand, the temperature of regeneration and cooling capacity has the same evolution tendency.

Shyi-Min et al.[60] reported a passive desiccant-cooling scheme operating according to the sequence of diurnal and nocturnal natural cycle. The concept used in the system is of desiccant enhanced nocturnal radiation cooling and dehumidification (DESRAD). He reported on a standalone solar desiccant radiant cooling(SDRC) system inherited from DESRAD.

Fatah et al.[12] studied a solar energy driven $LiBr - H_2O$ adsorption cooling machine called heat recovery system. The heat adds to driving solar power after recovering from the condenser of the machine. The coefficient of performance of the system increases to 1.2 times and hence was 58% higher than adsorption machine alone. Also, the temperature of the evaporator was raised from 11.5 to 19.3$^{\circ}C$.

Arshad [36] studied a mathematical model of the liquid absorber(dehumidifier). The study increased the performance by increasing the number of transfer units (NTU) of heat transfer between process air and desiccant solution. NTU determines the size of the absorber.

Adam[38] conducted a simulation study on a desiccant cooling system using an aqueous solution of $CaCl_2$ as the liquid desiccant. He studied the impact of desiccant solution's inlet temperature,

the space sensible heat ratio (SHR), heat exchanger effectiveness and ratio of liquid desiccant flow rate to the air flow rate(G_L/G_a).

2.2.4 Single effect hot water absorption chiller system

Figure 2.4 is a schematic representation of absorption chiller system. In the $LiBr - H_2O$ system, lithium bromide is the absorbent and water is the refrigerant. The necessary condition for boiling of water at low temperature is created by pumping of the chiller into a deep vacuum. The refrigerant vapour is attracted to absorber by a difference between lithium bromide solution and refrigerant water. They are absorbed by concentration of lithium bromide solution and performing continuous boiling of the refrigerant water. In the hot water operated chiller, the diluted solution in the absorber is pumped into the generator via a solution pump. The diluted solution concentrates into the concentrator when heated by hot water. The refrigerant vapour generated is condensed into water in the condenser. The refrigerant water enters the evaporator and pumps to the spray through the spraying device using the refrigerant pump. Heat transfer from the air-handling unit water to refrigerant causes refrigerant water to vaporise again, producing chilled water. Finally, chilled water is pumped to the air-handling unit producing cooled air for the building. On the other hand, the concentrated solution from the generator directly enters the absorber and repeats the cycle.

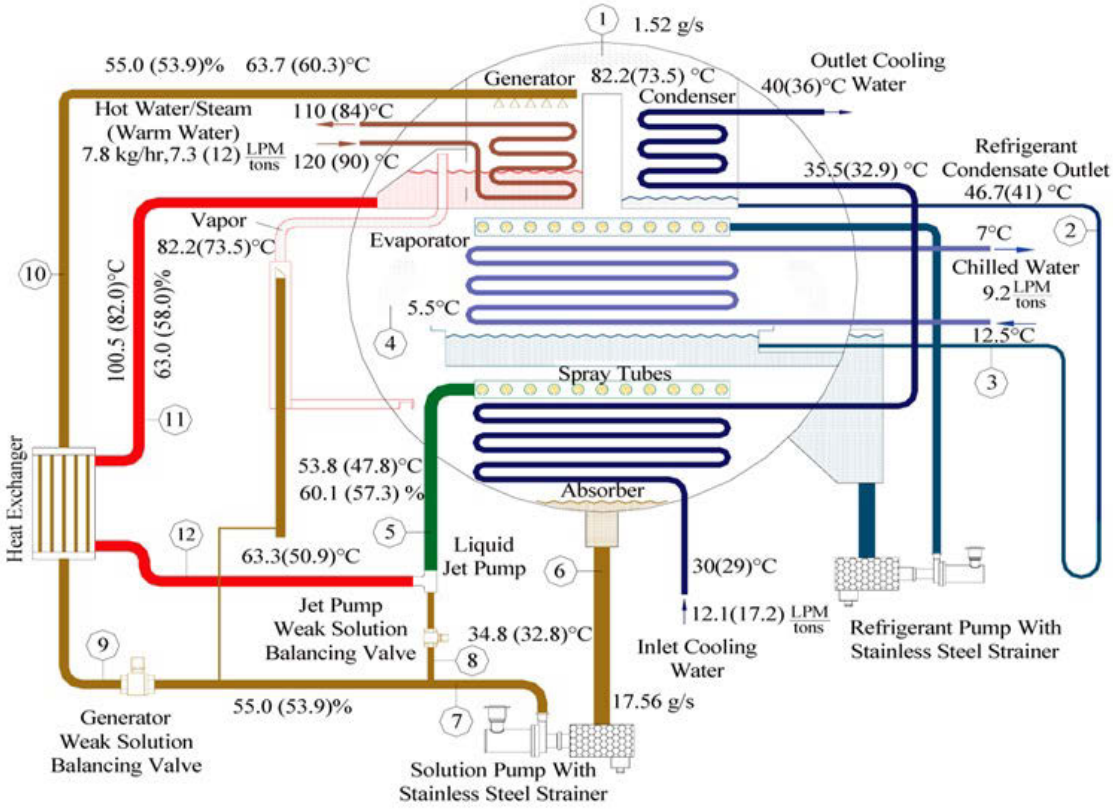

FIGURE 2.4: Single effect hot water absorption chillers actual cycle

Florides et al. [14] studied solar absorption cooling system for weather conditions of Nycosia, Cyprus using TRNSYS simulation program. A system optimisation was used to select appropriate solar collector, optimum storage tank size, collector slope and area. Two thermostat setting of the auxiliary boiler is used to choose these components. The final optimised system consists of 15 m^2 compound parabolic solar collector tilted by 30° from the horizontal and 0.6 m^3 hot-water storage tank.

Atmaca and Yigit [5] developed a modular computer program for a solar powered single stage absorption cooling system using lithium bromide-water solution as the working refrigerant. They inspected different cycle setups and solar energy parameters at Atlanta, Turkey. They studied the impact of hot water inlet temperatures on the coefficient of performance (COP) and

surface area of absorption cooling components. The increase in reference temperature decreases absorber surface area and heat exchanger surface area. Also, the system COP increases on the increase of the reference temperature. Atmaca and Yigit [5] showed evacuated, selective surface solar collector as the best option for the efficient operation of a solar-powered absorption cooling system. They showed that a solar-powered absorption cooling system required high-performance solar collectors.

Florides et al. [13] evaluated characteristics and performance of a single stage LiBr-water absorption machine. They used a computer program to input heat and mass transfer equations including working fluid properties. The sensitivity analysis showed that the difference between inlet and outlet concentrations of LiBr-water solution at the absorber reduces mass flow rate. The LiBr-water absorption cooling system has a high price compared to an electrical chiller of similar capacity. The electric chiller uses the electrical power produced from fossil fuels. However the absorption system uses renewable energy sources and waste heat.

Assilzadeh et al. [4] studied a solar absorption cooling system designed for the Malaysia climate and similar tropical regions using TRNSYS numerical simulations. They used Lithium bromide-water mixture as working fluid and evacuated tube solar collector as energy input to absorption cooling system. They showed that an evacuated tube collector provides high cooling performance at high temperature due to high efficiency under this weather condition. The cooling capacity of the system is significant during periods of high solar radiation energy. The author suggests that the reliability of the 3.5 kW system consisting of 35 m^2 evacuated tube solar collectors at slope 20° is increased by using a 0.8 m^3 hot-water storage tank in Malaysia's weather conditions.

Sayegh [58] investigates an absorption cooling system powered by solar energy with the use of a thermal storage tank, auxiliary heater and flat plate collector for weather condition of Aleppo,

Syria. The computational program prepared investigates effects of varying generator temperature between 80 to 100°C, and evaporator temperature between 5 − 15°C on the coefficient of performance (COP) and solar heat gain of absorption cooling system. Higher COP values are obtained by increasing generator temperature and temperature drop of the evaporator.

Balghouthi et al. [6] used TRNSYS and EES software using meteorological data file under climatic conditions of Tunis, the capital of Tunisia for selecting and sizing different installed solar systems. The system is optimised for a LiBr absorption chiller of capacity 11kW and building area of 150 m^2. The optimised system involves 30 m^2 flat plate collector area tilted by 35° from the horizontal and 0.8 m^3 hot-water storage tank.

Mateus and Oliviera [47] used a solar absorption cooling and heating system for building applications. Different buildings like residential, office and hotel from different locations and climates from Berlin, Lisbon and Rome, were studied for their research. The model ran for the whole year according to control rules of heating or cooling with combining cooling, heating and domestic hot water applications. The author concludes that residential house and hotel buildings have higher economic feasibility for solar vacuum tube collectors compared to the flat plate collectors. Conversely, flat plate collectors are more economical than vacuum tube collectors. The initial costs of the absorption chiller and solar collectors reduce for increasing market potential for integrated solar systems. The city of Rome achieved break-even situation for current energy costs. Their results show a reduction in solar collector area between 15 to 50% by using solar absorption cooling and heating systems.

2.2.5 Modelling methods for single effect hot water absorption chiller system

The literature review in this section provides insight into different modelling methods for single effect hot water absorption chiller system in Chapter 5. There are two kinds of models: mechanistic and empirical. The mechanistic process provides insight into the physical process or system while the empirical model provides the shape of the dataset for the observed model of the system. Researchers of absorption chillers use both mechanistic, and empirical approaches and these are present in the literature. Various authors report mechanistic or thermodynamic models. Joudi and Latfa [33] used the thermodynamic model of the $H_2O - LiBr$ absorption system using heat and mass transfer relationships for cycle components. Similarly, Kaynakli and Kilic [34] did a theoretical study on the performance of a $H_2O - LiBr$ absorption system. The influence of operating temperature and heat effectiveness on thermal loads of components and COP are investigated using thermodynamic analysis of the absorption cycle. Silverio and Figueiredo [61] used thermodynamic analysis for the steady-state simulation of the ammonia-water absorption system. The solution algorithm using the Substitution Newton-Raphson method used thermodynamic state relations and equations for solving pressure drops and heat transfer coefficients. Grossman and Zaltash [19] developed the modular simulation tool ABSIM, which investigates various absorption cycle configurations working with different fluids. ABSIM calculates internal state points and thermal load of components based on user-supplied cycle diagram, working fluid specification and given operating conditions. It is enabled through subroutines that contain governing equations for each component of the cycle. Garimella et al. [16] used ABSIM model to evaluate the performance of a Generator Absorber heat exchanger (GAX) heat pump. The thermodynamic modelling consists of input parameters such as heat transfer coefficients (U), heat transfer areas (A) of heat

exchangers and working fluid properties. Simple models provide good representation of absorption machine behaviour based on external parameters like experimental measurements or manufacturer catalogue data. Simple models can be used in simulation programmes or used for fault detection and control. The empirical and non-empirical model require less time and effort to develop and computation time is shorter compared to mechanistic models. The fitting coefficients of the models are found using regression method or minimising algorithms applied to the data set obtained from the manufacturer catalogue or experimental measurements. Several authors report the development of the empirical model for absorption equipment. Gordon and Ng [18] developed the model for predicting absorption chiller performance. The model employs both physical and empirical models. The physical principle predicts the performance of an absorption chiller fitted to experimental or manufacturer data using regression method. Ziegler and co-authors [25] predict the performance of an absorption chiller by two simple algebraic equations: one for cooling capacity and another for driving heat input. The literature review shows a gap in comparative studies on different modelling techniques for predicting absorption equipment performance. The studies evaluate the capability of models to predict energy performance.

2.2.6 Energy optimisation for single effect hot water absorption chiller system

The literature review in this section provides insight into energy optimisation for single effect hot water absorption chiller system in Chapter 6. A chiller plant provides cooling through chilled water to a building. Figure 4.2 is a schematic diagram of the chiller plant. The condenser cycle consists of chiller condensers, pumps, cooling towers and fan. The major components of the chilled water cycle are chiller evaporators and chilled water pumps. The ratio of electric

power consumed by load demand indicates the performance of a chiller plant. A chiller plant consumes electricity from 10% to 50% of total energy consumption (DOE 2003). Many researchers in the literature (Chang 2007, Beghi et al. 2011, Ma and Wang 2011, Sun and Reddy 2005, Arimante et al. 2000) consider energy conservation and optimal control of chiller plants. Some of the studies focus on individual component efficiency and others on targeted partial systems. Some of the research focuses on the condenser cycle (Braun and Doderrich 1990, Kirsner 1996) while other research focuses on chilled water loop (Olson and Liebman, 1990, Chang 2007). Most chiller plants are controlled manually or automatically by adjusting temperature or pressure settings (Ostendorp 2010). The chiller consumes a significant fraction of the power and is the most expensive component in a chiller plant. Therefore, optimising the performance of the chiller is necessary for power and cost savings. Hartman 2001 has done significant work in this area with the promotion of variable-speed drive chillers, pumps and cooling tower fans. This work is followed by Yu and Chan (2009) and Zheng and Wang (2009). The optimisation and control of a chiller plant are classified as enumeration-based and simulation-based methods. Bellenger and Becker 1996, Avery 2001 performed enumeration-based optimisation based on simulation of monitoring on performance map of the system. This process does not involve a mathematical optimisation technique. Avery (2001) suggests ways to improve accepted and practised primary/secondary cycle systems. His work shows that physical changes to the plant, such as installing temperature and pressure sensors and valves increases the efficiency of the plant. Bellenger and Becker (1996) developed a spreadsheet-based chiller optimisation model using manufacturer's data. It uses selecting cost-efficient chiller based on chiller performance data, cooling tower and pumping systems. Hydeman and Zhou(2007) use a parametric analysis technique to optimize the control sequence of chilled water plants. Morris and Blaine (2008) creates a spreadsheet-based optimisation tool

for the chiller plant. Modelling interaction between components consider the plant's response to load and outside air. A set of look-up tables are formed to help operators run the plant efficiently. This study involves no optimisation technique and is a basic model. The simulation-based method uses system optimisation theory with mathematical formulations. Olson and Liebman (1990) solves the chiller plant problem using the heuristic search and sequential quadratic programming (SQP). This study focuses on the optimisation problem based on the sequence of operation of the equipment but not on the performance levels of equipment. Later, Sun and Reddy (2005) use the SQP-based method to design optimal heating and cooling systems for buildings. The study uses a two-stage optimisation approach for the chiller plant. Lu et. al. (2004, 2005) studies global optimisation of heating, ventilation and air conditioning (HVAC) system. The work modifies the basic chiller plant model by Stoecker (1975) and shows component interactions. Ma and Wang (2011) uses the genetic algorithm to present a model-based optimal control strategy. System performance is predicted using simplified models based on recursive least squares estimation. Beghi et al.(2011) studies multiple chiller management for dynamic loading. The optimal chiller loading and sequencing problem are solved simultaneously by multi-phase genetic algorithm model. Chang et al. (2005) solves the optimal chiller sequencing problem using branch and bound and Lagrangian method of optimisation.

2.3 Opportunities for further research

On the basis of above literature survey in (section 2.2) it is felt by the authors that there is scope for doing further research in this field. The different possibilities are briefly discussed below:

2.3.1 Solar absorption air conditioning system

All solar absorption air conditioning systems use an ordinary flat plate or evacuated tubular solar collector readily available in the market. The performance of absorption air conditioning systems can increase by using new types of solar collectors.

The performance of air conditioning systems can increase by using horizontal N-S parabolic trough collectors with a minimum required collector area of 57.6 m^2. It is used for meeting peak cooling load of 17.5 kW solar energy, and also solar energy can be absorbed and stored in thermal storage tanks. Horizontal N-S parabolic trough collectors meet cooling load demands during the day and store solar energy for use after sunset.

Concentrating photovoltaic collectors operate at a higher temperature than flat plate collectors. The rejected heat collected from the CPV system leads to CPV/thermal systems providing both heat and electricity at high temperatures above $100^{\circ}C$ and can drive processes such as refrigeration, desalination and steam production.

For all weather conditions, it is necessary to install auxiliary power systems to supplement solar-powered cooling systems. These systems use a gas-fired auxiliary boiler for supplying auxiliary power at times when solar radiation is scarce. The combination of gas-fired heater and single stage absorption chiller are less efficient than traditional electric-driven compression systems.

The former uses 1.7 kWh of primary energy to produce 1 kWh of cooling power whereas the latter needs 0.7 kW. Thus a gas fired heater can be used when auxiliary power supplied is low. Auxiliary power systems for solar cooling systems are a better option of clean energy or renewable energy.

The wet cooling tower has a higher COP than the dry cooling tower, but a dry cooling tower can be selected to avoid problems of Legionella in wet cooling towers. The solar cooling system consists of $37.5m^2$ of flat plate collectors, 4.5 kW single-effect $LiBr - H_2O$ absorption chiller and a dry cooling tower. The geothermal system improves the performance of the absorption chiller. COP of the chiller is improved to 42% for geothermal systems compared to air cooled systems.

2.3.2 Solar adsorption air conditioning system

Solar adsorption air conditioning systems can be designed for environmental benefits of replacing CFCs and HCFCs and can be more efficient than current systems. The most important design aspect to be studied is the coupling of the heat exchanger to other components such as evaporator and condenser. One proposal for this study is using adsorbent bed container as evaporator-condenser heat exchanger surface. In this the vapour paths are very short and refrigerant vapour can move in a straight line to the condensing surface and vice versa and, as a result, small drops occur on the vapour side. A cheaper system can be obtained by reducing the volume of evaporator and condenser components. Another proposal for this study uses external evaporator and condenser that are connected with the reactor and uses valves between each part. Another machine design solution involves suitable materials for each part as plastics, aluminium, stainless steel and copper.

Adsorption cooling is possible for air conditioning, process cooling, etc. using chiller capacity and lower temperature heat source for waste heat and solar energy. The existing chilling capacity increases without increasing electricity consumption.

The solid sorption commercial chiller uses Silica gel. One of the disadvantages of using solid sorption compared with liquid sorbent systems are their needs to store sorbent and consequently heat or cold.

One can store the energy of collected sunlight as ice. Ice storage can offer compactness, safety and low expenses. Temperatures at night allow for efficient cooling, but some heat sink capacity has to be saved for daytime. A water storage chilled by night time is a solution to this problem.

The length of the cycle is an important parameter affecting the operation of gas-solid systems. Rotating systems applications use typical values of a few minutes whereas 1-3 h cycles operate in the plant using 150 kg of zeolite in two 'isothermal' reactors. A multibed system with internal heat recovery uses short cycles.

2.3.3 Solar Desiccant Air Conditioning System

Some research and development efforts for desiccant air conditioning system are

- Solving basic problems of the system like avoiding corrosion of the system and plant components.
- Improving transport processes in contacting columns such as absorber and desorber at partial load.

- Combining open liquid absorption systems with conventional refrigeration to reduce defrosting energy costs for example food preservation and transport.
- Combining open liquid absorption systems with conventional air conditioning systems to reduce or even eliminate the load on the chiller.
- Combine open liquid absorption systems with mobile air conditioning systems to reduce CO_2 emissions due to operation of such systems in cars, buses and trucks.
- Developing no chiller, no cooling tower air handling units.

2.3.4 Single effect hot water absorption chiller system

The Lithium bromide-water mixture as working fluid shows good performance for the solar absorption cooling systems. Future work involves studying the performance of solar absorption cooling systems using different types of mixtures for optimum cooling performance. The physical data of the system should produce the design specifications for each component of the system that is generator, evaporator, condenser and absorber. It results in the number of tubes of the heat exchanger. The coefficient of performance of the system varies with overall heat transfer coefficients of the heat exchanger.

Chapter 3

Calculating cooling load of the lift motor room

3.1 Introduction

In this chapter, the example of the lift motor at the top of UTS building 2 is illustrated for calculating cooling load by the cooling load temperature difference method and the radiant time series method. A cooling load calculation method determines sensible cooling load due to heat gain through structural components (walls, roofs, ceilings); through windows; infiltration and ventilation; and due to occupancy. The latent portion of the cooling load is evaluated separately. In this example measurements involving length, width and height of the lift motor room are taken for calculating the cooling load of the room. These dimensions are used to calculate the cooling load of the lift motor room by the cooling load temperature difference and radiant time series method. Radiant time series replaces cooling load temperature difference/ solar cooling

load / cooling load factor (CLTD/SCL/CLF) methods for calculating cooling load. Radiant time series estimates conductive heat gain on 24-term response part series and instantaneous radiant heat gains on 24-term "radiant time series" for calculating cooling loads. This chapter describes the radiant time series method and generation of response factors and radiant time series coefficients and gives a brief comparison with the CLTD method.

3.2 Cooling Load temperature difference/ Cooling Load Factor/Solar Cooling Load Calculation Method

3.2.1 Introduction

ASHRAE Cooling and Heating Load Manual in 1979 first introduced the Cooling Load temperature difference method. The sizing of HVAC equipment is done using total heat gain through building from the Cooling Load temperature difference method.The error in using the cooling load temperature process is less than twenty percent of peak cooling load and less than ten percent of least cooling load. The cooling load temperature difference method simplifies the cooling load calculation process by predetermined data. Different sections depending on different variables divide the data for the cooling load temperature difference method. These variables include orientation of the surface (e.g. walls or roof, 90 or 180 degrees), wall face orientation (N, NW, S, SE, etc.), building material of the envelope, thickness of building materials and time of day. The table of data was developed by using more complex transfer function method to determine various cooling loads for different types of heating.

3.2.2 Process for Calculating Cooling Load

The law of heat conduction also known as Fourier's Law, states that time rate of heat transfer through a material is proportional to the negative gradient in the temperature and to the area, at right angles to the gradient through which heat flows. This law is stated in integral form in which we look at the amount of energy flowing into or out of the body as a whole.

3.2.2.1 Integral form

By integrating the differential form over the material's total surface S, one can arrive at integral form of Fourier's Law:

$$\frac{\partial Q}{\partial t} = -k \oint_S \vec{\nabla} T \, d\vec{A},$$

$\frac{\partial Q}{\partial t}$ is the amount of heat transferred per unit time (in W),

$d\vec{A}$ is the oriented surface area element (m^2).

$$\frac{\Delta Q}{\Delta t} = -kA\frac{\Delta T}{\Delta x}, \tag{3.1}$$

where

A is the cross-sectional surface area,

ΔT is the temperature difference between ends,

Δx is the distance between the ends.

ΔT is the difference between outside surface temperature and inside surface temperature for the material of heat transfer.

$\Delta T = T_o - T_i$,

T_o = Outside surface temperature of material (K or $^\circ C, ^\circ F$) ,

T_i = Inside surface temperature of material (K or $^\circ C, ^\circ F$) .

3.2.2.2 Conductance

$$U = \frac{k}{\Delta x},$$

where U is the conductance, in W/(m^2K).

Fourier's Law can also be stated as

$$\frac{\Delta Q}{\Delta t} = UA(-\Delta T). \tag{3.2}$$

In a multilayer partition, the total conductance is related to conductance of its layers by,

$$\frac{1}{U} = \frac{1}{U_1} + \frac{1}{U_2} + \frac{1}{U_3} + \ldots\ldots\ldots$$

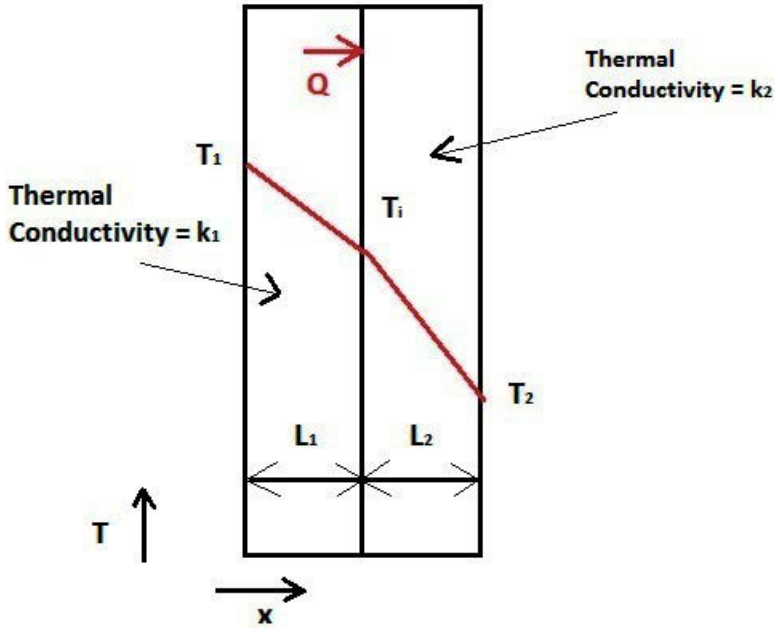

FIGURE 3.1: Heat transfer by conduction across composite wall

3.2.3 Calculating cooling or heating load of lift motor room

The cooling load for the lift motor room at the top of UTS building 2 calculated from ASHRAE Handbook 1997 Fundamentals[53].

3.2.3.1 Dimensions and area of lift motor room walls and roof

Height = H = 6.00 m

Length = L = 4.00 m

Width = W = 6.00 m

Roof area for the room = A_r =344.45 ft^2 = 24 m^2

Area of front wall facing North = A_{wn} =387.5 ft^2 = 36 m^2

Area of side wall facing East = A_{we} =344.45 ft^2 = 24 m^2

3.2.3.2 Sydney Outdoor design conditions

Location: 33.95°S 151.18°E

Outdoor design dry-bulb: 102.74°F = 39.3°C

Outdoor design wet-bulb: 74°F = 23.33°C

Indoor design dry-bulb: 78°F = 25.56°C

Daily Range: 12°F = 6.66°C

Relative Humidity: 50%

Wind Velocity: 2.5 mile

3.2.3.3 CALCULATIONS

Calculation of CLTD Correction:

$$\begin{aligned} CLTD_C &= [CLTD + (78 - TR) + (TM - 85)] \\ TR &= \text{Inside design temperature= } 78^\circ F = 25.56^\circ C \\ TM &= \text{mean outdoor temperature} \\ &= \text{Outdoor design dry bulb temperature}-\text{(Daily range/2)} \\ TM &= 102.74 - (12/2) = 102.74 - 6 = 96.74^\circ F = 35.97^\circ C \\ CLTD_C &= CLTD + (96.74 - 85) = CLTD + 11.74 \end{aligned} \tag{3.3}$$

3.2.4 Cooling Load Due to Heat Gain Through Structures

Cooling load temperature differences (CLTDs) method calculates sensible cooling load due to heat gain through walls, floors and ceilings of the lift motor room. It calculates cooling load using Table 1 and 2 from ASHRAE Handbook 1997 and U factors using summer conditions. Table 2 provides the variable of the mass of the walls. Daily range such as outdoor temperature swing on a design day affects equivalent temperature difference. Table 1 and 2 represents daily temperature ranges classified as high, medium and low. Table 1, 2 and 3 in Chapter 26 describe outdoor daily ranges of dry bulb temperature for different locations. Table 11 of Chapter 28 of ASHRAE Handbook 1997 is used to find U-Values for roofs and walls.

3.2.4.1 Roof

Table 11 of Chapter 28 of ASHRAE Handbook 1997 is used to find U-Values for roofs.

TABLE 3.1: R value for Roof

Roof Components	R Value(W/m^2K)
Inside Surface Resistance	0.121
70mm Insulation	1.584
Outside surface Resistance	0.059
Total	1.764

U_r = 0.566893 W/m^2K,

U_r = 0.099 $Btu/hft^{2\circ}F$.

Table 31 of Chapter 28 of ASHRAE Handbook 1997 is used to find roof numbers for Cooling load temperature difference calculation.

Roof Number 10

Table 30 of Chapter 28 of ASHRAE Handbook 1997 is used to find Cooling load temperature difference for 24 hours based on roof numbers.

TABLE 3.2: Cooling Load through Roof

Time of Day	CLTD	$CLTD_C$	Q(Btu/hr)	Q(kW)
9	28.8	40.54	1036.81	0.3039
10	45	56.74	1451.13	0.4253
11	59.4	71.14	1819.41	0.5332
12	73.8	85.54	2187.69	0.6411
13	82.8	94.54	2417.87	0.7086
14	88.2	99.94	2555.97	0.7491
15	88.2	99.94	2555.97	0.7491
16	82.8	94.54	2417.87	0.7086
17	73.8	85.54	2187.69	0.6411
18	59.4	71.14	1819.41	0.5332
19	34.2	45.94	1174.92	0.3443
20	25.2	36.94	944.74	0.2769
21	14.4	26.14	668.53	0.1959
22	9	20.74	530.43	0.15545
23	5.4	17.14	438.36	0.1285
24	1.8	13.54	346.29	0.10149
1	0	11.74	300.25	0.0880
2	-1.8	9.94	254.22	0.07450
3	-3.6	8.14	208.18	0.0610
4	-5.4	6.34	162.15	0.0475
5	-5.4	6.34	162.15	0.0475
6	-5.4	6.34	162.15	0.0475
7	0	11.74	300.25	0.880
8	12.6	24.34	622.50	0.1824

Equations:

$$\begin{aligned} Q_r &= U_r\, A_r\, CLTD_C \\ U_r &= 0.566893\ W/m^2K \\ A_r &= 24\ m^2 \end{aligned} \tag{3.4}$$

3.2.4.2 Wall Facing North

Table 11 of Chapter 28 of ASHRAE Handbook 1997 is used to find U-Values for walls.

TABLE 3.3: R Value for Wall

Wall Components	R Value(W/m^2K)
C4 160mm Common Brick	0.279
Total	0.279

U_{wn} =3.584 W/m^2K,

U_{wn} =0.6311 $Btu/hft^2{}^\circ F$.

Table 33B of Chapter 28 of ASHRAE Handbook 1997 is used to find wall numbers for Cooling load temperature difference calculation.

Wall Number 3

Table 32 of Chapter 28 of ASHRAE Handbook 1997 is used to find Cooling load temperature difference for 24 hours based on walls numbers.

Table 3.4: Cooling Load through Wall facing North

Time of Day	CLTD	$CLTD_C$	Q(Btu/hr)	Q(kW)
9	7.2	18.94	4631.81	1.3575
10	7.2	18.94	4631.81	1.3575
11	10.8	22.54	5512.20	1.6154
12	14.4	26.14	6392.59	1.8735
13	16.2	27.94	6832.78	2.0025
14	19.8	31.54	7713.17	2.2605
15	23.4	35.14	8593.55	2.5185
16	23.4	35.14	8593.55	2.5185
17	25.2	36.94	9033.75	2.6475
18	25.2	36.94	9033.75	2.6475
19	27	38.74	9473.94	2.7765
20	23.4	35.14	8593.55	2.5185
21	19.8	31.54	7713.17	2.2605
22	16.2	27.94	6832.78	2.0025
23	12.6	24.34	5952.39	1.7445
24	10.8	22.54	5512.20	1.6155
1	7.2	18.94	4631.81	1.3575
2	5.4	17.14	4191.62	1.2284
3	3.6	15.34	3751.43	1.0994
4	1.8	13.54	3311.23	0.9704
5	1.8	13.54	3311.23	0.9704
6	0	11.74	2871.04	0.8414
7	1.8	13.54	3311.23	0.9704
8	5.4	17.14	4191.62	1.2284

Equations:

$$\begin{aligned} Q_{wn} &= U_{wn}\, A_{wn}\, CLTD_C \\ U_{wn} &= 3.584\ W/m^2K \\ A_{wn} &= 36\ m^2 \end{aligned} \tag{3.5}$$

3.2.4.3 Wall Facing East

Table 11 of Chapter 28 of ASHRAE Handbook 1997 is used to find U-Values for walls.

TABLE 3.5: R Values for Wall facing East

Wall Components	R Value(W/m^2K)
C4 160mm Common Brick	0.279
Total	0.279

U_{we} =3.584 W/m^2K,

U_{we} =0.6311 $Btu/hft^{2\circ}F$.

Table 33B of Chapter 28 of ASHRAE Handbook 1997 is used to find wall numbers for Cooling load temperature difference calculation.

Wall Number 3

Table 32 of Chapter 28 of ASHRAE Handbook 1997 is used to find Cooling load temperature difference for 24 hours based on walls numbers.

Table 3.6: Cooling Load through Wall facing East

Time of Day	CLTD	$CLTD_C$	Q(Btu/hr)	Q(kW)
9	32.4	44.14	7196.35	2.1090
10	41.4	53.14	8663.66	2.5391
11	46.8	58.54	9544.05	2.7971
12	46.8	58.54	9544.05	2.7971
13	43.2	54.94	8957.12	2.6251
14	39.6	51.34	8370.20	2.4531
15	37.8	49.54	8076.73	2.3671
16	34.2	45.94	7489.81	2.1950
17	32.4	44.14	7196.35	2.1090
18	30.6	42.34	6902.88	2.0230
19	28.8	40.54	6609.42	1.9370
20	23.4	35.14	5729.04	1.6790
21	19.8	31.54	5142.11	1.5070
22	16.2	27.94	4555.19	1.3350
23	12.6	24.34	3968.26	1.1630
24	10.8	22.54	3674.8	1.0770
1	7.2	18.94	3087.88	0.9050
2	5.4	17.14	2794.41	0.8190
3	3.6	15.34	2500.95	0.7330
4	1.8	13.54	2207.49	0.6470
5	1.8	13.54	2207.49	0.6470
6	1.8	13.54	2207.49	0.6470
7	7.2	18.94	3087.88	0.9050
8	21.6	33.34	5435.57	1.5930

Equations:

$$\begin{aligned} Q_{we} &= U_{we}\, A_{we}\, CLTD_C \\ U_{we} &= 3.584\ W/m^2K \\ A_{we} &= 24\ m^2 \end{aligned} \tag{3.6}$$

3.2.5 VENTILATION

Ventilation load has two components 3.2.5.1) Sensible Load and 3.2.5.2) Latent Load

3.2.5.1 Sensible Load

$$\begin{aligned} Q_{sensible} &= 60\, CFM\, \rho\, C_P\, \Delta T \\ Q_{sensible} &= 60(hr/min) \times CFM(ft^3/min) \times 0.075(lbm/ft^3) \times \\ &\quad 0.24(Btu/lbm -^\circ F) \times \Delta T(^\circ F) \\ Q_{sensible} &= 1.08 \times CFM \times \Delta T \end{aligned} \tag{3.7}$$

ρ = Air Density (0.075 lbm/ft^3),

C_P = Specific heat of air (0.24 Btu/lb$^\circ F$).

Therefore,

CFM(Air flow rate) = 1×20 = 20 ft^3/min,

$Q_{sensible} = 1.08 \times CFM \times \Delta T$,

$\Delta T = (T_o - T_i)$,

Outdoor air temperature, $T_o = 102.74^\circ F$,

Indoor air temperature, $T_i = 78^\circ F$.

Therefore,

$Q_{sensible} = 1.08 \times 20 \times (102.74 - 78)$,

$Q_{sensible} = 21.6 \times 24.74 = 534\ Btu/hr = 156.499\ W$.

3.2.5.2 Latent Heat

$$Q_{latent} = 4840 \times CFM \times \Delta W \tag{3.8}$$

where:

CFM, Air flow rate = 1×20 = 20 ft^3/min,

$\Delta W = (W_o - W_i)$in lbm water/lbm dry air,

W_o,humidity ratio of outdoor air,

W_i,humidity ratio of indoor air.

From Psychrometric Chart:

I**ndoor**- 78°F dry bulb temperature at 50% relative humidity,

W_i = 0.0102 lbm water/ lbm dry air.

Outdoor - 102.74°F dry bulb temperature (DBT) at 50 % Relative Humidity,

W_o = 0.0226 lbm water/ lbm dry air,

$\Delta W = (W_o - W_i)$ = 0.0226 − 0.0102,

= 0.0124 lbm water/lbm dry air .

Therefore,

Q_{latent} = 4840 × 20 × 0.0124,

Q_{latent} = 1200 Btu/hr = 351.685 W.

3.3 Radiant time series method

3.3.1 Introduction

The radiant time series is derived from heat balance design and is a new method for performing cooling load calculations. All other simplified (non-heat-balance) methods such as Cooling load temperature difference/solar cooling load/cooling load factor (CLTD/SCL/CLF) are replaced by radiant time series design. Radiant time series computes conductive heat gain on 24-term response part series and instantaneous radiant heat gains on 24-term "radiant time series" for calculating cooling loads. Radiant time series is a computational procedure assuming radiant time series for wall/roof response factors. It involves computation of conductive heat gains, splitting of heat gains into radiant and convection portions and it converts heat gains into cooling loads. For conductive heat gains, the 24-term series of response factors relates conduction heat gain to 24-hourly sol-air temperatures and constant room temperatures.

3.3.2 Calculating cooling load of the lift motor room by radiant time series

3.3.2.1 Wall cooling load using sol-air temp, conduction and radiant time series

The cooling load from radiant time series is calculated from ASHRAE Handbook 2009 Fundamentals[22].

Sydney (Latitude = -33.85, Longitude = 151.2)

$$\begin{aligned} \tau_b &= 0.398 \\ \tau_d &= 2.308 \\ \rho_g &= 0.2 \end{aligned} \tag{3.9}$$

From monthly Sydney weather data

Solar angles:

$$\begin{aligned} \Psi &= \text{southwest orientation= } +45^\circ \\ \Sigma &= 90^\circ \text{for vertical surface} \end{aligned} \tag{3.10}$$

Solar position data and constants for January 21 are

$$\begin{aligned} ET &= -10.6\ min \\ \delta &= -20.10^\circ \\ E_o &= 447.1\ Btu/hft^2 = 1409.4828\ W/m^2 \end{aligned} \tag{3.11}$$

Apparent solar time:

$$\begin{aligned} AST &= LST + ET/60 + (LSM - LON)/15 \\ &= 17 + (-10.6/60) + [(150 - 151.21)/15] \\ &= 16.7426 \end{aligned} \tag{3.12}$$

Hour Angle H, degrees

$$\begin{aligned} H &= 15(AST - 12) \\ &= 15(16.7426 - 12) \\ &= 71.14^\circ \end{aligned} \tag{3.13}$$

Solar altitude β

$$\begin{aligned} \sin\beta &= \cos L\cos\delta + \cos H + \sin L\sin\delta \\ \beta &= 24^\circ \end{aligned} \tag{3.14}$$

Solar azimuth Φ

$$\begin{aligned} \cos\Phi &= (\sin\beta\sin L - \sin\delta)/(\cos\beta\cos L) \\ \Phi &= 81^\circ \end{aligned} \tag{3.15}$$

Surface solar azimuth γ

$$\gamma = \Phi - \Psi = 36^\circ \tag{3.16}$$

Incident angle θ

$$\begin{aligned} \cos\theta &= \cos\beta\cos g\sin\Sigma + \sin\beta\cos\Sigma \\ \theta &= 32^\circ \end{aligned} \tag{3.17}$$

Beam normal irradiance

$$\begin{aligned} E_b &= E_o exp(-\tau_b m^{ab}) \\ m &= \text{relative mass transfer} \\ &= 1/[sin\beta + 0.50572(6.07995 + \beta)^{-1.6364}] \\ &= 2 \\ ab &= \text{beam air mass exponent} \\ &= 1.219 - 0.043\tau_b - 0.151\tau_d - 0.204\tau_b\tau_d \\ &= 0.665987 \\ E_b &= 447.1 exp(-0.398 \times 2^{0.665987}) \\ &= 219\ Btu/hft^2 = 690.398\ W/m^2 \end{aligned} \tag{3.18}$$

Surface beam irradiance

$$\begin{aligned} E_{t,b} &= E_b \cos\theta \\ &= (219)\cos(32^\circ) \\ &= 185\ Btu/hft^2 \\ &= 583.213\ W/m^2 \end{aligned} \tag{3.19}$$

Ratio γ of sky diffuse radiation on vertical surface to sky diffuse radiation on horizontal surface

$$\begin{aligned} \gamma &= 0.55 + 0.437\cos\theta + 0.313\cos^2\theta \\ &= 0.55 + 0.437\cos(32^\circ) + 0.313\cos^2(32^\circ) \\ &= 1.15 \end{aligned} \tag{3.20}$$

Diffuse irradiance E_d−Horizontal Surfaces

$$\begin{aligned} E_d &= E_o exp(-\tau_d m^{ad}) \\ ad &= \text{diffuse air mass exponent} \\ &= 0.202 + 0.852\tau_b - 0.007\tau_d - 0.357\tau_b\tau_d \\ &= 0.197006 \\ E_d &= 447.1 exp(-2.308\times 2^{0.197006}) \\ &= 28.7\ Btu/hft^2 = 90.4768\ W/m^2 \end{aligned} \tag{3.21}$$

Diffuse irradiance $E_{t,d}$−vertical surfaces

$$\begin{aligned} E_{t,d} &= E_d\gamma \\ &= (28.7)(1.15) \\ &= 33.005\ Btu/hft^2 \\ &= 104.0483\ W/m^2 \end{aligned} \tag{3.22}$$

Ground Reflected Irradiance

$$\begin{aligned} E_{t,r} &= (E_b \sin\beta + E_d)\rho_g[(1 - \cos(90))]/2 \\ &= 11.778\ Btu/hft^2 = 37.1301\ W/m^2 \end{aligned} \tag{3.23}$$

Total surface irradiance

$$\begin{aligned} E_t &= E_b + E_d + E_r \\ &= 185 + 33.005 + 11.778 \\ &= 229.783\ Btu/hft^2 \\ &= 724.3909\ W/m^2 \end{aligned} \tag{3.24}$$

Sol-air temperature

$$\begin{aligned} T_e &= t_o + \alpha E_t/h_o + \epsilon\delta R/h_o \\ &= 148.6^\circ F = 64.8^\circ C \end{aligned} \tag{3.25}$$

Conductive heat gain is calculated:

$$
\begin{aligned}
q_{l,1} &= (0.6311)(387.5)(68.2-75) = -1663 Btu/hr = -0.4874 kW \\
q_{l,2} &= (0.6311)(387.5)(67.6-75) = -1809.7 Btu/hr = -0.5304 kW \\
q_{l,3} &= (0.6311)(387.5)(67.2-75) = -1907.5 Btu/hr = -0.5590 kW \\
q_{l,4} &= (0.6311)(387.5)(66.7-75) = -2029.8 Btu/hr = -0.5949 kW \\
q_{l,5} &= (0.6311)(387.5)(66.4-75) = -2103.1 Btu/hr = -0.6164 kW \\
q_{l,6} &= (0.6311)(387.5)(70.2-75) = -1173.9 Btu/hr = -0.3440 kW \\
q_{l,7} &= (0.6311)(387.5)(74.6-75) = -97.8 Btu/hr = -0.0287 kW \\
q_{l,8} &= (0.6311)(387.5)(80.2-75) = 1271.7 Btu/hr = 0.3727 kW \\
q_{l,9} &= (0.6311)(387.5)(85.5-75) = 2567.8 Btu/hr = 0.7525 kW \\
q_{l,10} &= (0.6311)(387.5)(90-75) = 3668.3 Btu/hr = 1.0751 kW \\
q_{l,11} &= (0.6311)(387.5)(93.6-75) = 4548.7 Btu/hr = 1.3331 kW \\
q_{l,12} &= (0.6311)(387.5)(96.1-75) = 5160 Btu/hr = 1.5123 kW \\
q_{l,13} &= (0.6311)(387.5)(105.2-75) = 7385.4 Btu/hr = 2.1645 kW \\
q_{l,14} &= (0.6311)(387.5)(125.6-75) = 12374.3 Btu/hr = 3.6265 kW \\
q_{l,15} &= (0.6311)(387.5)(141.8-75) = 16336 Btu/hr = 4.7876 kW \\
q_{l,16} &= (0.6311)(387.5)(150.5-75) = 18463.6 Btu/hr = 5.4111 kW \\
q_{l,17} &= (0.6311)(387.5)(148.6-75) = 17999 Btu/hr = 5.2750 kW \\
q_{l,18} &= (0.6311)(387.5)(129-75) = 13205.8 Btu/hr = 3.8702 kW \\
q_{l,19} &= (0.6311)(387.5)(80.2-75) = 1271.7 Btu/hr = 0.3727 kW \\
q_{l,20} &= (0.6311)(387.5)(74-75) = -244.6 Btu/hr = -0.0717 kW \\
q_{l,21} &= (0.6311)(387.5)(72.6-75) = -586.9 Btu/hr = -0.1720 kW \\
q_{l,22} &= (0.6311)(387.5)(71.3-75) = -904.8 Btu/hr = -0.2652 kW \\
q_{l,23} &= (0.6311)(387.5)(70-75) = -1222.8 Btu/hr = -0.3584 kW \\
q_{l,24} &= (0.6311)(387.5)(69.1-75) = -1442.9 Btu/hr = -0.4229 kW
\end{aligned}
\tag{3.26}
$$

Wall heat gain using conduction time series is:

$$\begin{aligned} q_{17} &= c_o q_{l,17} + c_1 q_{l,16} + c_2 q_{l,15} + c_3 q_{l,14} + \ldots\ldots\ldots + c_{23} q_{l,18} \\ &= 3620.34\ Btu/hr = 1.6010\ kW \end{aligned} \tag{3.27}$$

Convective heat gain is 54%

$$Q_c = (3620.34)(0.54) = 1954.98\ Btu/hr = 0.5729\ kW \tag{3.28}$$

Radiant Cooling load for wall from radiant time series

$$\begin{aligned} Q_{r,17} &= r_o(0.46)q_{l,17} + r_2(0.46)q_{l,16} + r_3(0.46)q_{l,15} + r_4(0.46)q_{l,14} \\ &\quad + \ldots\ldots\ldots + r_{23}(0.46)q_{l,18} \\ &= 6628.23\ Btu/hr = 1.9425\ kW \end{aligned} \tag{3.29}$$

The total wall cooling load at 5pm is

$$\begin{aligned} Q_{wall} &= Q_c + Q_{r,17} \\ &= 0.5729 + 1.9425 = 2.5154\ kW \end{aligned} \tag{3.30}$$

Similarly, cooling load is calculated for every hour for walls and roofs for the lift motor room.

3.3.2.2 Sydney Solar radiation

The solar radiation for Sydney is maximum for the month of January.

TABLE 3.7: Sydney Solar Radiation

Time	Beam	S. Beam	Diff	S. Diff	S. ref	Total	Total(W/m^2)
6	127	0	17.4	7.83	3.945	11.7753	37.1216
7	208	0	27.2	12.24	10.512	22.75182	71.7251
8	250	0	33.8	15.21	17.360	32.56982	102.676
9	274	0	38.4	17.28	23.879	41.15909	129.754
10	288	0	41.4	18.63	28.82642	47.45642	149.606
11	295	0	43.2	19.44	32.041	51.48093	162.294
12	298	0	43.9	21.95	33.305	55.25481	174.191
13	296	23	43.4	25.606	32.491	81.09727	255.659
14	290	87	41.9	29.749	29.554	146.303	461.220
15	277	142	39.1	33.626	24.815	200.4415	631.892
16	255	179	34.8	35.148	18.826	232.9743	734.452
17	219	185	28.7	33.005	11.778	229.7825	724.389
18	148	140	19.7	24.625	5.0471	169.6721	534.891
19	9	9	4.7	6.063	0.47	15.533	48.9678

Total solar radiation is zero from 8 pm to 5 am

S. = surface

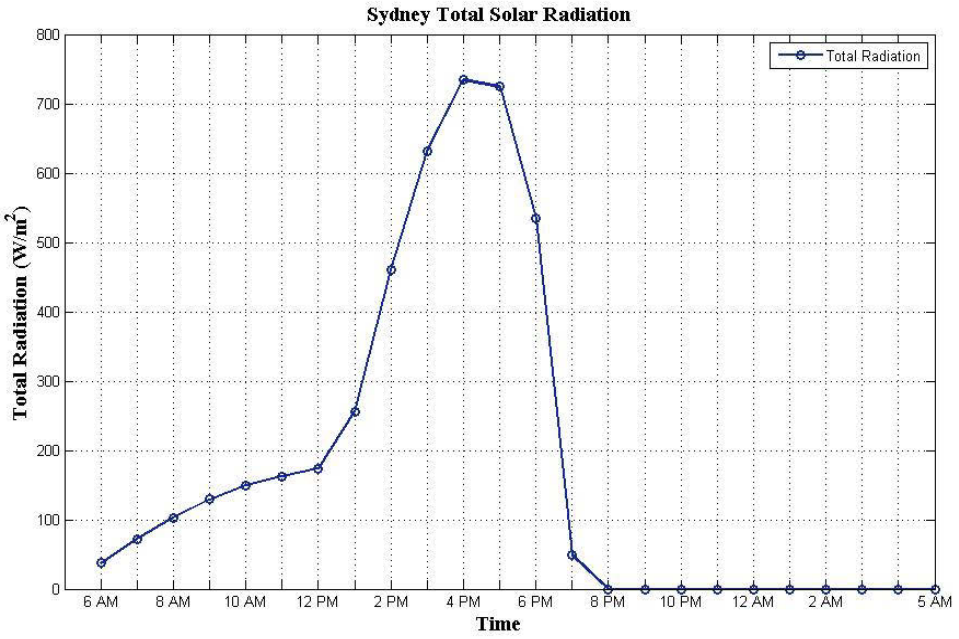

FIGURE 3.2: Sydney Solar Radiation

3.3.2.3 Outside temperature and Sol-air temperatures

TABLE 3.8: Outside and Sol-air Temperatures

Time	Outside Temperature(^oC)	Sol-air temperature(^oC)
6	19.278	21.222
7	19.889	23.667
8	21.333	26.778
9	22.889	29.722
10	24.333	32.222
11	25.611	34.222
12	26.444	35.611
13	27.111	40.667
14	27.556	52
15	27.556	61
16	27.056	65.8333
17	26.389	64.778
18	25.556	53.889
19	24.278	26.778
20	23.333	23.333
21	22.556	22.556
22	21.833	21.8333
23	21.111	21.111
24	20.6111	20.6111
1	20.111	20.111
2	19.778	19.778
3	19.556	19.556
4	19.278	19.278
5	19.111	19.111

3.4 Accuracy and Reliability of Various Calculation Methods

There are high uncertainties in input data to find cooling loads. This is due to unpredictable occupancy, human behaviour and outdoor weather conditions . It also involves lack of and variation in heat gain for modern equipment and introduction of new building products and HVAC equipment with unknown characteristics. The uncertainty exceeds the errors generated by simple methods compared to complex methods. Therefore, added time/effort for complex calculation method is not productive for better accuracy of results if uncertainties in input data are high. Therefore, simplified methods will have similar accuracy.

CLTD/SCL/CLF method described in 1997 ASHRAE Fundamentals is strict manual cooling load calculation method. This method will produce most conservative results based on peak load values in sizing equipment. The results got from CLTD/CLF depends on space and varies from model used to generate CLTD/CLF data in tables. Engineering judgement is required in interpreting custom tables and applying correction factors.

3.5 Comparison of Cooling load by CLTD and Radiant time series

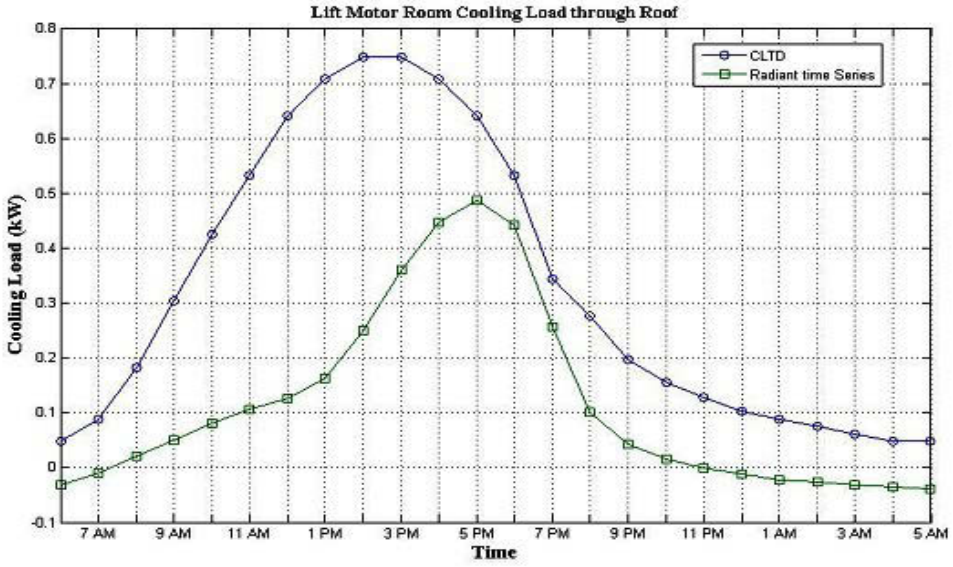

FIGURE 3.3: Cooling load of Roof

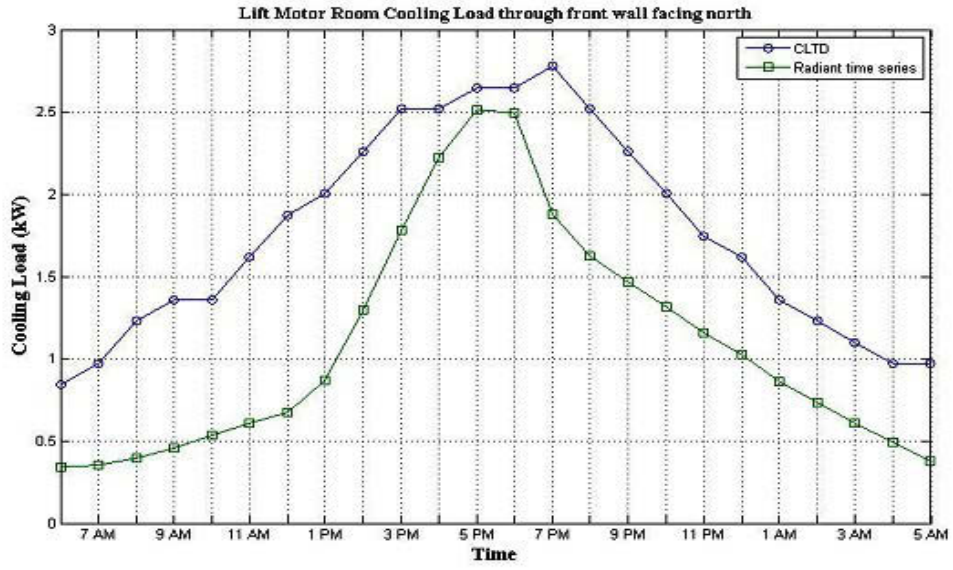

FIGURE 3.4: Cooling load of Front Wall facing North

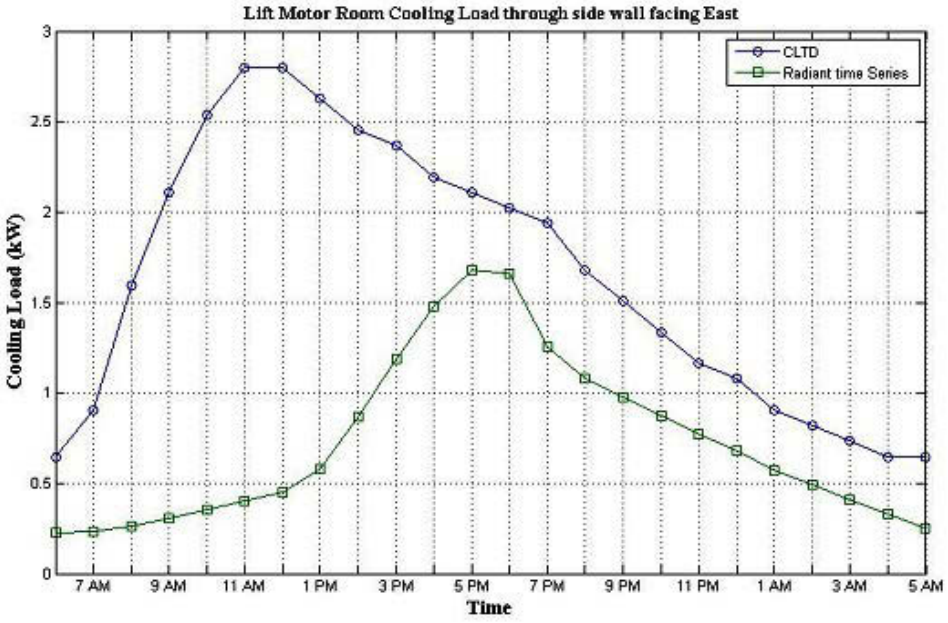

FIGURE 3.5: Cooling Load of Side Wall facing East

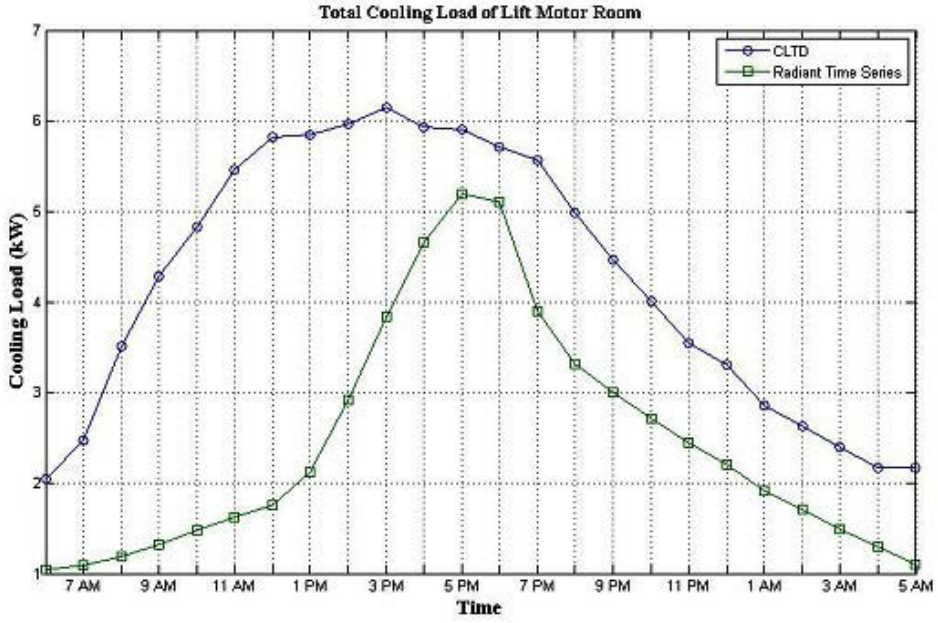

FIGURE 3.6: Total Cooling load of Lift Motor Room

3.6 Results and Discussions

The cooling load is calculated from the cooling load temperature difference method and radiant time series method. The peak cooling load is calculated from Fourier's law of conductance by the cooling load temperature difference method. The peak cooling load by cooling load temperature difference method is 6.14 kW at 3 pm whereas the peak cooling load by radiant time series process is 5.19 kW at 5 pm. Total solar radiation involving beam, diffuse, surface reflected and hence total radiation is a maximum at 5 pm by radiant time series process, therefore, peak cooling load is a maximum at 5 pm. The peak cooling load by Cooling load temperature difference method is at 3 pm as it does not take total solar radiation into account. It calculates cooling load on cooling load temperature difference which is a maximum at 3 pm for walls and roof.

3.7 Conclusion

CLTD is an old method of calculation whereas radiant time series is a new and more accurate method for calculating cooling load. The CLTD method takes into account annual design conditions and calculates average cooling load for whole year whereas radiant time series calculates cooling load for every month based on monthly design conditions. The CLTD method does not take solar radiation into account whereas radiant time series calculates cooling load on beam and diffuse solar radiation which is calculated from climatic station data for a chosen location. The CLTD method calculates cooling load only on heat conduction whereas radiant time series divides total heat into convection and radiation fraction and calculates cooling load on radiant time series for every hour.

Chapter 4

Testing the performance of absorption chiller

4.1 Introduction

There is rising concern of change in climate, and recent developments and progress in solar energy and use of waste heat. This has led to the development of small scale absorption chillers and heat pumps. This equipment has entered an early phase of standard generation, intended for private, business and mechanical application. Experimental work and performance evaluation of the complete operating range show they are ideal for diverse application. There is a few guidelines, standards and other expert recommendations apart from experimental work for absorption machines. The primary aim of IEA Annex 34 is development and revision of thermal driven technologies to develop their market position. It is very difficult to produce a correct model without experimental data, and neither simulation nor control strategy is available.

Internal components of absorption chiller are accessed by researchers based on external measurements. One of the usual practices in the literature is to present performance data with external operating conditions. The external measures suffice for characterizing absorption equipment and data for exploitation in various applications and provide a motivation for making simple procedure and guideline for future testing. The main purpose of this Chapter is to generate a simple method for performance evaluation of small capacity absorption chillers and heat pumps based on external measurements. The outcome will be the development of simple and correct models used in different applications. The procedure uses a test bench for testing different absorption machines through various operating modes. In the first stage, the system is developed based on tests on a Viuna absorption machine kept at the top of UTS building two. In the second phase, the developed systems is updated by adding new elements to complete it. The final process includes planning for tests, critical parameters for absorption machine and a method to calculate them and to develop a detector for steady-state conditions. It includes the uncertainty estimation and analysis of results with graphical and tabular display.

4.2 Viuna Absorption Chiller

FIGURE 4.1: Viuna Absorption chiller at the top of UTS building 2

Viuna single effect absorption chiller is the absorption machine chosen for test procedure and validating test bench. The single effect absorption chiller uses $LiBr - H_2O$ as the working fluid. Vapour compression systems produce gases like chlorofluorocarbons (CFCs) and hydrochlorofluorocarbons producing ozone depletion and global warming. According to the US Environmental Protection Agency [65] building energy consumption contributes 40% of greenhouse gas and other air pollutant emissions. Rodriguez-Hidalgo et al. [50] compares single-effect absorption chiller with the conventional system in Spain. CO_2 emission savings for single-effect absorption chiller is more than 20% for the coefficient of performance (COP) between 0.35 to 0.7. Florides et al. [15] showed that R22 in a 5 ton refrigeration system can produce about 18 g of CO_2/kWh of cooling supply. Different studies highlight the impact of

solar thermal energy on energy performance and greenhouse emission reduction in various HVAC systems like absorption, adsorption, desiccant, ejector and integrated photovoltaics system. Florides et al. [15] presented the method for performance analysis for a single stage LiBr-water absorption machine. The equations for working fluid properties is employed in the computer program as part of their research. The difference between inlet and outlet concentrations of the LiBr-water solution at the absorber reduces the mass flow rate.

4.2.1 System Description

The schematic of a single-effect central vapour-absorption cooling system integrated with vacuum solar collector is shown in Fig.4.2. The system comprises a water-cooled absorption chiller, an open circuit cross flow cooling tower, a fan-coil unit, chilled water, condenser water and hot water pumps, valves and connection tubes.

4.2.2 Operational Cycle

Figure 2.4 shows the absorption chiller cycle for Viuna single effect absorption chiller. In the $LiBr - H_2O$ system, lithium bromide is the absorbent and water is the refrigerant. The necessary condition for boiling of water at low temperature is created by pumping of chiller into a deep vacuum. The refrigerant vapour is attracted to absorber by a difference between lithium bromide solution and refrigerant water. They are absorbed by concentration of lithium bromide solution and performing continuous boiling of the refrigerant water. In the hot water operated chiller, the diluted solution in the absorber is pumped into the generator via a solution pump. The diluted solution concentrates into the concentrator when heating by hot water. The refrigerant vapour generated is condensed into water in the condenser. The refrigerant water enters the evaporator

and pumps to the spray through the spraying device using refrigerant pump. Heat transfer from air-handling unit water to refrigerant causes refrigerant water to vaporise again, producing chilled water. Finally, chilled water is pumped to the air-handling unit producing cooled air for the building. On the other hand, the concentrated solution from the generator directly enters absorber and repeats the cycle.

4.3 Experimental Set-Up

Experimental work covers measuring inlet and outlet cooling water, chilled water and hot water for an absorption chiller. The experiment is done on the top of UTS building 2 including the lift motor room and solar hot water absorption chiller including absorption chiller, cooling tower and fan coil. The cooling load is a lift motor room of UTS Building 2 together with a central cooling plant. The central cooling plant installed in the building consists of a water-cooled single-effect absorption chiller, a cross flow vertical cooling tower, a fan-coil unit, evacuated solar collectors, a chilled-water pump, a hot-water pump and condenser-water pump. The water absorption chiller with a rated capacity 6 kW(1.5 RT) operates at driving hot water temperature of $85°C$, coolant water temperature of $29.5°C$ and supply chilled water temperature of $7°C$. The rated hot water mass flow rate is 0.45 l/s. The designed supply and return chilled water temperatures are set respectively at 7° and $12°C$. The chilled water mass flow rate is 0.25 l/s. The heat rejection is performed by using a cross flow cooling tower, designed for 0.76 l/s cooled water flow rate. The fan-coil unit located in the room operates at 378 l/s air flow rate. The evacuated solar collectors comprise a $10m^2$ area for 135 evacuated tubes in nine bays, with an operating range of 75° to $95°C$. The COP of the chiller for normal condition is 0.725.

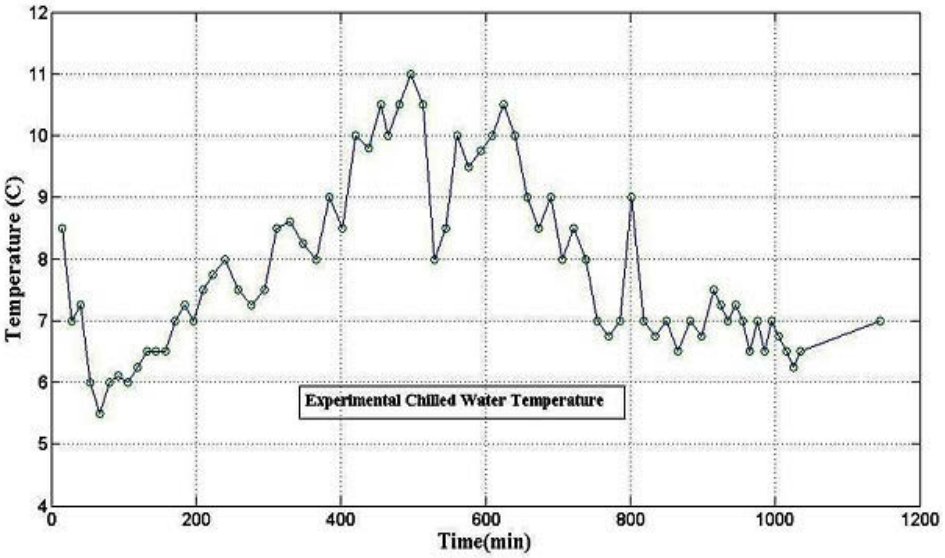

FIGURE 4.2: Experimental Chilled Water Temperature

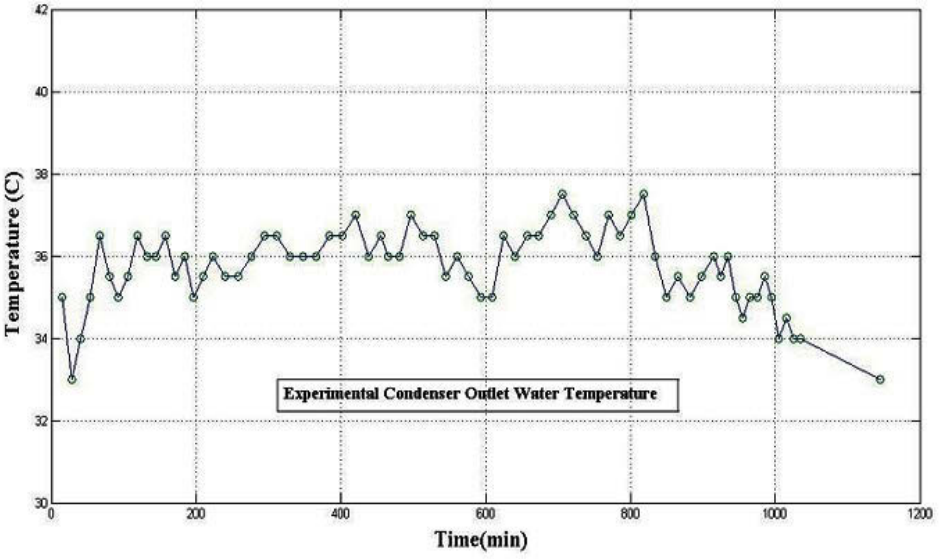

FIGURE 4.3: Experimental Condenser Outlet water Temperature

4.4 System Modelling

This section represents the thermodynamic modelling and analysis for the absorption chiller, cooling tower, fan coil unit and evacuated solar collectors.

4.4.1 Single Effect Absorption Chiller

The main components of the absorption chiller include the generator, condenser, evaporator and absorber to be modelled by using mass and energy balance laws. The mass and energy balances for the chiller are as proposed by Kong, Liu, Zhang, He, and Fang [40].

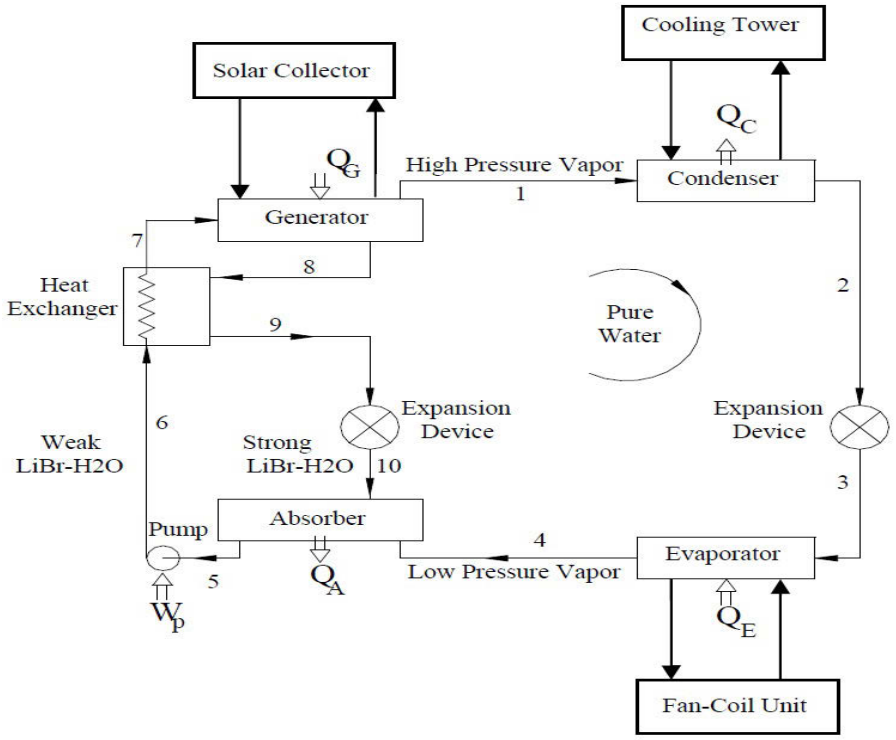

FIGURE 4.4: Schematic diagram of the proposed solar-powered single-effect hot water absorption air conditioning system

The mass balance equations for each component are as follows:

$$\frac{dM_C}{dt} = \dot{m}_1 - \dot{m}_2, \tag{4.1}$$

$$\frac{dM_E}{dt} = \dot{m}_3 - \dot{m}_4, \tag{4.2}$$

$$\frac{dM_A}{dt} = \dot{m}_4 + \dot{m}_{10} - \dot{m}_5, \tag{4.3}$$

$$\frac{dM_G}{dt} = \dot{m}_7 - \dot{m}_8 - \dot{m}_1, \tag{4.4}$$

$$\dot{m}_2 = \dot{m}_3, \tag{4.5}$$

$$\dot{m}_5 = \dot{m}_6 = \dot{m}_7, \tag{4.6}$$

$$\dot{m}_8 = \dot{m}_9 = \dot{m}_{10}, \tag{4.7}$$

where $\dot{m}$ is the water flow rate, M is the water mass and subscripts 1 to 10 indicate inlet and outlet of each component, as shown at the corresponding point in the figure.

The energy balances for the component are given as:

$$\frac{d}{dt}(M_C h_C) = \dot{m}_1 h_1 - \dot{m}_2 h_2 - Q_C, \tag{4.8}$$

$$\frac{d}{dt}(M_E h_E) = \dot{m}_3 h_3 - \dot{m}_4 h_4 - Q_E, \tag{4.9}$$

$$\frac{d}{dt}(M_A h_A) = \dot{m}_4 h_4 + \dot{m}_{10} h_{10} - \dot{m}_5 h_5 - Q_A, \tag{4.10}$$

$$\frac{d}{dt}(M_G h_G) = \dot{m}_7 h_7 - \dot{m}_8 h_8 - \dot{m}_1 h_1 - Q_G, \tag{4.11}$$

$$W_P = \dot{m}_6 h_6 - \dot{m}_5 h_5, \tag{4.12}$$

$$h_2 = h_3, \tag{4.13}$$

$$h_9 = h_{10}, \tag{4.14}$$

where h is the enthalpy, Q is the heat transfer rate, W_p is the input work of pump, and where subscripts A, C, E, G, and p represent the absorber, condenser, evaporator, generator and pump.

4.4.2 Evacuated Solar Collector

The performance equation of evacuated solar collectors is as proposed by Hayek, Assaf and Lteif[24]. The coefficients are found from Roper[57]. The performance equation of the evacuated solar collector can be given by:

$$\eta = 0.717 - 1.52\frac{T_{w,i} - T_{db}}{I_t} - 1.52\frac{(T_{w,i} - T_{db})^2}{I_t}, \tag{4.15}$$

where η is the collector efficiency, $T_{w,i}$ is the water temperature entering the collector, T_{db} is the ambient dry bulb temperature and I_t is the total solar radiation intensity absorbed by solar collectors.

4.4.3 Fan-Coil Unit

The purpose of the fan coil unit is to handle supply air in the building. The main parts of fan coil are cooling coil and supply fan. The heat transfer properties of water cooling coil have direct influence on performance of air-cooled chiller. The dynamics of air and water temperature through the cooling coil is as proposed by Vakiloroaya, Ha and Samali [66].

By using mass and energy laws the dynamics of air and water temperatures through the coil are described as:

$$M_{cc,w}(C_{p,w}\frac{dT_{cc,w}}{dt} + C_{p,w}v_w\frac{T_{chw,o} - T_{chw,i}}{l}) = Q_{cc}, \tag{4.16}$$

$$\rho_a V_{sup}(C_{p,a}\frac{dT_{sup}}{dt} + C_{p,a}v_a\frac{T_{sup} - T_{ret}}{l}) = -Q_{cc}, \tag{4.17}$$

where $M_{cc,w}$ is the cooling coil water mass, $T_{cc,w}$ the cooling coil water temperature, $C_{p,w}$ the water constant pressure specific heat, $C_{p,a}$ air constant pressure specific heat, v_w the water velocity, v_a the air velocity, T_{sup} the supply air temperature, T_{ret} is the return air temperature, $T_{chw,o}$ the chilled water temperature leaving the cooling coil, $T_{chw,i}$ the chilled water temperature entering cooling coil, l the cooling coil length, ρ_a the air density, V_{sup} the air volume and Q_{cc} is the cooling coil capacity.

The speed of the supply fan can be controlled for improving the cooling coil's performance. The total power consumption of the fan P_{fcu} as:

$$\begin{aligned} P_{fcu} \quad = \quad & 7.2 - 1.7T_{sup} + 0.07T_{sup}^2 + 0.03T_{sup}Q_b + 0.11T_{sup}T_{chw,o} - 0.01T_{sup}^2Q_b \\ & +0.04T_{sup}^2T_{chw,o} - 0.01T_{sup}Q_b^2 - 0.02T_{sup}T_{chw,o}^2 - 0.03T_{chw,o}Q_b, \end{aligned} \tag{4.18}$$

where Q_b is the building cooling demand and all coefficients are found by curve-fitting of real data.

4.4.4 Cooling Tower

The thermal and hydraulic model of cooling tower is combined for thermal and hydraulic performance of cooling tower. The ratio of cooling tower water flow rate to ambient dry air flow rate is proposed by Soylemez[62] and can be determined by

$$(\dot{m}_{w,ct}/\dot{m}_{a,ct})_{opt} = \frac{C_{p,a}}{C_{p,w}} + \frac{3238.7 h_{fg,w} P_{amb} e^{18.6-(5206.9/T_w)}}{(C_{p,w} T_w^2)(P_{amb} - e^{18.6-(5206.9/T_w)})^2}, \tag{4.19}$$

whrere $\dot{m}_{w,ct}$ is the cooling tower water flow rate, $\dot{m}_{a,ct}$ is the cooling tower air flow rate, $h_{fg,w}$ is the latent heat of evaporation of water, P_{amb} is the ambient pressure, and T_w is the mean temperature of cooling tower water.

4.5 Model Validation

Several tests is facilitated under different operating conditions to the above mentioned instrumented system. The following parameters are measured by experiment: temperatures of water entering and leaving cooling tower, chiller and fan-coil unit, and the total power consumption of the plant. Six platinum resistance thermometers of the PT100 type are used with calibrated accuracy of $\pm 0.50°C$ for temperature range from – $50°C$ to $+260°C$ to measure water temperature before and after each component. All PT100 sensors and pressure transducers are integrated with a computer-based DT500 data-logger. The power of the air-conditioner is measured by digital ac/dc power clamp multimeter of precision ±3.5%. The system performance is monitored continuously at various weather condition by field tests for two weeks. The tests are carried for 10 hours a day and measured data is monitored in 15 minute intervals. All measurements are computerised and recorded for further analysis.

4.6 Data Modelling

The thermal load of the evaporator was calculated by using equation 4.20:

$$\dot{Q}_{eva} = \dot{V}_{chw}\, \rho_{chw}\, C_{p_{chw}}\, (T_{chw,in} - T_{chw,out}), \tag{4.20}$$

where $\dot{V}_{chw}$ is the volumetric flow rate of the chilled water circuit, ρ_{chw} is the density and $C_{p_{chw}}$ is the specific heat of water at constant pressure. The last two parameters are calculated on average value of the inlet and outlet temperatures of chilled water, $T_{chw,in}$ and $T_{chw,out}$. The fluid properties

from table or software is applied when fluid in the external heat carrier is different. Similarly, generator load was calculated by using equation 4.21:

$$\dot{Q}_{gen} = \dot{V}_{hw}\, \rho_{hw}\, C_{p_{hw}}\, (T_{hw,in} - T_{hw,out}). \tag{4.21}$$

The absorber and condenser load were calculated as a single load since common practice in absorption machines is that the same external water circuit is used for both components. This is described by equation 4.22:

$$\dot{Q}_{ac} = \dot{V}_{cw}\, \rho_{cw}\, C_{p_{cw}}\, (T_{cw,out} - T_{cw,in}). \tag{4.22}$$

Three different indicators were used to evaluate the performance of the absorption machine operating as chiller: thermal coefficient of performance (COP), energy efficiency ratio (EER) and overall coefficient of performance. Thermal COP assesses thermal performance as ratio of cooling capacity to heat supplied to the generator for activation (equation 4.23):

$$COP_{chiller,th} = \frac{\dot{Q}_{eva}}{\dot{Q}_{gen}}\ . \tag{4.23}$$

The Energy Efficiency Ratio is defined as ratio of cooling capacity to the electricity consumption of the absorption chiller by equation 4.24:

$$EER_{chiller} = \frac{\dot{Q}_{eva}}{\frac{E}{\eta}}\ . \tag{4.24}$$

Here E is the electricity consumption and η is the overall generating efficiency of the Spanish electricity system taken as equal to 0.33 according to best practice standard.

Overall COP was used to assess the performance by including both electrical consumption and heat supplied to the generator into one equation(4.25):

$$COP_{chiller,all} = \frac{\dot{Q}_{eva}}{\dot{Q}_{gen} + \frac{E}{\eta}} \ . \tag{4.25}$$

4.7 Results and Discussions

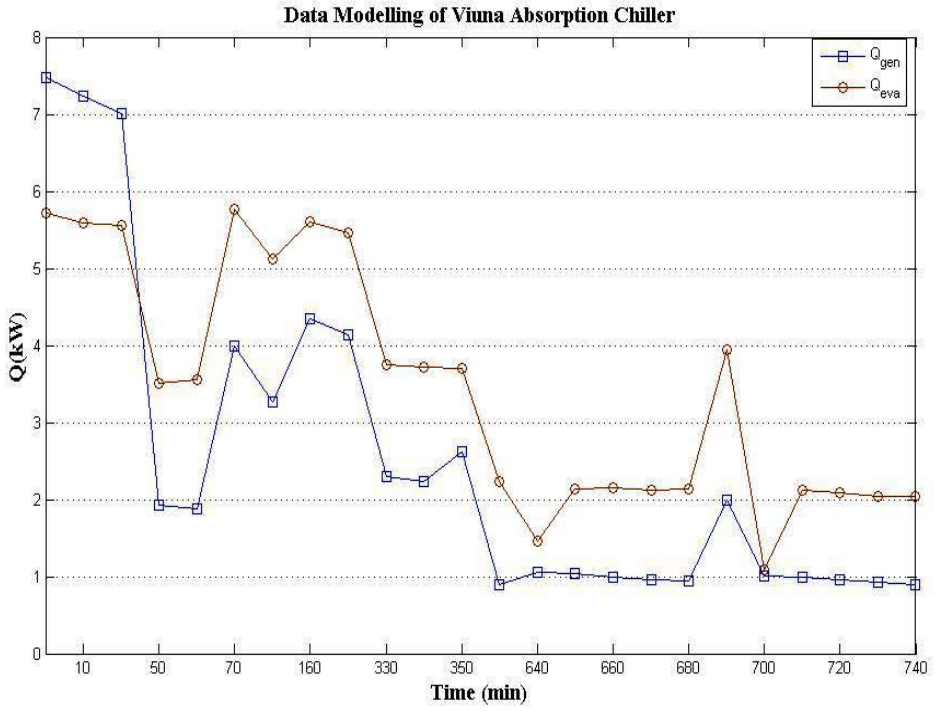

FIGURE 4.5: Data modelling of Viuna absorption chiller

The performance of absorption chiller is evaluated by varying the temperature of external circuits. The figure above shows heat absorbed by generator and absorber and heat rejected by evaporator based on experimental data for hot water, cooling water and chilled water temperatures for the absorption chiller for three hours. The pattern of variation of the heat absorbed by absorber and generator is found to be similar. The heat rejected by the evaporator indicates the cooling rate of the absorption chiller.

4.8 Conclusion

The absorption machine performance is tested using a comprehensive procedure for small capacity commercial units. The measurement of external parameters monitors and the process allows the creation of a complete performance map for absorption machines based on highly accurate data. The study of a single effect absorption chiller system includes system modelling for absorption chiller, evacuated solar collectors, cooling tower and fan coil unit. The obtained data is used to form the database that is further used for model development.

Chapter 5

Modelling methods

5.1 Introduction

A model is a mathematical representation of physical state or process and is used to understand better the process and mechanism and to comprehend the results. The process or system can be improved by using the model based on analysis of simulated data. This Chapter aims at comparing different modelling approaches to predict the performance of absorption chillers. The simulation software package serves for the comparative evaluation of simple but accurate models of absorption chillers. The annual simulation of complex building systems produces a high level of performance prediction for minimum input parameters of the chiller models. Also, this chapter provides statistical information that helps in selecting appropriate models. For this purpose, three different absorption chiller models were examined: First Law of thermodynamics model, the adapted characteristic equation model and multivariate polynomial model.

5.2 Database of modelling

The dataset is obtained for a Viuna hot water absorption chiller. The water absorption chiller has capacity of 6 kW(1.5 RT) and operates at hot water temperature of 85°C, coolant water temperature of 29.5°C and supply chilled water temperature of 7°C. The estimated hot water mass flow rate is 0.45 l/s. The designed supply and return chilled water temperatures are set respectively at 7° and 12°C. The chilled water mass flow rate is 0.25 l/s. The heat rejection is performed by using a cross flow cooling tower, designed for 0.76 l/s cooled water flow rate. The fan-coil unit located in the room operates at 378 l/s air flow rate. The evacuated solar collectors comprise a $10m^2$ area for 135 evacuated tubes in nine bays, in an operating range of 75° to 95°C. The COP of the chiller for the normal condition is 0.725.

5.3 Models

5.3.1 Adapted Characteristic Equation model ΔΔ t'

Ziegler et al. [25] developed an approximate method for modelling absorption chillers and represents cooling capacity and driving heat input by simple algebraic equations. These equations are expressed as a function of characteristic temperature function ($\Delta\Delta t$) which depends on the average temperature of external heat carrier fluids. The heat transfer from heat transfer equations in four major components is related to driving heat temperature difference in heat exchangers. The authors determine relationships between external temperatures and driving heat temperature difference using Duhring's rule. The total heat transfer between absorption chiller and ambient is proportional to characteristic temperature difference as seen from equation:

$$\Delta\Delta t = (T_{gen} - T_{abs}) - R(T_{con} - T_{eva}) \approx T_{gen} - (1 - R)T_{ac} + RT_{eva}. \tag{5.1}$$

A linear function of heat flow and external temperatures are reduced from a complex response to all external heat carrier temperatures. A constant between 1.1-1.2 of R is used to relate vapour pressure line to one of pure water. The predicted cooling capacity deviates from linear behaviour at high driving temperatures due to higher internal losses. Kuhn and Ziegler[35] propose an improved model of adapted characteristic equation method using numerical fit to catalogue or experimental data. Thus, adapted characteristic temperature function ($\Delta\Delta t'$) takes the form (5.2):

$$\Delta\Delta t' = T_{gen} - a\, T_{ac} + e\, T_{eva}, \tag{5.2}$$

and the linear characteristic equation for component loads with (5.3):

$$\dot{Q}_{(k)} = s' \; T_{gen} - s' \; a \; T_{ac} + s' \; e \; T_{eva} + r. \tag{5.3}$$

The catalogue or experimental data are fitted using multiple linear regression algorithms to find the four parameters(s', a, e, r). This algorithm minimises residual sum of squares by choosing regression coefficients. Puig et al. [54] analyses and confirms the capability of ($\Delta\Delta t'$) method to obtain good results and better accuracy than the original method ($\Delta\Delta t$) . Equations for arithmetic mean temperatures (5.4) - (5.6) and external mean temperatures (5.7) - (5.9) are obtained by combining equation (5.3) and solves efficiently. The performance of the absorption chiller is predicted from three temperatures of each external circuit and fixed flow rates of external heat carriers.

$$T_{eva}^{in} = 2 \; T_{eva} - T_{eva}^{out}, \tag{5.4}$$

$$T_{gen}^{out} = 2 \; T_{gen} - T_{gen}^{in}, \tag{5.5}$$

$$T_{ac}^{out} = 2 \; T_{ac} - T_{ac}^{in}, \tag{5.6}$$

$$\dot{Q}_{eva} = 2 \; m_{eva} \; C_{Peva} \; (T_{eva} - T_{eva}^{out}), \tag{5.7}$$

$$\dot{Q}_{gen} = 2 \; m_{gen} \; C_{Pgen} \; (T_{gen}^{in} - T_{gen}), \tag{5.8}$$

$$\dot{Q}_{ac} = 2 \; m_{ac} \; C_{Pac} \; (T_{ac} - T_{ac}^{in}). \tag{5.9}$$

5.3.2 Multivariable Polynomial Regression(MPR)

The absorption chiller was formulated based on the multivariable polynomial regression model. MPR models are useful tools for describing non-linear relationships between input and output variables. The parameters of the MPR model are calculated by fitting experimental data minimising sum of squares using a polynomial function. MPR models are applied in various fields such as forecasting, control, optimisation, fault detection and diagnosis[41 , 55 , 37]. A polynomial regression model contains squared and higher order terms of estimator variables. It has been decided to apply second order polynomials to predict absorption chiller performance. MPR models are developed to calculate thermal loads of the absorption chiller by using measurements of external chillers: generator inlet temperature, absorber/condenser inlet temperature and evaporator outlet temperature. The second order model of absorption chillers can be represented using Eq. 5.10:

$$\begin{aligned} \dot{Q}_k &= \beta_{0,k} + \beta_{1,k} T^{in}_{gen} + \beta_{2,k} T^{in}_{ac} + \beta_{3,k} T^{out}_{eva} + \beta_{4,k} T^{in}_{gen} T^{in}_{ac} + \beta_{5,k} T^{in}_{gen} T^{out}_{eva} \\ &\quad + \beta_{6,k} T^{in}_{ac} T^{out}_{eva} + \beta_{7,k} (T^{in}_{gen})^2 + \beta_{8,k} (T^{in}_{ac})^2 + \beta_{9,k} (T^{out}_{eva})^2. \end{aligned} \tag{5.10}$$

The ten coefficients in the above model are fitted from experimental data. These coefficients have no physical meaning and are not able to be interpreted in physical terms.

5.4 Results and Discussions

5.4.1 Model Parameters

5.4.1.1 Adapted Characteristic Equation model ΔΔ t'

The same experimental dataset were applied for the $\Delta\Delta t'$ method. Multiple linear regression fits resulted in the following coefficients for characteristic functions of absorption chillers (Table 5.1).

TABLE 5.1: Multiple linear regression fit parameters ($\Delta\Delta t'$)

	s'	s'a	s'e	r
$\dot{Q}_{eva}$	-58.849	0.8965	-0.1422	0.3486
$\dot{Q}_{gen}$	-116.6290	1.6668	0.0008	-0.0114

5.4.1.2 MPR

The regression fitting parameters ($\beta_{i,k}$) for different heat loads (k) are found from 2^{nd} order polynomial fit applied to experimental data of absorption chiller for MPR models from Table 5.2.

TABLE 5.2: Fitting Coefficients of MPR models

k	$\dot{Q}_{eva}$	$\dot{Q}_{gen}$
β_0	-5067.9	-71.7560
β_1	143.7	-0.1221
β_2	-0.2	0.0006
β_3	-47.6	1.2075
β_4	0.1	0.0003
β_5	0.4	-0.0268
β_6	0.3	0.0114
β_7	-1	0.0167
β_8	-0.1	-0.0014
β_9	0.7	0.0305

5.4.2 Evaluation of the models

5.4.2.1 Simple Comparison

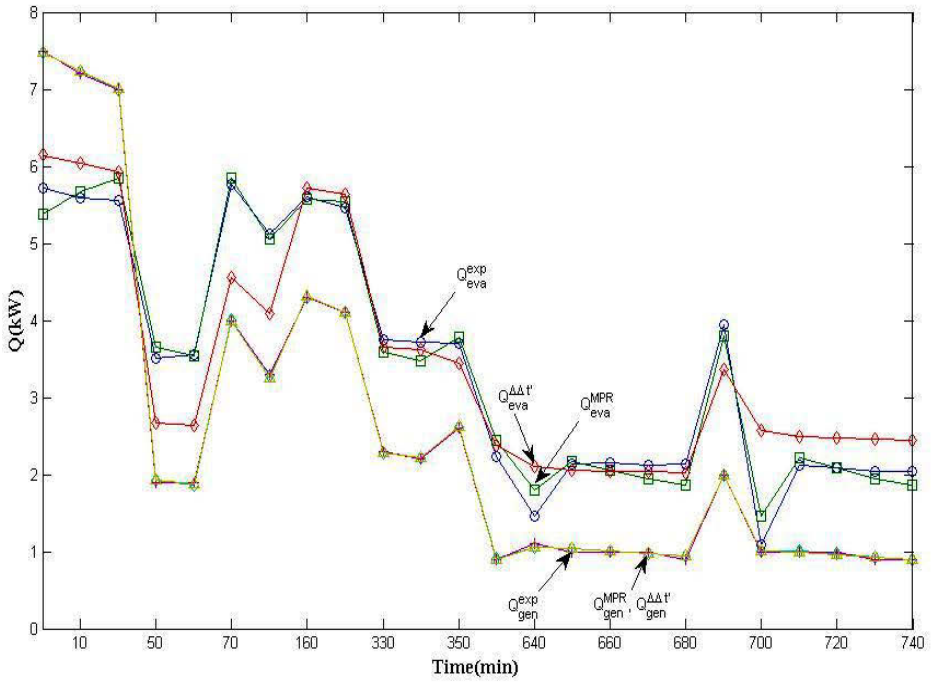

FIGURE 5.1: Cross validation empirical models with experimental data from chiller

Two empirical models Adapted Characteristic equation ΔΔ t' and MPR showed close agreement with experimental data for the same absorption machine in the small solar-assisted installation. Figure 5.1 shows the comparison of 12.3 hours profile for absorption chiller that shows a majority of compared empirical models have good prediction capability. The mean deviation is less than 5% which means models are useful simulation tools. It can establish correlations that are valid for a range of data (or points) used for modelling. The model will deviate radically by moving away from the range of models. The profile used for comparison was close to the data used for modelling.

5.4.2.2 Statistical Indicators

The goodness-of-fit of models are evaluated from statistical indicators. Several statistical indicators like residual sum of squares (SS_{res}), the coefficient of determination (R^2), the root mean square error (RMSE), are used to predict statistical performance analysis of different models. The similarity between predicted and observed data is found from the residual sum of squares and coefficient of determination. The similarity between predicted and observed data are found from the residual sum of squares and coefficient of determination. Residual value is found after fitting a model through the difference between values predicted by the model (y_i) and observed values ($\hat{y}$). The sum of squares of these differences is called the residual sum of squares (5.11) and is a measure of the difference between data and estimated model. A smaller SS_{res} indicates the better fit of observed data.

$$\begin{aligned} \epsilon_i &= y_i - \hat{y}_i \\ SS_{res} &= \sum_{i=1}^{N} \epsilon_i^2 \end{aligned} \tag{5.11}$$

.

The coefficient of determination is another parameter that quantifies the goodness of fit. The R^2 is calculated from residual sum of squares and total sum of squares (SS_{tot}) by equation 5.12:

$$R^2 = 1 - \frac{SS_{res}}{SS_{tot}}, \tag{5.12}$$

$$SS_{tot} = \sum_{i=1}^{N} (\hat{y}_i - \bar{y}_i)^2. \tag{5.13}$$

R^2 is the statistical measure of how well the model prediction approximates to the observed data. R^2 of 1 indicates that model prediction perfectly fits observed data. Apart from R^2 value other model parameters should be used for interpreting the performance of the absorption chiller.

The RMSE is the statistical indicator that measures the precision of the model and is calculated as the square root of the variance of residuals (equation 5.14). RMSE indicates the absolute fit of the model to the observed data.

$$RMSE = \sqrt{\frac{1}{N}\sum_{i=1}^{N}\epsilon_i^2} \tag{5.14}$$

Two different models of Viuna absorption chiller are compared in Figure 5.2 , 5.3, 5.4, 5.5 with predicted chilling capacity and driving heat input(Q_{eva} and Q_{gen}). R^2 value of each model shows the comparison of predictive capabilities. MPR modelling ($R^2 > 0.99$) predicts chiller performance better than adapted characterisitic equation models.

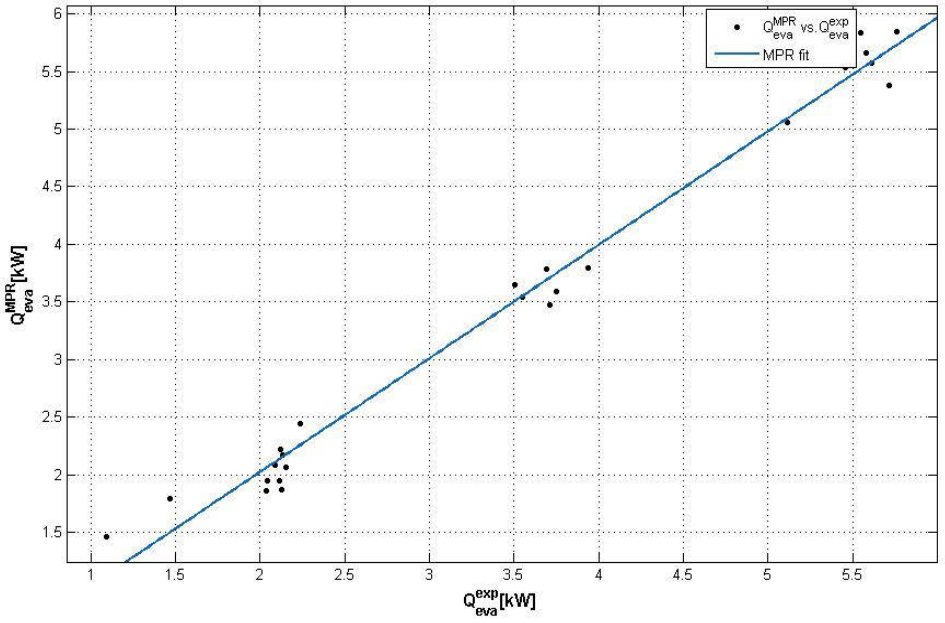

FIGURE 5.2: MPR Comparison between measured and predicted evaporator

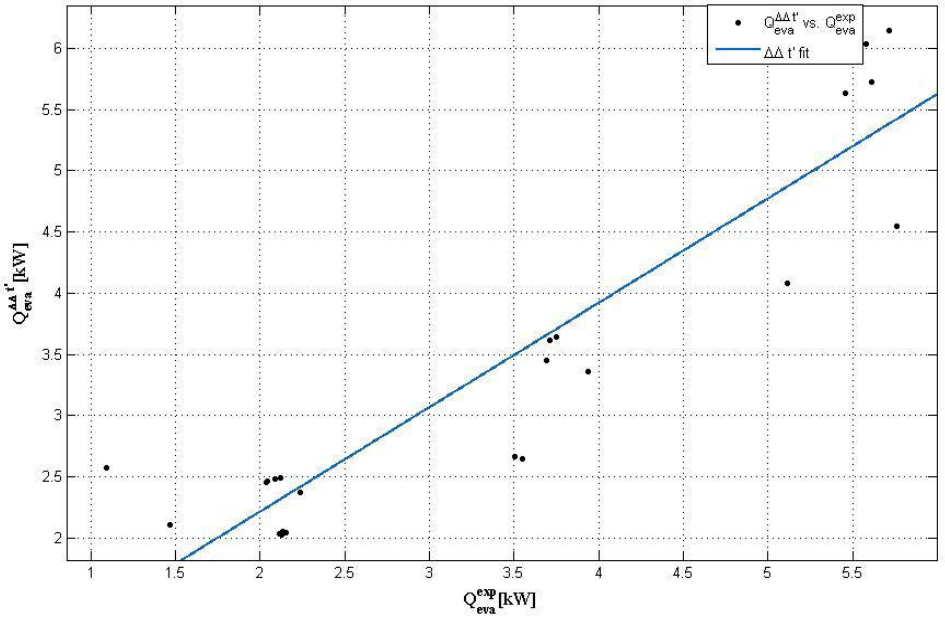

FIGURE 5.3: $\Delta\Delta t'$ Comparison between measured and predicted evaporator

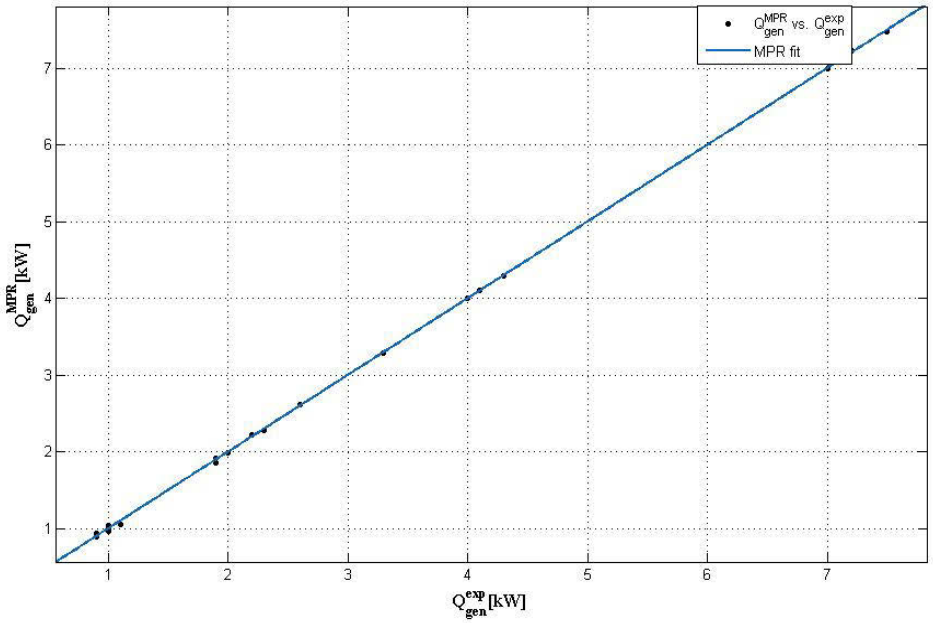

FIGURE 5.4: MPR Comparison between measured and predicted generator

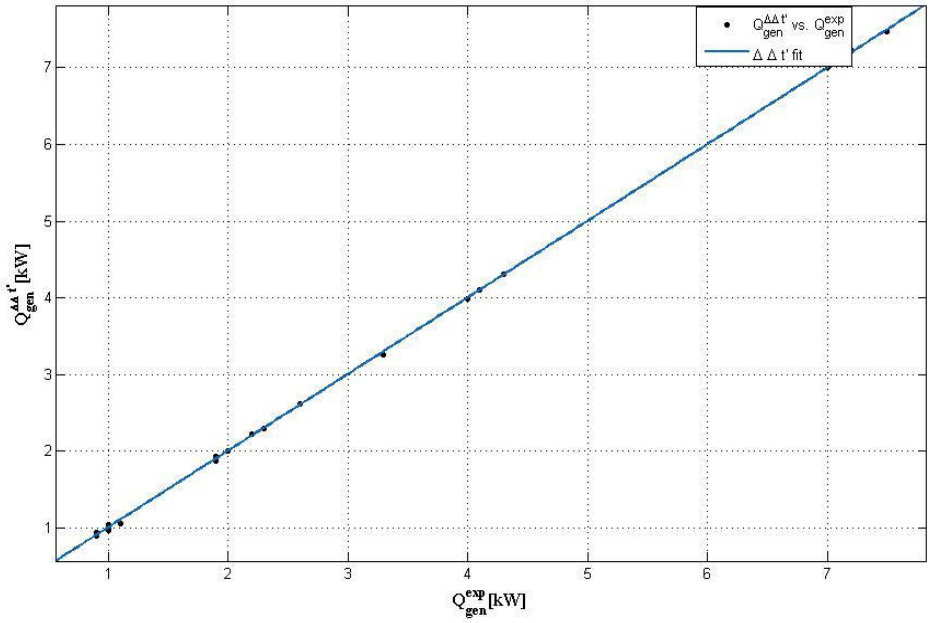

FIGURE 5.5: $\Delta\Delta t'$ Comparison between measured and predicted generator

TABLE 5.3: Statistical Indicators - Viuna

Parameter	Load	$\Delta\Delta t'$	MPR
R^2	Q_{eva}	0.8465	0.9861
	Q_{gen}	0.9999	0.9999
RMSE	Q_{eva}	0.5688	0.1883
	Q_{gen}	0.02578	0.02367
SS_{res}	Q_{eva}	7.117	0.7805
	Q_{gen}	0.01462	0.01233

5.5 Conclusion

The steady-state modelling of a small capacity absorption chiller are presented by a comprehensive comparison of different methods. All the models focus on measurements of external water circuits. Two different methods ($\Delta\Delta t'$ and MPR) are applied to model Viuna absorption chiller performance. Excellent statistical indicators (R^2 around 0.99) shows that either of the two methods ($\Delta\Delta t'$ and MPR) predicts the performance of absorption systems. These methods are used for other purposes like control and monitoring, fault detection and optimisation.

Chapter 6

Energy Optimisation of Chiller Plant

6.1 Introduction

A chiller plant is a very high power-consuming unit in a building. Most studies in the literature use either enumeration or simulation-based models. The enumeration-based models have no mathematical basis while simulation based models do not span the entire performance of components and do not produce good solutions. The results are not valid unless physical changes apply to the plant for enumeration-based models. This study uses a novel formulation technique combining the two methods. The method uses performance map of equipment to build the models along with systems optimisation theory using hybrid optimisation method to optimise chiller plants. A software model is developed for HVAC plant to achieve energy savings. Chiller plant optimisation is addressed in the literature using two different types of optimisation: operation-mode optimisation and set-point optimisation. In the present study, a hybrid algorithm is developed which overcomes the drawbacks of two-stage optimisation. This

algorithm uses one optimisation instead of two optimisations for set-point and operation modes. A classical optimisation technique-SQP-is combined with modified branch and bound method of integer optimisation for solving the chiller plant optimisation problem.

6.2 Chiller plant optimisation problem

The objective of chiller plant optimisation is to minimize the total power consumed by main components. The main energy consuming components are chillers, pumps and cooling tower fans. The condenser water loop is considered for optimisation of power on input load requirement and outside air temperatures. Design variables are percentage load of chiller, generator inlet temperature, absorber condenser inlet temperture, evaporator outlet water temperature and percentage of cooling tower fan speed. The problem is expressed as:

$$Minf(\vec{X}) = w_1 P_{ch}(\vec{X}) + w_2 P_p(\vec{X}) + w_3 P_{ctf}(\vec{X}). \tag{6.1}$$

where $\vec{X} = \{ \mathrm{PL}_{ch}, T^{in}_{gen}, T^{in}_{ac}, T^{out}_{eva}, PS_f \}$

(1) Input load equilibrium constraint

This constraint ensures that total input load required (as input variable) matches the load obtained for percentage loading of each chiller and maximum capacity of the chiller:

$$IL(\vec{X}) = (PL_{ch} Ch_{max})/100 \tag{6.2}$$

where Ch_{max} is maximum chiller capacity.

(2) Upper and lower bounds on the design variables

The design variables is limited to certain bounds of operation based on overall chiller plant and equipment specifications indicated by manufacturer. The bounds are specified as:

$40 \leq PL_{ch} \leq 100$

$70°C \leq T^{in}_{gen} \leq 90°C$

$26°C \leq T^{in}_{ac} \leq 35°C$

$7°C \leq T^{out}_{eva} \leq 12°C$

$30 \leq PS_{f} \leq 100$

6.3 Single effect absorption chiller

The single effect absorption chiller consists of generator, condenser, absorber and evaporator. In the hot water absorption chiller, hot water flows and returns from vacuum solar collectors. Cooling water flows and returns from cooling tower and chilled water flows and returns from the fan coil unit.

6.3.1 Chiller Model

The absorption chiller was formulated based on the multivariable polynomial regression model. MPR models are useful tools for describing non-linear relationships between input and output variables. The parameters of MPR model are calculated by fitting experimental data minimising sum of squares using a polynomial function. MPR models are applied in various fields such as

forecasting, control, optimisation, fault detection and diagnosis [41 , 55 , 37]. A polynomial regression model contains squared and higher order terms of estimator variables. It has been decided to apply second order polynomials and predict absorption chiller performance. MPR models are developed to calculate thermal loads of the absorption chiller by using measurements of external chillers: generator inlet temperature, absorber/condenser inlet temperature and evaporator outlet temperature.

The ten coefficients in the above model are fitted from experimental data. These coefficients have no physical meaning and cannot be interpreted in physical terms.

The second order model of absorption chillers can be represented using Eq. 6.3:

$$\begin{aligned} \dot{Q}_k &= \beta_{0,k} + \beta_{1,k} T^{in}_{gen} + \beta_{2,k} T^{in}_{ac} + \beta_{3,k} T^{out}_{eva} + \beta_{4,k} T^{in}_{gen} T^{in}_{ac} + \beta_{5,k} T^{in}_{gen} T^{out}_{eva} + \beta_{6,k} T^{in}_{ac} T^{out}_{eva} \\ &\quad + \beta_{7,k} (T^{in}_{gen})^2 + \beta_{8,k} (T^{in}_{ac})^2 + \beta_{9,k} (T^{out}_{eva})^2 . \end{aligned} \tag{6.3}$$

System's coefficient of performance is given by

$$COP = \frac{Q_{eva}}{Q_{gen}} . \tag{6.4}$$

The system of performance (SP) is defines as 1/COP

$$PL_{ch} = (\frac{Q_{eva}}{Q_{cap}}) \times 100 . \tag{6.5}$$

The part load percentage of the chiller is calculated as the ratio of heat rejected by the evaporator, the cooling rate of the operating chiller, to the cooling capacity of the chiller.

The chiller power is calculated as:

$$P_{ch} = \frac{SP \times PL_{ch}}{100} . \tag{6.6}$$

Thus the present chiller model can predict required power consumption of the chiller depending on the percentage load at which the chiller functions, PL_{ch}. The percentage load of the chiller is calculated as the ratio of operating cooling rate to maximum chiller capacity.

TABLE 6.1: Notation Description for Chiller

Notation	Description
COP	Coefficient of Performance
Q_{eva}	Heat rejected by evaporator, Cooling rate
Q_{gen}	Heat absorbed by generator
Q_{cap}	Cooling capacity of chiller
PL_{ch}	Part Load of Chiller
T_{gen}^{in}	Generator inlet temperature
T_{ac}^{in}	Absorber Condenser inlet temperature
T_{eva}^{out}	Evaporator outlet temperature

6.3.2 Model Calibration

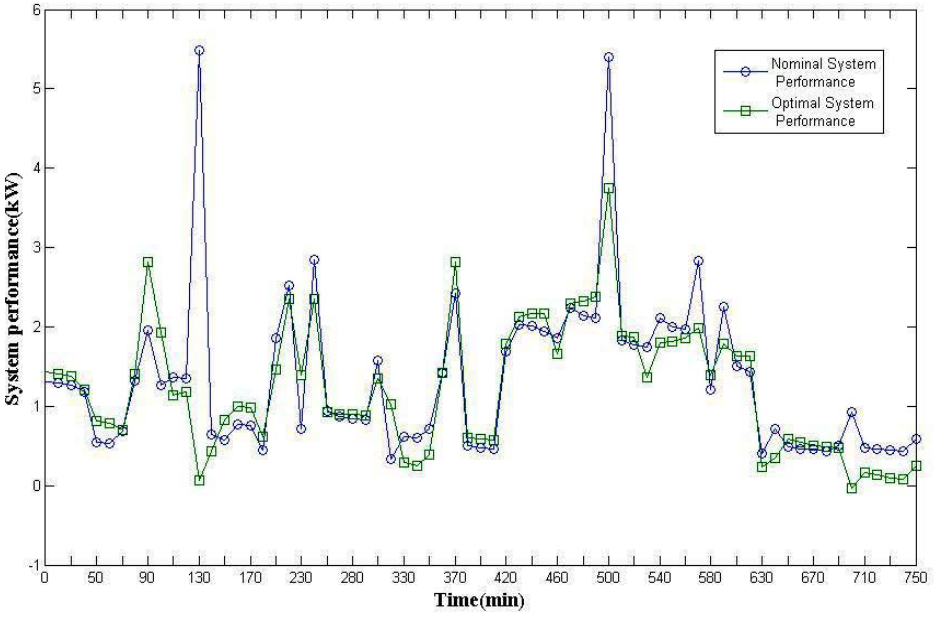

FIGURE 6.1: System Performance

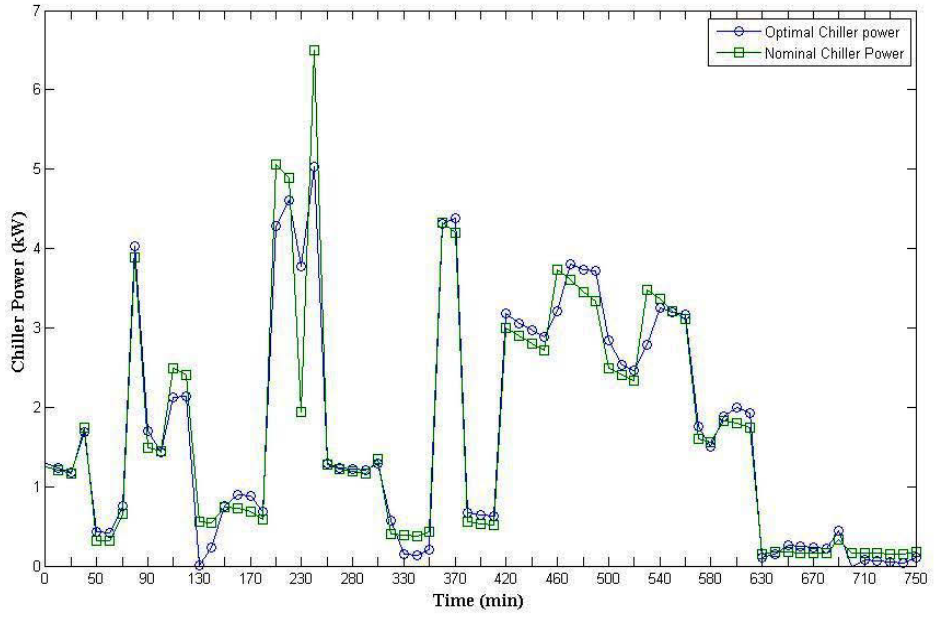

FIGURE 6.2: Chiller Power

A multivariable polynomial regression method is used to fit heat rejected by evaporator and heat absorbed by the generator. The COP of the chiller is calculated as the ratio of heat rejected by the evaporator and heat absorbed by the generator from the multivariable polynomial regression method. The system performance is estimated as 1/COP for the chiller for both nominal and optimal modes as shown in Figure 6.1. Figure 6.2 displays the variation of chiller power consumption for different time intervals. The chiller power curve has maximum and minimum for input load. The nominal chiller power varies from 0.1485 kW to 6.4987 kW whereas the optimal chiller power varies from 0.0132 kW to 5.0371 kW. The pattern of variation for both nominal and optimal modes of operation for the chiller is similar.

TABLE 6.2: Calibrated Parameter Values for Chiller

k	$\dot{Q}_{eva}$	$\dot{Q}_{gen}$
β_0	-133.2703	-288.7422
β_1	4.3602	10.5361
β_2	-5.9775	-7.9637
β_3	13.5639	-17.9224
β_4	-0.0337	0.0660
β_5	-0.1131	0.3353
β_6	-0.1745	-0.3932
β_7	-0.0119	-0.0836
β_8	0.1526	0.0922
β_9	-0.0422	0.3898

6.4 Primary Pump

The variable speed primary pump finds flow rate through the evaporator of the chiller. It plays a key role in finding the cooling load on chillers, and resulting chiller COP.

6.4.1 Model

The chilled water pump is optimised as proposed by Haves[23]. The chilled water pump used in the chiller plant has pressure rise, also know as pump head, for a nominal pump speed N_o and is modelled as a quadratic function:

$$\Delta P_o(q_o) = a_o + a_1 q_o + a_2 q_o^2, \tag{6.7}$$

where q_o is the nominal volumetric flow rate and ΔP_o is the nominal pressure across the pump. Similarly, the efficiency curve of the pump for a nominal pump speed is modelled as a quadratic function

$$\eta(q_o) = b_o + b_1 q_o + b_2 q_o^2. \tag{6.8}$$

The pressure and efficiency curves use the following laws for addressing the variable speed operation of the pump

$$\frac{q}{q_o} = \frac{N}{N_o}, \tag{6.9}$$

whereas the ratio of pump speed N to nominal pump speed is denoted as R. If N_o is maximum pump speed, then $0 \leq R \leq 1$. The general pump pressure curve takes the form

$$\Delta P = R^2(\Delta P_o)(q/R), \tag{6.10}$$

where $\Delta P_o = P_o - P_i$, and the pump power is calculated as:

$$P = \frac{\Delta P q}{\eta(q/R)} \ . \tag{6.11}$$

Assuming variable speed drive and pump motor eject heat to ambient mechanical space, the energy balance between inlet and outlet of the pump is

$$0 = m(h_i - h_o). \tag{6.12}$$

TABLE 6.3: Notation Description for Pump

Notation	Description
a	Coefficients for quadratic pressure difference curve
b	Coefficients for quadratic efficiency curve
N	Pump motor speed
P	Pump Power[W]
q	Volumetric flow rate [m^3/s]
R	ratio of drive speed to nominal speed[rpm/rpm]
ρ	fluid density[kg/m^3]
i	Pump inlet
o	Pump outlet

6.4.2 Model Calibration

The figures 6.3, 6.4 and 6.5 illustrate the quality of curve fit for the selected pump. The pump power is found from equation 6.11 as shown in Figure 6.5.

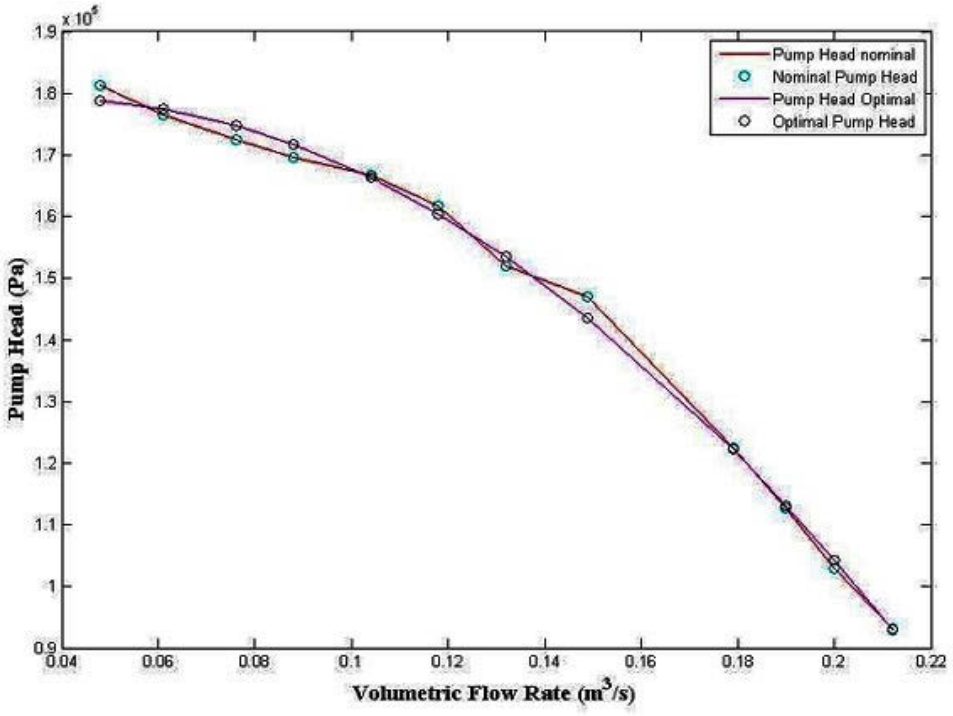

FIGURE 6.3: Pump Head

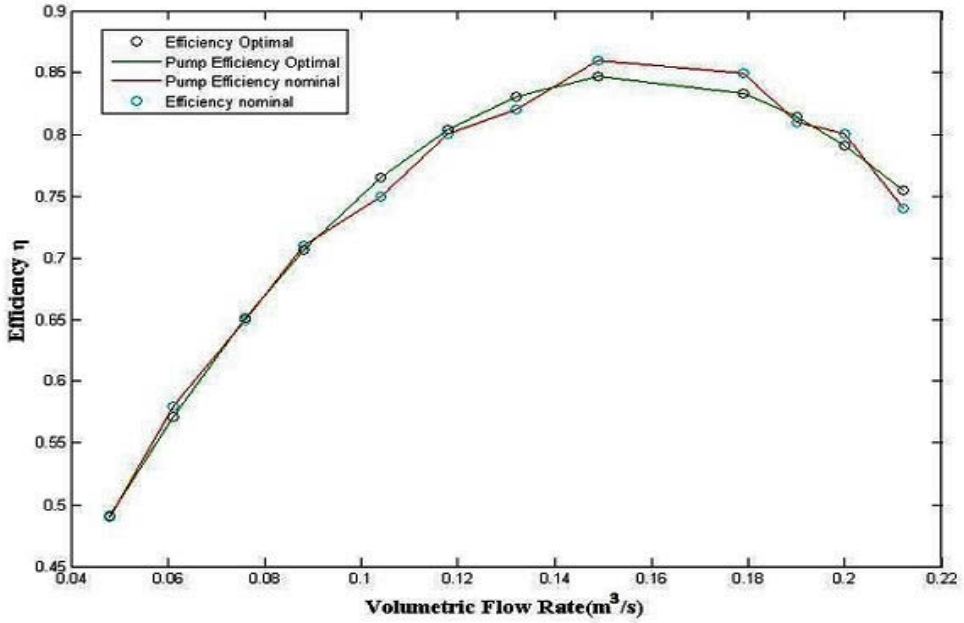

FIGURE 6.4: Pump Efficiency

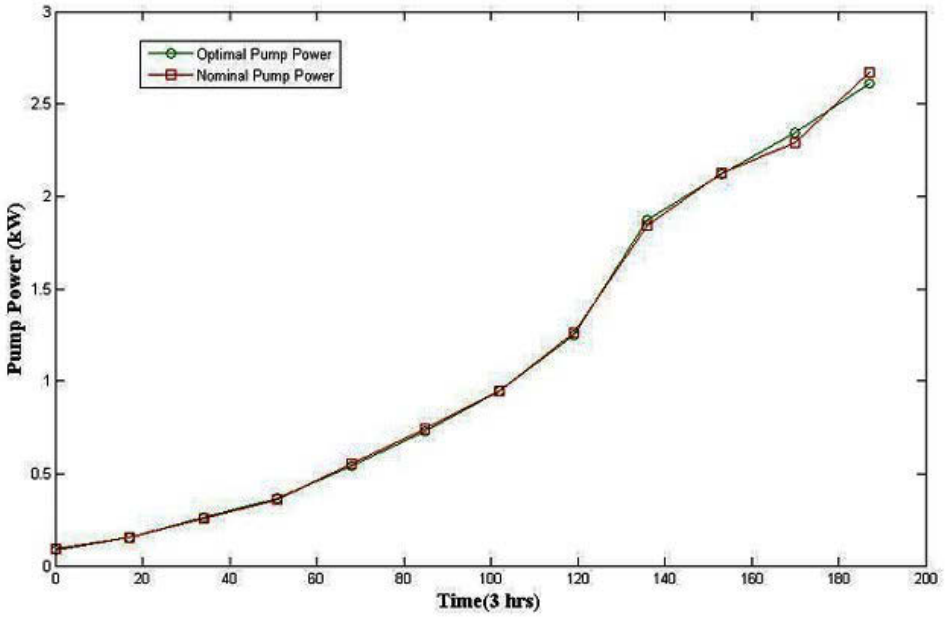

FIGURE 6.5: Pump Power

Like the pump curve, the system curve $\Delta P = C_0 + C_1 + C_2 q^2$ represents pressure loss as a function of flow rate. The primary pump was unable to achieve 225 kg/s flow rate. Instead, the primary pump was only able to produce 212 kg/s. Therefore, system curve is fit using data processing limited number of points with the pump at less than full speed. The pressure drop across the evaporator of each chiller specified by design specifications is used to calculate the turbulent pressure loss as quadratic terms. The pressure drop in the primary loop pipe models as the linear function of flow rate, and the coefficient C_1 tunes to fit measured flow rates data given pump speed.

TABLE 6.4: Calibrated parameter values for chiller pump

$A_0 = 1.754 \times 10^5$	$A_1 = 2.030 \times 10^5$
$A_2 = -2.7932 \times 10^6$	$B_0 = 1.036 \times 10^{-1}$
$B_1 = 9.5258 \times 10^0$	$B_2 = -3.0442 \times 10^1$
$C_0 = 0 \times 10^0$	$C_1 = 1.9072 \times 10^5$
$C_2 = -4.4047 \times 10^5$	

6.5 Cooling Tower

6.5.1 Model

The power consumed by a fan drive is represented by a cubic function as proposed by Haves[23].

$$P_{fan} = P_{fan,0}(N_{fan}/N_{fan,0})^3 \tag{6.13}$$

TABLE 6.5: Notation Description for Cooling Tower

Notation	Description
N_{fan}	fan speed(rpm)
$N_{fan,0}$	design fan speed(rpm)
P_{fan}	fan power[kW]

6.5.2 Model Calibration

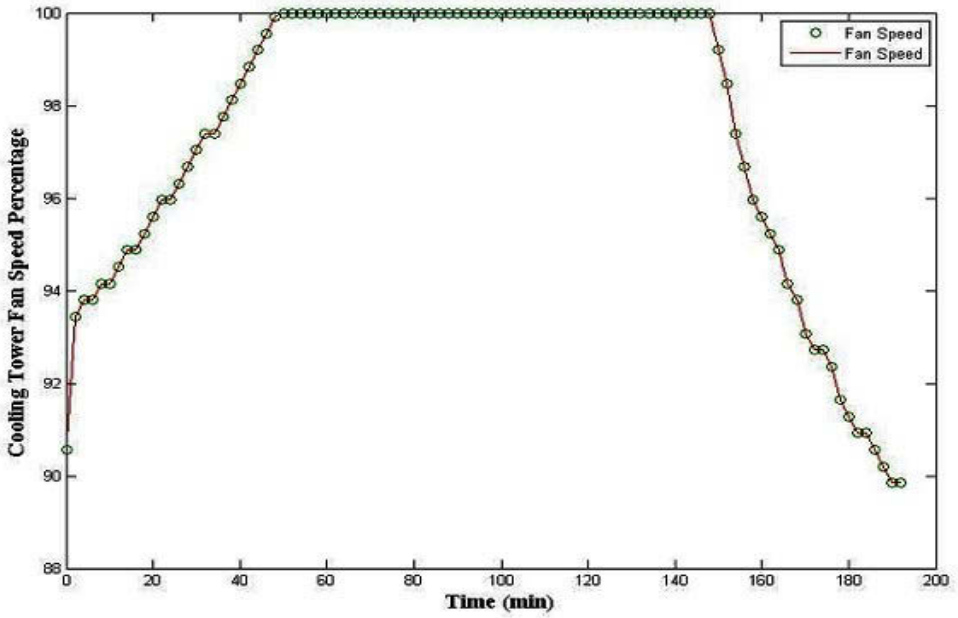

FIGURE 6.6: Cooling Tower Fan Speed

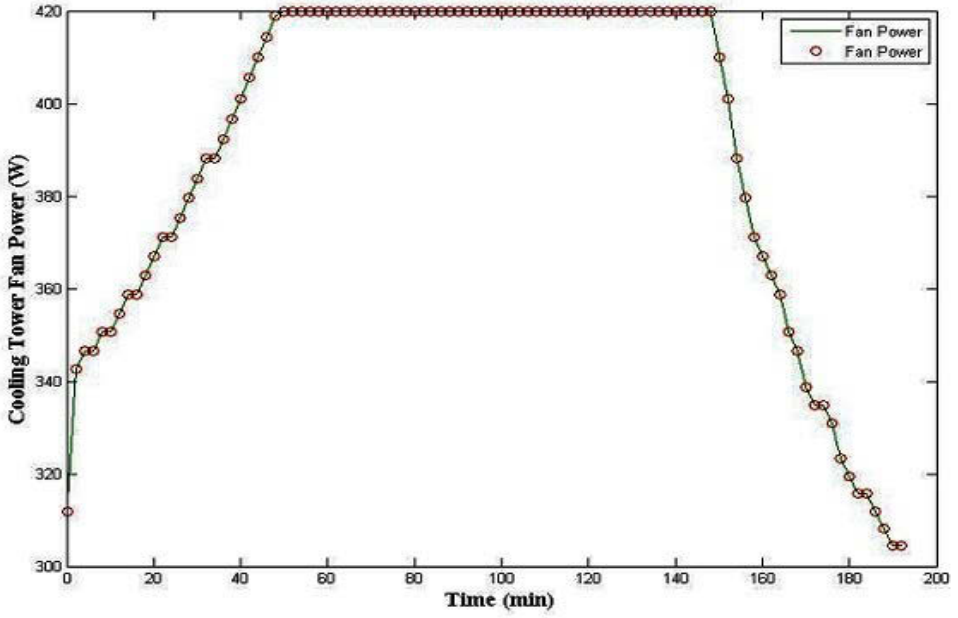

FIGURE 6.7: Cooling Tower Fan Power

The variation in cooling tower fan speed percentage is found from leaving water temperature for cooling tower. The fan speed percentage changes with respect to the leaving water temperature for the cooling tower as shown in Figure 6.5. The variation in cooling tower fan speed is found from input conditions shown in Figure 6.6. The cooling tower fan speed percentage increases from 90% to 100% for chiller charging period. It remains constant at 100% for one hour and decreases from 100% to 90% for the last half hour. The cooling tower fan power increases from 310 W to 420 W as a cubic function of fan speed percentage for one hour. It remains constant at 420 W of maximum power for one hour and decreases to 300 W as a cubic function of fan speed percentage for last half hour.

TABLE 6.6: Calibrated cooling tower parameters

$N_{fan,0} = 100\%$	$P_{fan,0} = 420W$

6.6 Chiller Plant Optimisation Problem

The objective of chiller plant optimisation is minimising the total power consumed by the main components. The main energy-consuming components in a chiller plant are chillers, pumps and cooling tower fans. The design variables are percentage load of chillers, pump head and efficiency and the percentage of cooling tower fan speed. The problem is expressed as:

$$Minf(\vec{X}) = w_1 P_{ch}(\vec{X}) + w_2 P_p(\vec{X}) + w_3 P_{ctf}(\vec{X}). \tag{6.14}$$

The above power calculations for nominal and optimal modes of operation are used to plot bar graph for chiller, cooling tower fan and chilled water pump.

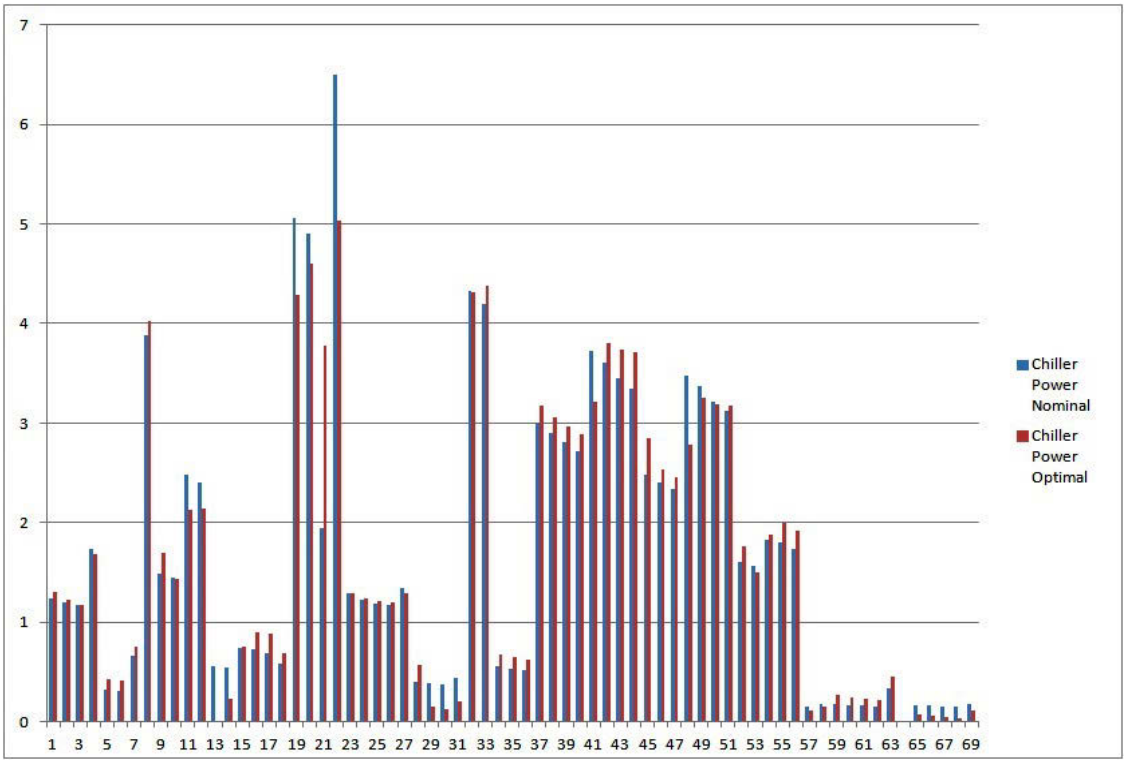

FIGURE 6.8: Chiller Power bar graph

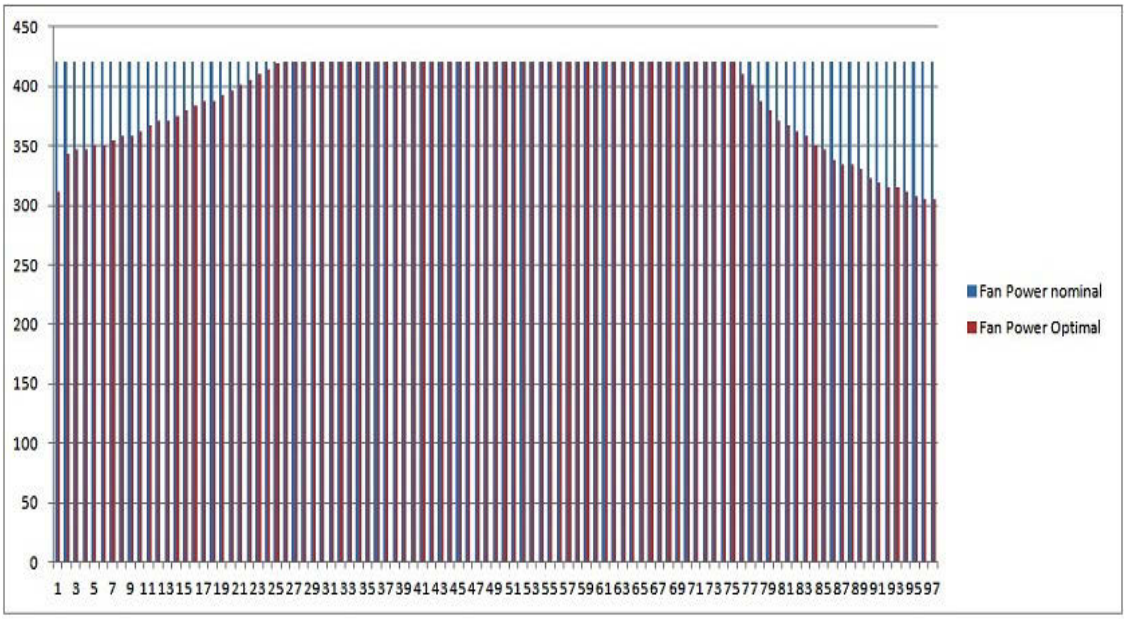

FIGURE 6.9: Cooling Tower fan power bar graph

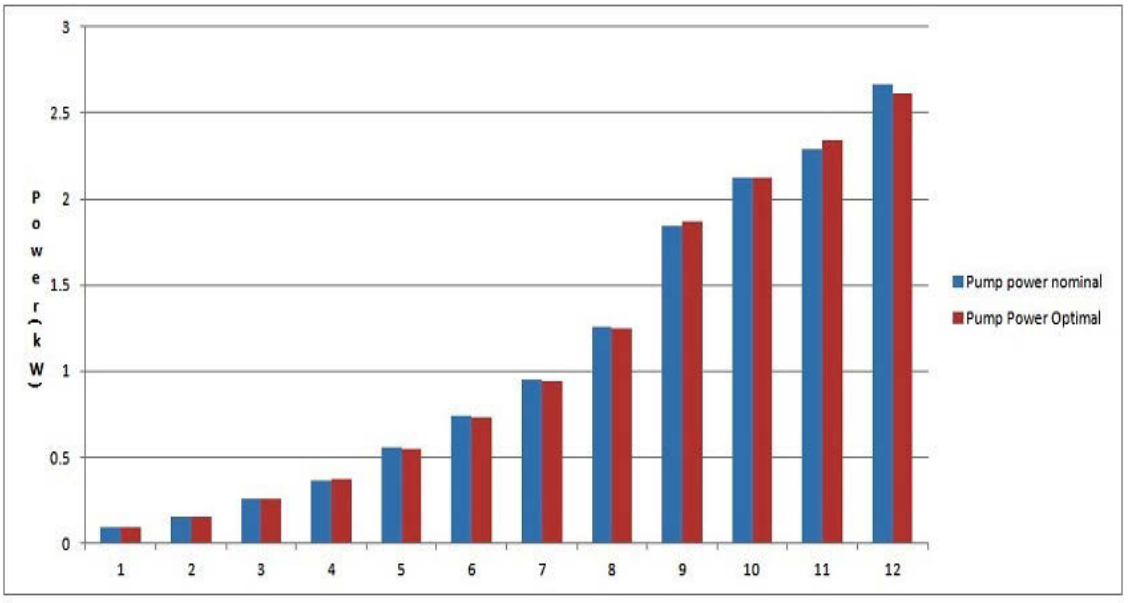

FIGURE 6.10: Pump Power bar graph

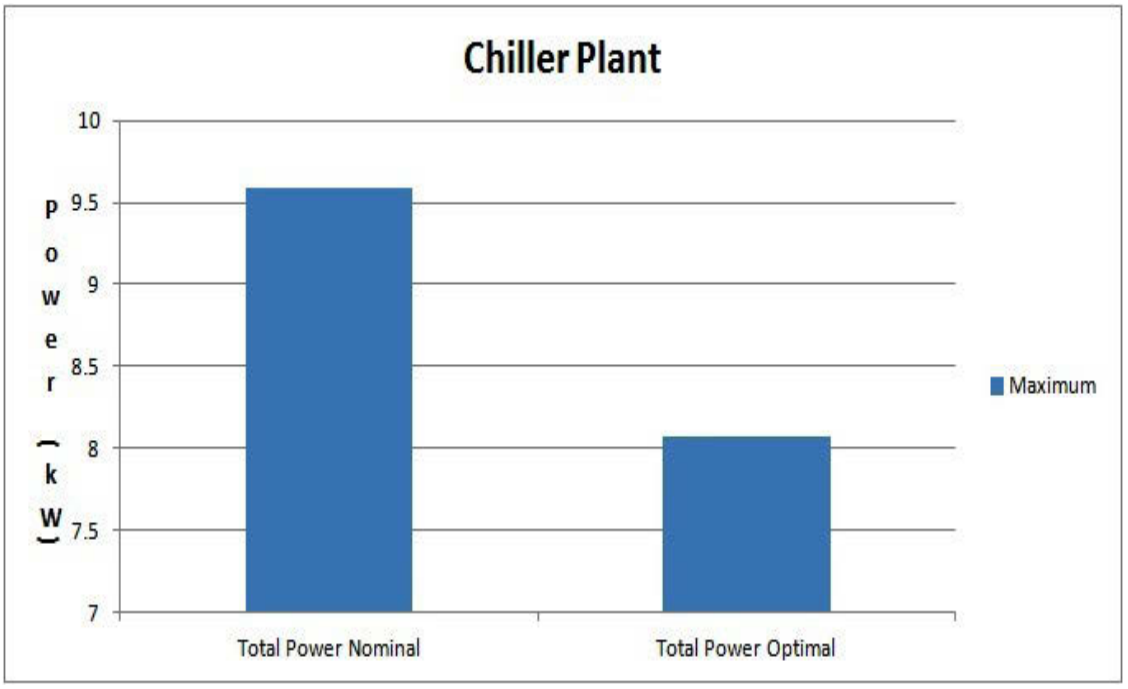

FIGURE 6.11: Total Power bar graph

From the bar graphs for chiller, cooling tower fan and pump, the weighting factors can be calculated from the maximum for chiller, cooling tower fan and pump for nominal and optimal performance.

$W_1 = 1.290167; W_2 = 1.022759; W_3 = 1$

Total nominal Power Consumption for chiller plant =

$Pump_{nominal} + Towerfan_{nominal} + Chiller_{nominal} = 2.668316 + 0.42 + 6.4987 = 9.587kW.$

Total optimal Power Consumption for chiller plant =

$Pump_{optimal} + Towerfan_{optimal} + Chiller_{optimal} = 2.608938 + 0.42 + 5.0371 = 8.066kW.$

The average power consumption for the nominal mode is 9.587 kW whereas optimisation method results gave an average power consumption of 8.066 kW. Hence using the optimisation

mode decreases power consumption by 1.521 kW. This shows the amount of savings in power and operating cost of the chiller plant. The power savings are mainly due to optimal chiller loading and power consumed by chilled water pumps. However, the energy savings for the chiller plant are small as a small capacity absorption chiller is used for optimisation. However, high capacity absorption chillers may lead to very considerable energy savings by the above optimisation approach.

6.7 Conclusion

In this research, the optimisation problem is presented for water-cooled chilled water plants. The chiller plant optimisation problem is formulated by developing multi-variable regression models using equipment performance data. The water-cooled chiller plant optimisation involves the optimal combination of equipment and operating levels for minimum electrical power consumption. The numerical results indicate the validity and effectiveness of the chiller plant formulation and hybrid optimisation strategy.

Chapter 7

Conclusion and Future Work

7.1 Summary and Conclusion

The work carried out in this thesis meets the aim of developing methods for testing, modelling and optimisation strategy for the small capacity absorption machine. It is developed from important experimental work and forms the basis for simple and accurate models for small capacity absorption machines. Models are formed based on external circuit parameters using several approaches.

A comprehensive literature review in Chapter 2 provides a better understanding of absorption technologies. The study provides valuable information for an absorption machine, from operating principles to usability and applications. A particular emphasis is given for small capacity absorption machines according to the main aim of the thesis. The latest achievements in a small capacity absorption machine are presented as a review of actual trends and most important applications for use such as solar cooling. There is comprehensive progress in results

from the last two decades. However, most of the barriers are overcome to make them competitive with vapour compression units. There are different reasons that prevent absorption machine potential in primary energy savings and environmental benefits. These are high initial cost, lower performance, lack of serial production, poor system design and inadequate control. Regulations and incentives are very important measures for further development. However, intensive work on simulations, optimisation and control strategy improvements are some of the actions that will fill the gap compared with conventional systems. The development of appropriate standards, best practice guides and test procedures are further steps that will fill the gap compared with conventional systems.

Chapter 3 provides the radiant time series method for performing design cooling load calculations, derived from the heat balance method. Radiant time series replaces cooling load temperature difference/ solar cooling load / cooling load factor (CLTD/SCL/CLF). Radiant time series calculates conductive heat gain on 24-term response part series and instantaneous radiant heat gains on 24-term ”radiant time series” for calculating cooling loads. This chapter describes the radiant time series method and generation of response factors and radiant time series coefficients and gives a brief comparison with the CLTD method.

The final result is the test procedure that has important steps such as test planning, data modelling, the uncertainty estimation and analysis of results. Measurement of external parameters are monitored, and the process creates performance of absorption machine. System modelling is performed for absorption chiller, evacuated solar collectors, cooling tower and fan coil. Data is used to form the database that is further used for model development. The data collected during these tests are used for modelling and analysis of different modelling methods which predicts performance of small capacity absorption chillers. Two different modelling

methods are the applied adapted characteristic equation ($\Delta\Delta t'$) and the multivariable polynomial regression (MPR) model. Excellent statistical indicators (R^2 value around 0.99) and close agreement with experimental data show that either of the two methods ($\Delta\Delta t'$, MPR) can be used to get a high level of prediction.

Towards the end, the optimisation problem is presented for water-cooled chilled water plants. The chiller plant optimisation problem is planned by developing multi-variable regression models using equipment performance data. Power consumption of absorption chiller, chilled water pump and cooling tower fan are calculated after optimisation of the chiller plant. Total energy consumption of the chiller plant are compared for nominal and optimal modes of operation. Numerical results show the validity and effectiveness of the chiller plant formulation and hybrid optimisation strategy.

7.2 Thesis Contribution

The thesis contributes to the following knowledge:

1) Cooling load of the lift motor room are compared by Cooling load temperature difference and Radiant time series method.

- Radiant time series is a better and more accurate method for calculating cooling load for the room than cooling load temperature difference method. It calculates cooling load on beam and diffuse solar radiation for every hour for the room.

2) Thermodynamic modelling is performed for solar hot water air conditioning system.

- Experimental chilled water and condenser outlet water temperature results are plotted in Matlab for absorption chiller.

- Thermodynamic modelling of the absorption chiller, cooling tower, fan coil and evacuated solar collectors is performed.

3) Performance of solar hot water absorption chiller is analysed.

- Multivariable polynomial Regression and Adapted Characteristic Equation models are used for performance analysis of absorption chiller.

- Experimental data is compared with Multivariable Polynomial Regression and Adapted Characteristic Equation models for absorption chiller.

4) Total Power consumption of chiller plant is minimised for energy optimisation of solar hot water absorption chiller system.

7.3 Future Work

Most questions are further explored besides the significant contribution of this research. The primary constraint of the models in this research is operating constant flow rates in external water circuits. Therefore, the future tasks include improving the models by variable flow rates. This should lead to more detailed and correct models with more parameters which can be better adjusted in control systems and simulation tools. Another future task is to develop a method for air-cooled absorption machines including economic analysis compared to vapour compression machines. Artificial Neural Network has the ability to map non - linear problems to develop

dynamic models. It includes transient behaviour (start up and shut down period) and thermal inertia of small capacity absorption machines. The performance prediction of HVAC systems is performed by implementing dynamic models in simulation tools. A step further is to develop the method, or a better software tool useful for designing and sizing of absorption chillers plants to work at greatest efficiency.

Appendix A

The steady state design method is used to size the system components. The major design parameters of chilled water of the cooling system is shown in the Table. These parameters represent design day load conditions.

Parameter[unit]	Description	Magnitude
	Cooling Load Estimation by Radiant time series method	
$T_o[^\circ C]$	Outside air temperature	39.3
$RH(\%)$	Relative humidity ratio	50
$T_i[^\circ C]$	Indoor air temperature	25.6
$A_r[m^2]$	Roof Area	24
$A_{wn}[m^2]$	North Wall Area	36
$A_{we}[m^2]$	East Wall Area	24
$E_t[W/m^2]$	Total surface irradiance	734.5
$Q_r[W]$	Cooling Load through roof	486.4
$Q_{wn}[W]$	Cooling Load through wall facing north	2515.5
$Q_{we}[W]$	Cooling Load through wall facing east	1677
$Q_{sensible}[W]$	Sensible cooling load due to Ventilation	156.5
$Q_{Latent}[W]$	Latent cooling load due to Ventilation	351.7
$Q_t[W]$	Total Cooling Load of Lift motor room	5187.1
	Cooling Coil	
$Q_{cc}[W]$	Design Coil Load for Cooling	7000
$T_{sup}[^\circ C]$	Supply air temperature	13
$T_{ret}[^\circ C]$	Return air temperature	25
$T_{chw,i}[^\circ C]$	ChW temperature entering the cooling coil	7
$T_{chw,o}[^\circ C]$	ChW temperature leaving the cooling coil	12
$m_{cc,a}[l/s]$	Air flow rate of cooling coil for the zone	378

$m_{chw}[l/s]$	Chilled water mass flow rate	0.25
	Cooling Coil Fan	
$P_{fcu}[W]$	Power of the fan in cooling coil	45
	Chiller	
COP	COP of the Chiller	0.725
$P_{ch}[kW]$	Power of the chiller	6
	Cooling Tower	
$T_{cw,o}[^{\circ}C]$	Cooled water temperature leaving the cooling tower	29
$T_{cw,i}[^{\circ}C]$	Cooled water temperature entering the cooling tower	34
$m_{cw}[l/s]$	Cooling water mass flow rate	0.76
	Cooling tower fan	
$P_{fan}[W]$	Power of the fan in cooling tower	420

Bibliography

[1] Aksoy, B 2013, BP Global Review by energy type: Primary energy, Word-press blog, weblog post, 12 September, viewed 16 February 2015, https://batuaksoy.wordpress.com/2013/09/12/primary-energy/.

[2] Alizadeh S, Saman WY. An experimental study of a forced flow solar collector/regenerator using liquid desiccant. *Solar Energy* 2002;73(5):345-62.

[3] ASHRAE. Absorption air-conditioning and refrigeration equipment. *In: ASHRAE Guide and Data Book, Equipment*. Chapter 14. New York : ASHRAE, 1972.

[4] Assilzadeh, F., Kalogirou, S.A., Ali, Y., and Sopian, K., "Simulation and optimization of a LiBr solar absorption cooling system with evacuated tube collectors", *Renewable Energy*, vol. 30, no. 8, pp. 1143-1159, 2005.

[5] Atmaca, I., and Yigit, A., "Simulation of solar-powered absorption cooling system", *Renewable Energy*, vol. 28, no. 8, pp.1277-1293, 2003.

[6] Balghouthi, M., Chahbani, M.H., and Guizani, A., "Feasibility of solar absorption air condition in Tunisia", *Building and Environment*, vol. 43, no. 9, pp. 1459-1470, 2008.

[7] Blinn JC, Mitchell JW, Duffie JA. Modeling of transient performance of residential solar air-conditioning systems. *In: Proceedings of the ISES, Silver Jubilee Congress*, Atlanta, Georgia, May 1979. vol.1. p.705-9.

[8] Bliss RW. The derivation of several plate efficiency factors useful in the design of flat plate collectors. *Solar Energy* 1959;3(4):55-64.

[9] Butz LW, Beckman WA, Duffie JA. Simulation of a solar heating and cooling systems. *Solar Energy* 1974;16:129-36.

[10] Charters WWS, Chen WD. Some design aspects of air cooled solar powered $LiBr - H_2O$ absorption cycle airconditioning systems. *In: Proceedings of the ISES, Silver Jubilee Congress*, Atlanta, Georgia, May 1979. Vol. 1. p.725-8.

[11] Dai YJ, Wang RZ, Zhang HF, Yu JD. Use of desiccant cooling to improve the performance of vapour compression air conditioning. *Applied Thermal Engineering* 2001;21:1185-201.

[12] Fathalah K, Aly SE. Study of a waste heat driven modified packed desiccant bed dehumidifier. *Energy Conversion Management* 1996;37(4):457-71.

[13] Florides, G.A., Kalogirou, S.A., Tassou, S.A., and Wrobel, L.C., "Design and construction of LiBr-water absorption machine", *Energy Conversion Management*, vol. 44, no. 15, pp. 2483-2508, 2003.

[14] Florides, G.A., Kalogirou, S.A., Tassou, S.A., and Wrobel, L.C., "Modelling and simulation of an absorption solar cooling system for Cyprus", *Solar Energy*, vol. 72, no. 1, pp. 43-51, 2002.

[15] G.A. Florides, S.A. Kalogirou, S.A. Tassou, and L.C. Wrobel, "Modelling, simulation and warming impact assessment of a domestic-size absorption solar cooling system," *Applied Thermal Engineering*, vol. 22, pp. 1313-1325, 2002.

[16] Garimella S., Christensen R.N., Lacy D. Performance evaluation of a generator-absorber heat-exchange heat pump. *Applied Thermal Engineering* 1996; 16(7): 591-604.

[17] Ginestet S, Stabat P, Marchio D. Control of open cycle desiccant cooling systems minimising energy consumption. Centre denergetique, Ecole de Mines de Paris gineste@cenerg.ensmp, marchio@cenerg.ensmp,gineste@cenerg.ensmp.

[18] Gordon J.M., Ng K.C. A general thermodynamic model for absorption chillers: Theory and experiment. *Heat Recovery Systems and CHP* 1995; 15(1): 73-83.

[19] Grossman G., Zaltash A. ABSIM - modular simulation of advanced absorption systems. *International Journal of Refrigeration* 2001; 24(6): 531-43.

[20] Ha, Q. and Vakiloroaya, V., 2013. A new single-effect hot-water absorption chiller air conditioner using solar energy, *Power Engineering Conference (AUPEC), 2013 Australasian Universities* 2013, IEEE, pp. 1-6.

[21] Halliday SP, Beggs CB, Sleigh PA. The use of solar desiccant cooling in the UK: a feasibility study. *Applied Thermal Engineering* 2002;22:1327-38.

[22] Handbook, A.S.H.R.A.E., 2009. Fundamentals Atlanta: American Society of Heating, Air-Conditioning and Refrigeration Engineers. Inc.

[23] Haves, P., 2010. Model predictive control of HVAC systems: Implementation and testing at the University of California, Merced. Lawrence Berkeley National Laboratory.

[24] Hayek, M., Assaf, J. and Lteif, W., 2011. Experimental investigation of the performance of evacuated-tube solar collectors under eastern mediterranean climatic conditions. *Energy Procedia*, 6, pp. 618-626.

[25] Hellmann H.- M., Ziegler F.F. Simple absorption heat pump modules for system simulation programs. *ASHRAE Transactions* 1999; 105.

[26] Henning H-M, Erpenbeck T, Hindenburg C, Santamaria IS. The potential of solar energy use in desiccant cycles. *International Journal of Refrigeration* 2001;24:220-9.

[27] Hottel HC, Whillier A. Evaluation of flat-plate solar collector performance. *In: Transcripts of the Conference on Solar Energy, University of Arizona, II (Thermal Processes)* 1955. P. 74-104.

[28] Hu HL. Computer simulation and system performance analysis of the solar powered air-conditioning and heat providing system. Master thesis, Guangzhou Institute of Energy Conversion, Chinese Academy of Sciences, 1991.

[29] IEA, Energy Technology Perspectives 2010. Scenarios Strategies to 2050.

[30] International Energy Outlook 2010. US. Department of Energy, Washington, DC 20585, DOE/EIA- 0484(2010); July 2010.

[31] Jain S, Dhar PL. Evaluation of solid desiccant-based evaporative cooling cycles for typical hot and humid climates.*International Journal of Refrigeration* 1995;18(5):287-96.

[32] Jain S, Dhar PL, Kaushik SC. Experiments studies on the dehumidifier and regenerator on a liquid desiccant cooling system. *Applied Engineering* 2000;20:253-67.

[33] Joudi K.A., Lafta A.H. Simulation of a simple absorption refrigeration system. *Energy Conversion and Management* 2001; 42(13): 1575-605.

[34] Kaynakli O., Kilic M. Theoretical study on the effect of operating conditions on performance of absorption refrigeration system. *Energy Conversion and Management* 2007; 48(2): 599-607.

[35] Kühn A., Ziegler F. Operational results of a 10 kW absorption chiller and adaptation of the characteristic equation. *In: Proceedings of First International Conference on Solar Air Conditioning* 2005; Bad-Staffelstein, Germany.

[36] Khan AY, Martinez JL. Modelling and parametric analysis of heat and mass transfer performance of a hybrid liquid desiccant absorber. *Energy Conversion Management* 1998;37(10):1095-112.

[37] Kim M., Yoon S.H., Payne W.V., Domanski P.A. Development of the reference model for a residential heat pump system for cooling mode fault detection and diagnosis. *Journal of Mechanical Science and Technology* 2010; 24(7): 1481-9.

[38] Kinsara AA, Omar M, Rabghi A, Alsayes MM. Parametric study of an energy efficient air conditioning system using liquid desiccant. *Applied Thermal Engineering* 1997;18(5):327-35.

[39] Klien SA, Duffie JA, Beckman WA. Transient considerations of flat-plate collectors. *Trans ASME, Journal of Engineering for Power* 1974;96A:109.

[40] Kong, D., Liu, J., Zhang, L., He, H. and Fang, Z., 2010. Thermodynamic and experimental analysis of an ammonia-water absorption chiller. *Energy and Power Engineering*, 2(04), pp. 298.

[41] Lee T.-S., Lu W.-C. An evaluation of empirically-based models for predicting energy performance of vapor-compression water chillers. *Applied Energy* 2010; 87(11): 3486-93.

[42] Leite A.P.F., Belo F.A., Martins M.M., Riffel D.B. Central air conditioning based on adsorption and solar energy. *Applied Thermal Engineering* 2011; 31: p.50-58.

[43] Li CH, Wang RZ, Lu YZ. Investigation of a novel combined cycle of solar powered adsorption-ejection refrigeration system. *Renewable Energy* 2002;26:611-22.

[44] Li, Z.F, Sumathy, K. Technology development in the solar absorption air-conditioning systems. *Renewable and Sustainable Energy Reviews* 2000;4:p.267-293.

[45] Lof GOG, Tybot RA. The design and cost of optimised systems for residential heating and cooling by solar energy. *Solar Energy* 1974;16:9-18.

[46] Mansoori GA, Patel V. Thermodynamics basis for the choice of working fluids for solar absorption cooling systems. *Solar Energy* 1979;22:483-91.

[47] Mateus, T., and Oliveira, A.C., "Energy and economic analysis of an integrated solar absorption cooling and heating system in different building types and climates", *Applied Energy*, vol. 86, no. 6, pp. 949-957, 2009.

[48] Mavroudaki P, Beggs CB, Sleigh PA, Halliday SP. The potential for Solar powered single-stage desiccant cooling in southern Euro. *Applied Thermal Engineering* 2002;22:1129-40.

[49] Mazzei P, Minichiello F, Palma D. Desiccant HVAC systems for commercial buildings. *Applied Thermal Engineering* 2002;22:545-60.

[50] M.C. Rodrıguez Hidalgo, P. Rodrıguez Aumente, M. Izquierdo Millan, A. Lecuona Neumann, and R. Salgado Mangual, "Energy and carbon emission savings in Spanish

housing air-conditioning using solar driven absorption system," *Applied Thermal Engineering*, vol. 28, pp. 1734–1744, 2008.

[51] Munner T, Uppal AH. Modeling and simulation of a solar absorption cooling system. *Applied Energy* 1985;19:209-29.

[52] Nunez T, Mittelbach W, Henning HM. Development of an adsorption chiller and heat pump for domestic heating and air-conditioning applications. *In: Proceedings of the third international conference on heat powered cycles (HPC 2004)*; 2004.

[53] Parsons, R.A. (1997). 1997. *ASHRAE Handbook: 1997 Fundamentals* .

[54] Puig-Arnavat M., Lopez-Villada J., Bruno J.C., Coronas A. Analysis and parameter identification for characteristic equations of single- and double-effect absorption chillers by means of multivariable regression. *International Journal of Refrigeration* 2010; 33(1): 70-8.

[55] Reddy T.A., Niebur D., Andersen K.K., Pericolo P.P., Cabrera G. Evaluation of the Suitability of Different Chiller Performance Models for On- Line Training Applied to Automated Fault Detection and Diagnosis (RP-1139). *HVAC&R Research* 2003; 9(4): 385-414.

[56] Restuccia G, Freni A, Vasta S, Aristov Y. Selective water sorbent for solid sorption chiller: experimental results and modelling. *International Journal of Refrigeration* 2004;27(3):284-93.

[57] Roper, L.D., Solar Collectors Orientation, viewed 17 April 2015, www.roperld.com/science/solarcollectorsorientation.pdf.

[58] Sayegh, M.A., "The solar contribution to air conditioning systems for residential buildings", *Desalination*, vol. 209, vol. 1-3, pp. 171-176, 2007.

[59] Shen CM, Worek WM. The second-law analysis of a recirculation cycle desiccant cooling system: cosorption of water vapour and carbon dioxide. *Atmospheric Environment* 1996;30(9):1429-35.

[60] Shy-Min LU, Wen-Jyh YAN. Development and experimental validation of a full-scale solar desiccant enhanced radiative cooling. *Renewable Energy* 1995;6(7):821-7.

[61] Silverio R.J.R., Figueiredo J.R. Steady state simulation of the operation of an evaporative cooled water-ammonia absorption scale ice maker with experimental basis. *Journal of the Brazilian Society of Mechanical Sciences and Engineering* 2006; 28: 413-21.

[62] Soylemez, M., 2004. On the optimum performance of forced draft counter flow cooling towers. *Energy Conversion and Management*, 45(15), pp. 2335-2341.

[63] Techajunta S, Chirarattananon S, Exell RHB. Experiments in a solar simulator on solid desiccant regeneration and air dehumidification for air dehumidification for air conditioning in tropical humid climate. *Renewable Energy* 1999;17:549-68.

[64] TRNSYS. A transient system simulation program. Solar Energy Laboratory, University of Winconsin-Madison, Engineering Experimental Station Report 38, June, 1979.

[65] United State Environment Protection Agency. EPA green building strategy, 2008, http://www.epa.gov/greenbuilding/pubs/about.htm.

[66] Vakiloroaya , V., Ha, Q. and Samali, B., 2013. Energy-efficient HVAC systems: Simulation–empirical modelling and gradient optimization. *Automation in Construction*, 31, pp. 176-185.

[67] Wang RZ, Wu JY, Xu YX, Wang W. Performance researchers and improvements on heat regenerative adsorption refrigerator and heat pump. *Energy Conversion Management* 2001;42(2):233-49.

[68] Wilbur PJ, Mancini TR. A comparison of solar absorption air-conditioning systems. *Solar Energy* 1976;18:568-76.

[69] Wilbur PJ, Mitchell CE. Solar absorption air-conditioning alternatives. *Solar Energy* 1975;17:193-9.

[70] Yamaguchi S.,Jeong J., Saito K.,Miyauchi H.,Harada,M. Hybrid liquid desiccant air-conditioning system:Experiments and simulations, *Applied Thermal Engineering* 2011; 31: p.3741-3747.